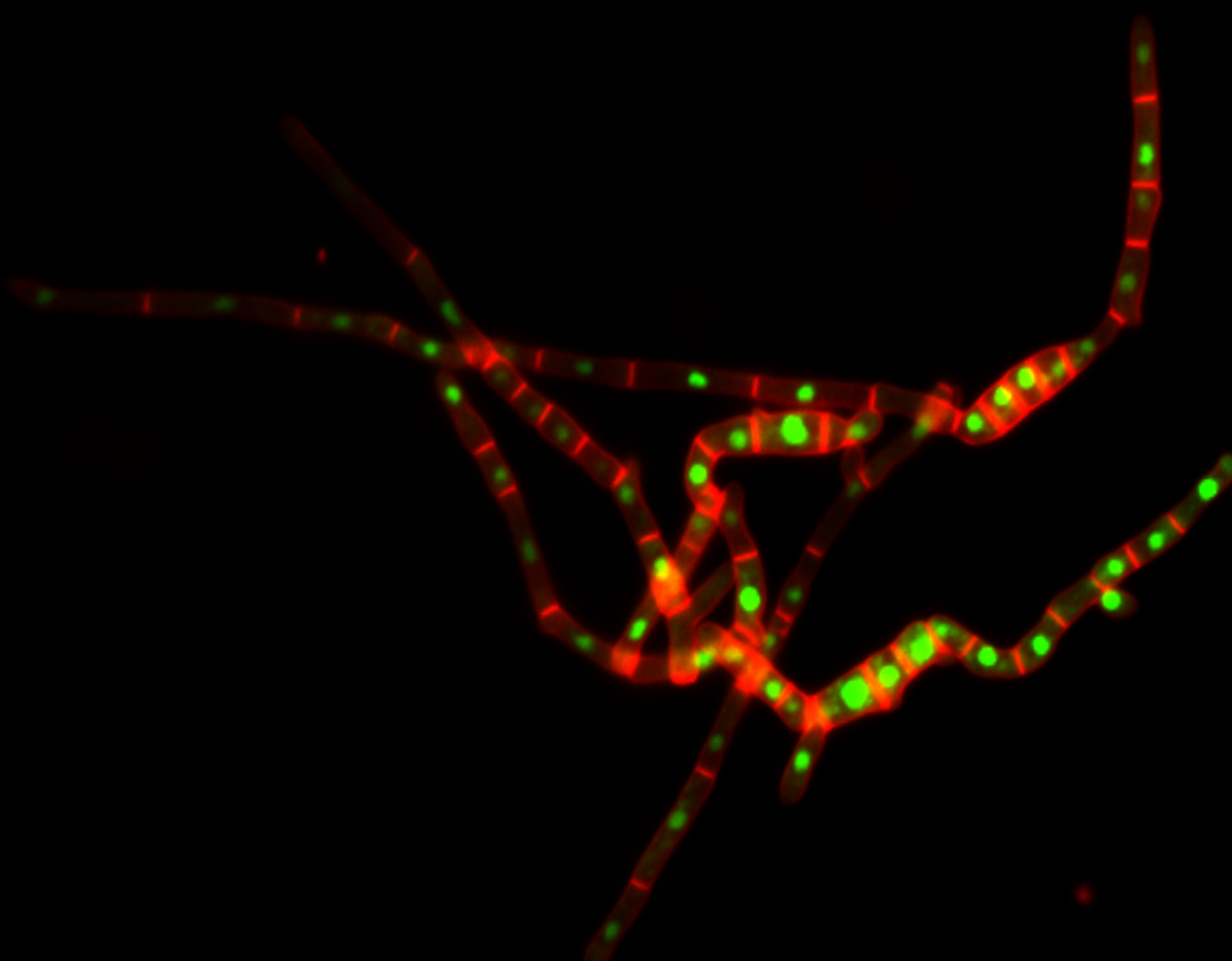**VNiVERSiDAD Ð SALAMANCA**

CAMPUS DE EXCELENCIA INTERNACIONAL

ibfg

TESIS DOCTORAL

Relationships between the cell cycle and the differentiation programs associated to virulence in the phytopathogen fungus *Ustilago maydis*

Sónia Castanheira Dias
Salamanca, 2014

Departamento de Biología Funcional y Genómica

Instituto de Biología Funcional y Genómica

(USAL/CSIC)

VNiVERSiDAD Ð SALAMANCA

Relationships between the cell cycle and the differentiation programs associated to virulence in the phytopathogen fungus *Ustilago maydis*

TESIS DOCTORAL

Sónia Castanheira Dias
Salamanca 2014

UNIVERSIDAD DE SALAMANCA

Departamento de Biología Funcional y Genómica
Instituto de Biología Funcional y Genómica
(USAL/CSIC)

Relationships between the cell cycle and the differentiation programs associated to virulence in the phytopathogen fungus *Ustilago maydis*

Memoria presentada por Sónia Castanheira Dias para optar
al grado de Doctor en Biología.

Salamanca, 2014

Acknowledgments

The day I had the interview in Madrid in 2010 for the Marie Curie fellowship within ARIADNE project, I would never imagine how such incredible experiences were waiting for me. I would like to express my endless gratitude to my advisor, for accepting me in his laboratory. I could not have imagined having a better advisor. Many thanks Pepe for your continuous support, for your patience, enthusiasm, motivation, good humour, immense scientific knowledge, your excellent guidance and also for providing me a very well organized laboratory and so good conditions to do good science.

Besides a unique boss, I also had unique and best labmates that undoubtedly I will miss them a lot. Many thank Maria Tenorio, Sara Rivera, Antonio de la Torre and Paola Bardetti. Sharing the laboratory with you has made the days at work a pleasure and I have learnt and laugh very much with you.

I would also like to thank to my first labmates, during the first year and half in Madrid (now it seems it has been ages ago): Natalia Carbó and Carmen de Sena. Thanks Carmen for making me company during the two first "lonely" months at IBFG after moving from CNB. I was also glad to share lab with Arturo Calzada and Fernando Devesa. Unexpectedelly, I had his company during a part of the writing thesis, what was a good surprise.

Thanks to the Ariadne PhD students team for the excellent moments spent together during the workshops and summer courses: Miriam Oses, Filomena Nogueira, Elisabetta Marchegiani, Mennat El Ghalid, Vikram Naik, Clara Baldin, Lisa Wasserström, Therése Oscarsson, Katja Schäfer, Elisabetth Grund, Pankaj Mehrotra, Soodeh Moghaddas and Marino Moretti. I have to give a special thank to Filo for listening me always I needed, for helping me with English writing and her helpful advice. Behind her apparent madness, there is an exceptional person.

I would like to thank all PIs of ARIADNE: Jüergen Wendland, Antonio Di Pietro, Regine Kahmann, Neil Gow, Nicholas Talbot, Marc-Henri Lebrun, Axel Brakhage and Valerie Toquin. A special thank to Elena for taking charge of Ariadne review.

I wish to thank prof. Francisco del Rey, Paco Soriano and Alegria for their very useful help in bureaucracy aspects.

All the research groups within IBFG for the insightful comments and hard questions during seminars and lab meetings both hold weekly.

To my friends of social activities in Salamanca who have been like a family: Marta Tormos, Daniel, "Amandinha", Diana and Paola.

Thanks to Gorjana for welcoming me always at her home in Madrid. To David, Camilla and all the fellows from IBFG for those out work activities.

A very special thanks to Ale for his constant presence and infinite patience. Definitely, I am very luck having meeting you. Thank you for making me smile even in the not so good moments.

To my family, that sadly has decreased during my thesis dissertation. I dedicate this thesis to the lovely memory of my brother Bruno, my grandfather José, my father João and my uncle José.

"Valeu a pena? Tudo vale a pena Se a alma não é pequena."
Fernando Pessoa

Table of contents

Resumen en español

1. Justificación del estudio

Ustilago maydis es el agente responsable del carbón del maíz. El desarrollo patógeno en este hongo está íntimamente vinculado a la diferenciación sexual y se acompaña de numerosas transiciones morfológicas asociadas a un control preciso del ciclo celular. Esto hace que este hongo sea un excelente modelo para identificar dianas del ciclo celular que jueguen papeles esenciales en las enfermedades causadas por hongos. Dado que en la mayoría de las situaciones, los fungicidas no son efectivos en el control de la enfermedad si el patógeno ya ha entrado penetrado en los tejidos de la planta, la enfermedad debe impedirse durante las primeras etapas de la infección. *U. maydis* debe tomar dos decisiones cruciales de desarrollo, que ocurren en la superficie de la planta, antes de penetrar el tejido vegetal. La primera tiene lugar cuando dos células haploides son capaces de reconocerse mediante un sistema feromona-receptor. Las células detienen su ciclo celular, forman cada una un tubo de conjugación que crece a favor de gradiente de feromona hasta aparearse. La segunda decisión es la formación de la hifa dicariótica, que implica tanto una detención específica del ciclo celular en G2 como una activación de un fuerte crecimiento polar (Pérez-Martín and Castillo-Lluva, 2008). Por lo tanto, entender los mecanismos moleculares implicados en el apareamiento y en la formación del filamento infectivo es crucial en el diseño de antifúngicos. Nuestro objetivo ha sido dilucidar los mecanismos responsables de estas paradas de ciclo celular con el fin de desacoplar la detención del ciclo del resto de los procesos durante la formación de las hifas infectivas y de este modo averiguar sus consecuencias en el proceso infectivo.

2. Parada de ciclo celular en G2 inducida por el factor b

El complejo de proteínas homeodominio bE/bW es el factor clave para el cambio de crecimiento como levadura a crecimiento filamentoso y su formación es suficiente para la iniciación de la fase patógena. La expresión ectópica y inducible de las subunidades b compatibles, bajo el control de promotores regulables, conduce a la formación de un filamento monocariótico en cultivo líquido. Esto mimetiza el filamento dicariótico con respecto al crecimiento

filamentoso y a la parada de ciclo celular. Estudios previos en nuestro laboratorio indicaron que la hifa infecciosa producida tras la expresión de las proteínas b compatibles está parada en la fase G2 del ciclo celular (Mielnichuk et al., 2009). También indicaron que la parada del ciclo celular, inducida por el factor b, es mediada por la acumulación de la forma inactiva fosforilada de Cdk1. La acumulación de Cdk1 fosforilada después de la producción del factor b fue debida a la inactivación de la fosfatasa Cdc25 por Bmh1, una proteína 14-3-3 que retiene Cdc25 en el citoplasma. La retención citoplasmática de Cdc25 requiere la fosforilación previa de sus sitios de unión 14-3-3. Sorprendentemente, se encontró que Chk1, una quinasa implicada en la respuesta al daño del ADN, era responsable de la fosforolación de Cdc25 (de Sena-Tomas et al., 2011; Mielnichuk et al., 2009). Sin embargo, Chk1 se activa transitoriamente durante la formación de la hifa infecciosa. Teniendo en cuenta que la detención del ciclo celular inducida por b se puede mantener durante un largo periodo de tiempo, nos hemos planteado la hipótesis de que son necesarios factores adicionales para sostener una parada del ciclo celular a largo plazo.

2.1. Resultados

- La inducción de la expresión de los genes b tuvo como resultado la disminución específica del gen *hsl1* que codifica una quinasa tipo Nim1.

- La quinasa Hsl1 es un regulador de la transición G2/M del ciclo celular en *U. maydis.*

- La disminución de *hsl1* y la activación de Chk1 colaboran en la parada del ciclo celular inducida por el factor b.

- Las cepas incapaces de detener el ciclo celular se vieron gravemente afectadas en la virulencia.

- La parada del ciclo celular parece ser necesaria para la formación de apresorio.

3. Parada de ciclo celular en la fase G2 inducida por feromona

Estudios llevados a cabo en las levaduras de fisión *Schizosaccharomyces pombe* y de gemación *Saccharomyces cerevisae* han mostrado que la exposición de las células a feromonas de tipo de apareamiento opuesto conduce a una parada del ciclo celular. Como consecuencia, las células sincronizan su ciclo celular en la misma fase antes de la fusión y crecen a favor de un gradiente de feromona de una manera polarizada, dando lugar a las estructuras de apareamiento. En nuestro laboratorio, estudios previos indicaron que las células de *U. maydis* tras la exposición a feromonas también paran el ciclo celular. Sin embargo, a diferencia de *S. pombe* y *S. cerevisae*, que paran el ciclo celular en G1, las células de *U. maydis* detienen su ciclo celular en G2 tras la exposición a las feromonas. El mecanismo que *U. maydis* utiliza para detener el ciclo en G2 aún no se ha caracterizado. Como en las levaduras de fisión y de gemación, en *U. maydis* una vía conservada de MAP kinasas transmite la señal de la feromona desde los receptores de feromona situados en la membrana citoplasmática. La integridad de esta vía es necesaria para la inducción de la parada de ciclo celular (Garcia-Muse et al., 2003;(Garcia-Muse et al., 2003b; Muller et al., 2003). Sin embargo, no se habían caracterizado hasta el momento efectores localizados por debajo de esta vía de MAP kinasas requeridos específicamente para la parada de ciclo celular. En esta parte del estudio, hemos llevado a cabo intentos de caracterizar el mecanismo detrás de la parada de ciclo celular inducida por feromona en *U. maydis*.

3.1. Resultados

- La expresión del alelo constitutivamente activo *fuz7^{DD}* mimetiza la parada de ciclo en G2 inducida por feromona.
- La fosforilación inhibitoria de Cdk1 es necesaria para la parada del ciclo celular en G2 inducida por *fuz7^{DD}*.
- La feromona y el factor b utilizan mecanismos diferentes para detener el ciclo celular.
- Los niveles de la fosfatasa Cdc25 disminuyen tras la inducción de *fuz7^{DD}*.

8

- El complejo Cdk5-Pcl12 es necesario para la parada del ciclo celular inducido por *fuz7^{DD}*.

- La sobreexpresión de *pcl12* mimetiza la parada del ciclo celular inducida *fuz7^{DD}*.

- La quinasa Crk1 del tipo Ime2 es necesaria para la parada del ciclo celular inducida *fuz7^{DD}*.

- Crk1 es necesaria para la parada del ciclo celular inducida *pcl12*.

- La fosforilación del motivo TEY de Crk1 es necesario para sostener las paradas de ciclo celular inducidas tanto por *fuz7^{DD}* como por *pcl12*.

4. Conclusiones del estudio

1. Los niveles de expression de hsl1 son disminuidos tras la inducción del factor b independientemente de la parade de ciclo celular.

2. Hsl1 en *U. maydis* es una quinasa del tipo Nim1 que actúa como un regulador negativo de Wee1.

3. Dos mecanismos diferentes que involucran Hsl1 y Chk1 sostienen la parada del ciclo celular en G2 tras la inducción del factor b.

4. La parada del ciclo celular en G2 en las hifas infecciosas es importante para la virulencia.

5. La parada del ciclo celular en G2 es esencial para la formación del apresorio.

6. Feromona y el factor b utilizan mecanismos distintos para detener el ciclo celular

7. Pcl12 es suficiente y necesario para la detención del ciclo celular

8. Crk1 fosforilación en el sitio TXY es necesario para la parada del ciclo celular inducido por feromona.

9. Los niveles de Cdc25 estan aparentemente disminuidos tras la indución de feromona.

Abbreviations

C: DNA content

cDNA: Coding DNA

CFW: Calcofluor white

CMD: Complete medium with glucose

CMA: Complete medium with arabinose

DAPI: 4',6-diamidino-2-phenylindole

DEPC: Diethyl pyrocarbonate

DNA: Deoxyribonucleic acid

dNTP: Deoxyribonucleotide

FACS: Fluorescence-activated cell sorting

G: Gap

GFP: Green fluorescent protein

mRNA: messenger RNA

NLS: Nuclear localization signal

O.D: Optical density

PCR: Polymerase chain reaction

Phleo: Phleomycin or bleomycin

RNA: Ribonucleic acid

rpm: Revolutions per minute

RT-PCR: Reverse transcription polymerase chain reaction

SDS: Sodium dodecyl sulfate

SSC: Saline-sodium citrate buffer

Introduction

1. Connection between the cell cycle and developmental processes

In eukaryotes, developmental processes often involve differentiation, cell cycle modulation, and the induction of a new morphogenetic program. Control of the cell cycle is essential for the development of an organism. In fact, a number of studies in *Caenorhabditis elegans* and *Drosophila melanogaster* have given insights into the importance of co-ordinating cell cycle progression and cell differentiation to generate specific tissues and organs during development (Budirahardja and Gönczy, 2009). For example, during *D. melanogaster* eye development, an altered cell cycle progression prevents proper photoreceptor differentiation. Similarly, during vulval developmental in *C. elegans*, cells must synchronize cell cycle prior differentiation. Other case is the requirement of a cell cycle arrest in G1-phase preceding differentiation of neural progenitors (Hindley and Philpott, 2012). Thus, there is growing evidence that a cross-talk between the processes of differentiation and cell cycle progression must exist to determine cell fate and make the appropriate developmental decision.

2. Developmental decisions in fungi: Sexual differentiation

In fungi able to reproduce sexually, a crucial developmental decision is the mating process. Fungal haploid cells secrete pheromones, which are recognized by their cognate receptors located on the cell membrane of opposite mating type. Pheromone binding leads to activation of a conserved mitogen-activated protein kinase (MAPK) module, which ultimately results in cell cycle arrest, polarized morphogenesis towards the partner cell, and eventually cell fusion.

2.1. Pheromone response pathway in Ascomycete yeasts

The ascomycetes *Schizosaccharomyces pombe* and *Saccharomyces cerevisiae* are well known as been used as fungal models for many years. Since then, they have often served as paradigms for studying the cell cycle in

other organisms, including the connection between cell cycle regulation and sexual development.

2.1.1. Pheromone-mediated cell cycle arrest in *Saccharomyces cerevisiae*

So far, the best-understood system with respect to the molecular mechanism of pheromone-induced cell cycle arrest is that of the yeast *S. cerevisiae*. This budding yeast has two different mating types named a and α. Upon pheromone-receptor interaction, the pheromone pathway composed of MAP3K Ste11, MAP2K Ste7 and MAPK Fus3, is activated and promotes the phosphorylation and activation of Far1 Cdk inhibitor as well as the activation of Ste12 transcription factor, which in turns regulates transcription of mating-specific genes. As a consequence, cells arrest their cell cycle progression at G1 phase and grow towards the mating partner in a polarized manner, giving rise to mating projections termed shmoo. Arrest of cell cycle progression results from the inhibition of the function of complexes formed by G1 cyclins and the CDK (Cdc28). Such inhibition occurs via the Far1 Cdk inhibitor, which is up regulated and gets phosphorylated upon activation of the pheromone cascade. Recently, Pope and colleagues (2014) have shed new light on the mechanism by which Far1 inactivates the function of Cdk. They unravelled a novel mechanism undertaken by budding yeast for regulation of CDK/cyclin complex. This mechanism relies on disrupted interactions between cyclin-Cdk complexes and their substrates through Far1. The cyclins Cln1 and Cln2 recognize Cdk substrates via specific docking sites, which in turn trigger substrates phosphorylation (Bhaduri and Pryciak, 2011; Kõivomägi et al., 2011). Far1 inhibits these docking interactions, by competing with substrates for association with G1 cyclins. Besides disrupting substrate docking, Far1 is also able to disrupt Cdk kinase activity.
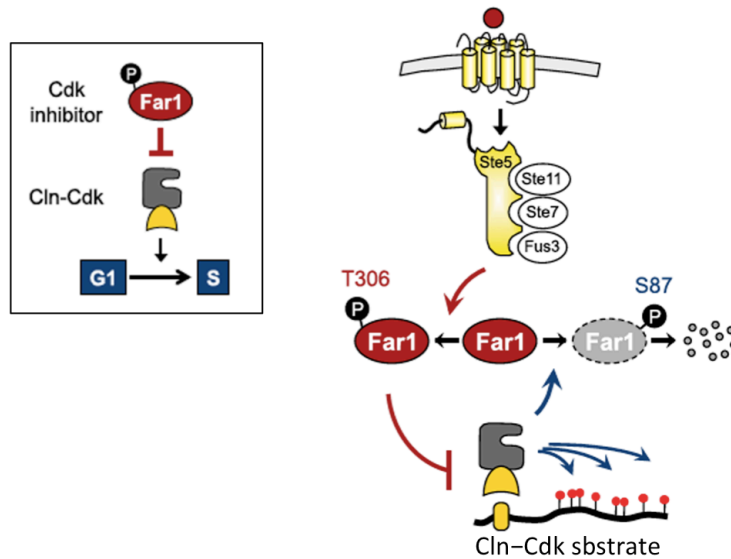
Figure 1: Scheme of pheromone-mediated cell cycle arrest via CKI protein Far1 in *S. cerevisiae* (Pope et al., 2014)**.** Far1 Cdk inhibitor antagonizes both kinase activity and substrate recognition by Cln1/2-Cdk complexes. Phosphorylation at residue T306 by the MAPK Fus3 promotes Far1 function, whereas phosphorylation at residue S87 by Cdk promotes its degradation.

2.1.2. Pheromone-mediated cell cycle arrest in *Schizosaccharomyces pombe*

The fission yeast *S. pombe* has two mating types, called h+ and h-. Cells of opposite mating types communicate by mating pheromones only under starvation for nutrients. The pheromones secreted by h+ and h- cells are P-factor and M-factor, respectively. The first studies on cell-cycle control by pheromone were not easy in *S. pombe*. This was due to the requirement for mating of nutrients deprivation, which automatically leads *S. pombe* cells to arrest in G1. However, by using a mutant deleted for *cyr1* (encoding for adenylate cyclase), which uncouples sexual differentiation from nutritional starvation, this problem was overcome. The h+ cells had no detectable cAMP in the absence of Cyr1 and responded to the M-factor in rich medium. In response to pheromones, cells underwent a transient cell cycle arrest at G1 phase and elongated to form shmoo structure (Davey and Nielsen, 1994). Additionally, studies done by Imai and Yamamoto (1994) revealed that using the synthetic P-factor in combination with *cyr1* and *sxa2,* which encodes a protease thought to degrade P-factor, deletion mutations enhanced the susceptibility to P-factor

even in the presence of nutrients. P-factor induced responses toward mating and also a cell cycle arrest at the G1 phase confirming that *S. pombe* cells arrest the cell cycle at G1 phase in response to pheromone. Further studies have demonstrated that pheromone blocks entry into S-phase by degradating both Cig2 and Cdc13 B-cyclins associated to Cdc2 kinase, via the Ste9-APC/ complex (Blanco et al., 2000; Kitamura et al., 1998; Yamaguchi et al., 1997; Yamaguchi et al., 2000). The Cdk inhibitor Rum1 is also required to maintain cell cycle arrest (Moreno and Nurse, 1994). Rum1 binds both Cdc13 and Cig2 and it is specifically required for Cdc13 proteolysis (Davey, 1998; Stern and Nurse, 1997; Stern and Nurse, 1998). Thus, in response to pheromone, *S. pombe* cells arrest their cell cycle through down-regulation of Cdc2/CLB activity. This inhibition is achieved through mitotic cyclins degradation as well as through the function of the Cdk inihitor, Rum1.

In *S. pombe* the integration of nutritional and pheromone signals converges on the high mobility group (HMG) transcription factor Ste11. Furthermore, Ste11 activates many genes that are required for the switch from cellular proliferation to sexual differentiation (Otsubo and Yamamoto, 2012). Importantly, the role of PKA in *S. pombe* is to mediate repression of Ste11 and thereby cAMP induces a negative effect on mating.
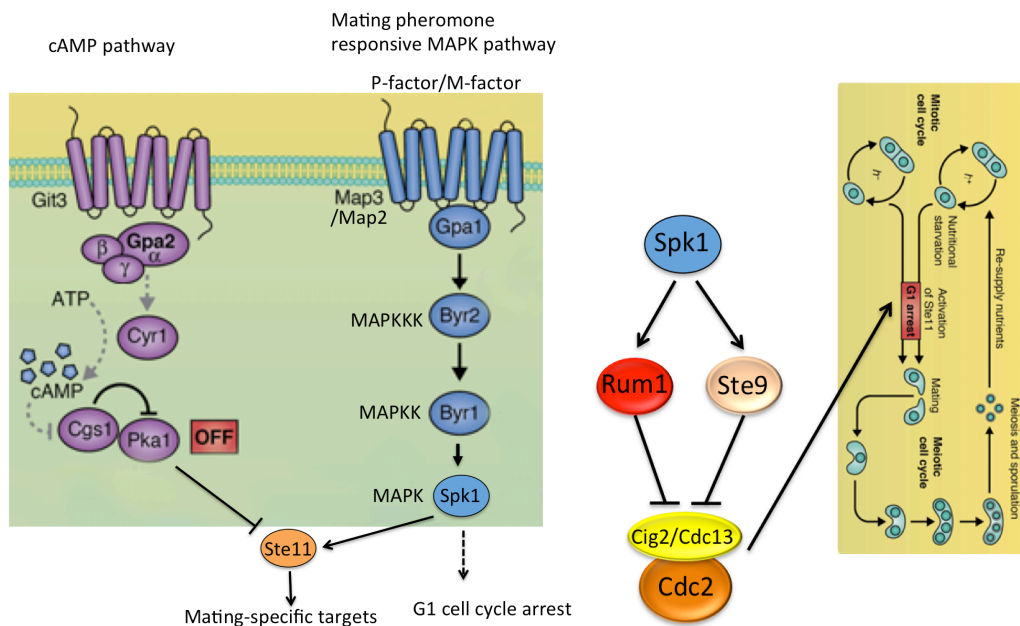
Figure 2: Pheromone-induced cell cycle arrest at G1 phase in *S. pombe* (Adapted from Otsubo and Yamamoto, 2012)*.* Two parallel signalling pathways regulate mating in *S. pombe*. One is a nutrient-sensing pathway that, in presence of abundant nutrients, stimulates cAMP production to repress *ste11* expression and inhibit mating. The second responds to pheromones through a conserved MAPK signalling pathway, leading to a G1 cell cycle arrest and formation of mating structures.

3. Morphogenic differentiation and cell cycle in pathogenic fungi

Pathogenic fungi show a great variability in their lifestyles and in the symptoms they cause (Perez-Nadales et al., 2014). These characteristics make more difficult the searches for common antifungal targets. Nevertheless, several fungal pathogens undergo morphogenetic changes from a yeast-like form to a filamentous form, and this dimorphic behaviour has been considered to be crucial for pathogenicity. The switching requires a tight coordination of several processes, such as cell cycle control, the change to a polarized growth, and in the case of fungal plant pathogens, also the differentiation into specialized cell structures to breach the leaf surface and proliferate inside the plant. Moreover, it has been stated that cell cycle and fungal morphogenesis have to be adjusted in response to extracellular (environmental) and intracellular (developmental) signals. Also, the integration of both signals by the cell machinery will determine whether pathogenic fungi will trigger virulence mechanisms (Pérez-Martín, 2012).

3.1. *Magnaporthe oryzae*

Morphological changes are required for fungal pathogens to cause disease. Conserved signalling pathways regulate morphogenic differentiation in response to environmental and host physiological stimuli. A well-known example includes the rice blast ascomycete *M. oryzae*, in which conidia must undergo differentiation into specialized infection structure termed appresoria to breach the leaf surface. Appressorium morphogenesis starts with a polarized germ tube. On an inductive surface, the germ tube tip switches from apical to isotropic growth and forms an initial appressorium. Turgor generation and melanisation matures the appressorium. Such physiological changes in the appressorium are tightly regulated by the cell cycle. By using Histone-GFP as a

marker for nucleus, it was found that only the nucleus at the germ tube divides and mitosis always precedes appressorium development. Upon appressorium maturation, the other nuclei left in the conidia are degraded in an autophagic cell death mechanism. The appressorium morphogenesis is regulated by three distinct cell cycle checkpoints. Initiation of appressorium morphogenesis is regulated at S-phase. Arresting S-phase with inhibitor of DNA synthesis (hydroxyurea) or *nim1^{I327E}* mutation prevents germ tubes from swelling and initiating appressorium formation. Mitotic entry is necessary for appressorium development. Blocking entry into mitosis by using a thermosensitive allele of NimA (*never in mitosis*) kinase (*nimA^{E37G}*) inhibits nuclear division, appressorium formation and also autophagic cell death. Mitotic entry is not only necessary but also sufficient for appressorium development. *bim1^{F1763*}* mutants in which the function of anapase promoting complex (APC) is disrupted or mutants in which the expression of B type cyclins is stabilized prevents mitotic progression and exit. Although these mutants are unable to cause plant infection, the appressorium is able to mature.
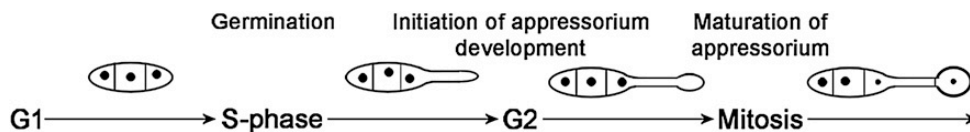
Figure 3: Coordination between infection structure development and cell cycle progression in *M. oryzae* (Taken from Saunders et al., 2010).

3.2. *Candida albicans*

The human fungal pathogenic *Candida albicans* is able to undergo morphological changes between budding yeast, pseudohyphae, and hyphae. The developmental switch from a yeast form to a hyphal form is required for its pathogenicity. Differentiation of hyphae is induced by environmental cues in a cell cycle-independent manner as reported by (Hazan et al., 2002). They demonstrated that the timing of cell cycle-regulated events and the levels of inhibitory Tyr18 phosphorylation of Cdc28 mediated by the mitosis inhibitor protein kinase Swe1 are identical between synchronous yeast and hyphal apical cells. However different mutations or drug treatments that interrupt nuclear progression lead to unscheduled polarized or highly polarized growth.

18

In some cases, the phenotypic alterations are accompanied by the expression of hyphae-specific genes (Berman, 2006). Also, cell cycle factors have been reported to influence hyphal morphology. For example, G1 cyclin Ccn1 is necessary to maintain hyphal growth on solid media and in liquid Lee's medium (Loeb et al., 1999); Hgc1 that is a G1 cyclin-related protein is essential for hyphal formation (Zheng and Wang, 2004); B type cyclins Clb2 and Clb4 regulate negatively polarized growth (Bensen et al., 2005).

Bachewich and Whiteway (2005) gave insights into how the cell cycle may be directly coupled to development. They reported that in the absence of G1 cyclin Cln3 under yeast growth conditions causes the yeast cells to arrest in G1, increase in size and develop into hyphae and pseudohyphae. In contrast, the absence of Cln3 in environment-induced hyphae does not inhibit growth or the cell cycle. These results suggested that the cell cycle may not be regulated in the same manner in yeast and hyphal cells. The authors proposed that absence of a G1 cyclin could activate developmental pathways and uncouple differentiation from the normal environmental controls. The G1 phase could play a role in regulating hyphal and pseudohyphal in *C. albicans*.
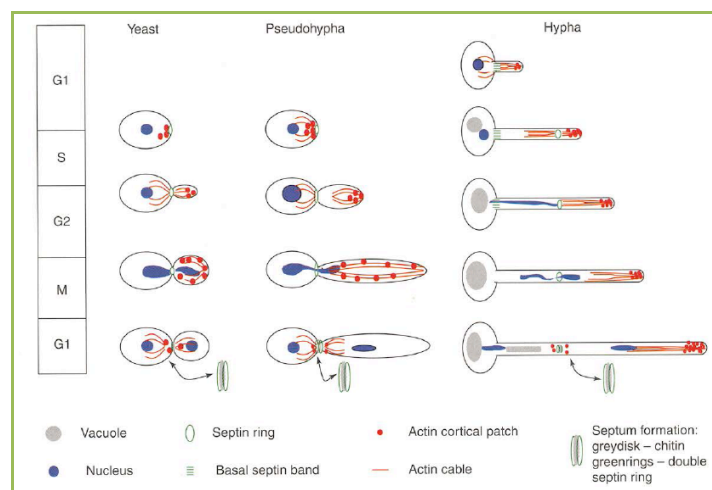
Figure 4: Cell cycle progression in hyphal cells (Taken from Sudbery et al., 2004).

4. *Ustilago maydis:* a model to unravel the mechanisms of morphogenesis and virulence associated to the cell cycle

U. maydis, a basidiomycete fungus, belongs to the Ustilaginales group of plant pathogens that can infect around 4000 species of angiosperms (Martínez-

Espinoza et al., 2002). This fungus infects all aerial organs of its plant maize and establishes a biotrophic interaction, which ultimately results in formation of plant tumors. In México, the diseased fresh ears are appreciated as demonstrated by their use in preparation of traditional dishes known as "huitlacoche". However, under certain conditions smut disease may lead to high economic losses worldwide. For example, in United States, a loss of 1% equals to $189 million per year (Martínez-Espinoza et al., 2002). As a result, there is a need for improved molecular knowledge of *U. maydis* pathogenesis and furthering the development of antifungals.

 U. maydis has been considered an excellent model system to study the relationship between cell cycle, morphogenesis and pathogenicity. In this fungus virulence and sexual cycle are intimately intertwined as demonstrated by the generation of the infectious stage, which requires the mating of two compatible haploid cells in order to form the infective dikaryotic filament. In addition, *U. maydis* undergoes a number of different morphological and genetic changes during its life cycle: a haploid unicellular form called sporidia, which is non-pathogenic and divides by budding; a dikaryotic filamentous form, which is pathogenic and grows by apical cell extension; and a diploid form, the teliospore, which undergoes meiosis to produce sporidia. Therefore, an accurate control of the cell cycle as well as morphogenesis would be required during these transitions.

4.1. *Ustilago maydis* life cycle

 In the field, corn smut infections are spread by air-borne diploid teliospores. Germination of the teliospore is coupled to meiosis, resulting in pairs of sexually compatible sporidia. Transition from a non-pathogenic to a pathogenic form requires the fusion of two haploid compatible cells of opposite mating types since pathogenic development is associated to sexual reproduction. This process is dependent on pheromone signal transduction, regulated by a tetrapolar mating system that is specified by the biallelic *a* locus and the multiallelic *b* locus (Feldbrugge et al., 2004). Upon recognition of two haploid compatible cells that differ in the *a* locus, the cell cycle arrests in G2 phase, the budding is stopped and conjugation tubes started to be formed

(Perez-Martin et al., 2006). These structures usually appear at one tip and grow toward each other until they fuse. Once the cytoplasmic fusion is achieved, no kariogamy is induced, resulting in a dikaryotic cell, a hallmark of many basidiomycete. In addition, if cells harbor different mating type *b* locus, the dikaryon grows in a polar manner producing the infective filament. Hypha extends apically, and the cytoplasm accumulates at the tip of the cell compartment, whereas older parts become vacuolated and are sealed off through the insertion of regularly spaced septa at the distal pole resulting in the formation of characteristic empty sections, which often collapse (Steinberg and Perez-Martin, 2008). Such kind of growth enables the fungus to migrate along the plant surface most likely to find an appropriate point of entry. Eventually, hyphae stop polar growth in response to both chemical and physical signals from the plant. Hyphal tips swell to form poorly differentiated appressorium that will penetrate the cuticle via the action of lytic enzymes (Brefort et al., 2009). Once the filament enters the plant, cell cycle is reactivated. The formation of empty sections ceases and mitotic divisions take place, concomitant with the development of clamp-like structures that allow the correct sorting of nuclei to maintain the dikaryotic status. By this way, the fungus proliferates to a network of filaments with septated cell compartments each containing a pair of nuclei (Banuett and Herskowitz, 1996; Snetselaar and Mims, 1992). The massive proliferation of fungal hyphae is responsible for the induction of plant tumors. Strikingly, plant does not trigger any visible protective response and only 2-3 days after infection a stress reaction can be observed. Consequently, antocyanin is produced and partial necrosis at areas of initial penetration appears. Finally, hyphal proliferation inside the tumors is followed by sporogenesis, a poorly understood process that includes karyogamy to produce diploid nuclei, hyphal fragmentation, and differentiation into melanized diploid teliospores. Eventually the tumors dry up and rupture occurs, resulting in the release of the diploid spores, which are dispersed by air thus closing the fungus life cycle.
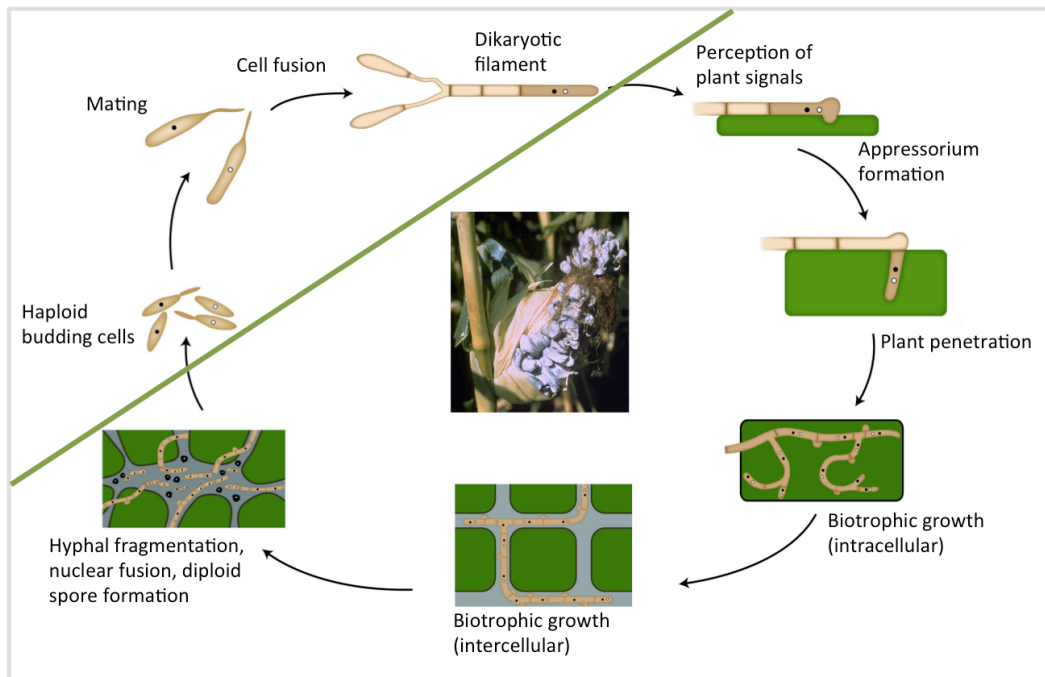
Figure 5: Schematic diagram of *U. maydis* life cycle (Adapted from Perez-Nadales et al., 2014). In the yeast stage, haploid yeast like cells grow by polar budding and are non-pathogenic. Upon pheromone-dependent recognition that takes place on the plant surface, the fungus switches to hyphal tip growth and forms conjugation tubes that grow toward the mating partner. Subsequently, these cells fuse to form a dikaryotic hypha. A green line separates processes mentioned from those that take place inside the plant tissue. Following appressorium formation, hypha is able to penetrate the plant tissue, where the fungus proliferates and causes the symptoms of maize smut disease. The picture in the middle shows tumor formation on a corn cob.

4.2. *U. maydis* mating type loci

Many pathogenic fungi are capable of undergoing sexual reproduction (Butler, 2010; Morrow and Fraser, 2009; Ni et al., 2011). Sexual reproduction in fungi is governed by their mating type locus (Bölker and Kahmann, 1993). *U. maydis* is a heterothallic fungus (two compatible mating types are required for a complete sexual cycle), whose sexual development is regulated by the a and b mating type loci. Successful mating relies first in a cellular recognition that depends on the mating type determinants encoded in the locus *a*. In each of the two alleles of the locus, designated *a1* and *a2*, two genes encode for a lipopeptide-pheromone precursor (*mfa*) and a seven transmembrane receptor (*pra*). Recognition of each pheromone by its respective pheromone receptor in the opposite mating partner elicits a response in each cell that is transmitted by

a MAPK cascade. The mechanisms triggered by this cascade result in the formation of conjugation tubes that eventually fuse.

Once cytoplasmic fusion takes place, the second mating type determinant encoded by the *b* locus, induces progression of the sexual process. The *b* locus is composed of two divergently transcribed genes that encodes the two unrelated homeodomain transcription factors bE and bW. These two proteins can form a heterodimeric complex, but only in the case the proteins are derived from different alleles (Gillissen et al., 1992; Kamper et al., 1995). Therefore, the production of this regulator is linked to the mating process that, after cell fusion, leads to the interaction of the two subunits, each one provided by each compatible mating partner. The bE/bW homeodomain protein complex is the key factor for the switch from budding to filamentous growth and its formation is sufficient for initiation of the pathogenic phase (Bölker et al., 1995b). The bE/bW complex is able to trigger a regulatory cascade with 345 direct and indirect targets (Heimel et al., 2010). Among these, there are genes involved in the establishment of the biotrophic phase, cell cycle regulation and the dimorphic transition from budding to polarized growth. The *a* and *b* loci are cross-controlled: activation of the pheromone-dependent signalling pathway leads to an induction of *bE* and *bW* genes via the *prf1* transcription factor, whereas the formation of an active bE/bW heterodimer after cell fusion leads to the downregulation of the *a*-pathway (Heimel et al., 2010).
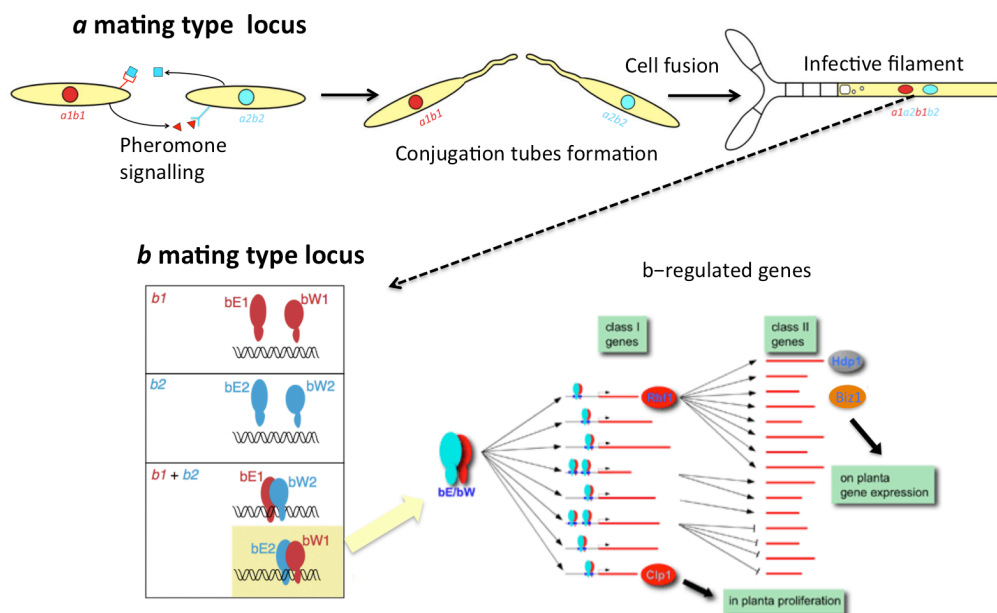
Figure 6: Control of sexual development and pathogenicity by *U. maydis* a and b mating type loci. Schematic view of interactions between pheromones and receptors encoded by the a locus. This locus encodes for lipopeptide pheromones (represented by triangle and square) and cognate pheromone receptors (represented by matching symbols). The multi-allelic b locus encodes for a pair of unrelated homeodomain proteins termed bE and bW. Only combinations of *bE* and *bW* of different allelic origin are active. Class I genes are directly regulated by bE/bW. The majority of the indirectly regulated class II genes are controlled by the b-dependent transcription factor Rbf1, and the expression of the transcription factors Hdp1 and Biz1 is dependent on Rbf1.

4.3. Pheromone response pathway in *U. maydis*

U. maydis haploid cells are non-pathogenic and grow by yeast-like budding. However, when compatible mating partners are exposed to both nutritional deprivation and pheromone, transcription of mating genes is enhanced and thus sexual development is initiated. Binding of pheromones (Mfa) to their cognate receptors (Pra) induces morphological switch from yeast-like to filamentous growth, which results in formation of conjugation tubes. Conjugation tubes of compatible cells grow towards each other and fuse at their tips. The pheromone signal is transmitted by a mitogen-activated protein kinase (MAPK) cascade, which includes the MAPK kinase kinase Ubc4/Kpp4, the MAPK kinase Ubc5/Fuz7 and the MAP kinase Ubc3/Kpp2. In addition to MAPK cascade, the cyclic AMP/protein kinase A (cAMP/PKA) plays a crucial role in controlling environmental-induced outcomes in *U. maydis*. These two pathways integrate both nutritional and pheromone signals in order to control sexual development. The integration has been proposed to occur through the high-mobility-group (HMG) domain transcription factor Prf1, which is differentially phosphorylated by PKA and the MAPK Kpp2 to activate *a* and *b* genes expression. Induction of the *a* genes requires PKA phosphorylation sites, whereas induction of b genes requires both PKA and MAPK phosphorylation sites. A complex cross talk between the cAMP and MAPK pathways has been reported in several studies. For example, haploid cells deleted for *uac1*, encoding adenylate cyclase, or for *adr1*, encoding the catalytic subunit of protein kinase A, results in a constitutive filamentous growth. Mutations in components of the MAPK cascade are able to supress filamentous phenotype of strains defective in Uac1. Integration of the cAMP and MAPK pathways has also been demonstrated through the study of Crk1, which encodes for an Ime2-

like kinase (Garrido and Perez-Martin, 2003(Garrido and Perez-Martin, 2003; Garrido et al., 2004). Additionally, cells defective in components either of the cAMP pathway or defective in genes encoding components of the MAPK pathway are severely impaired in the ability to mate. This indicates that MAPK and PKA transduction pathways operate antagonistically in morphogenesis, and synergistically in sexual differentiation.
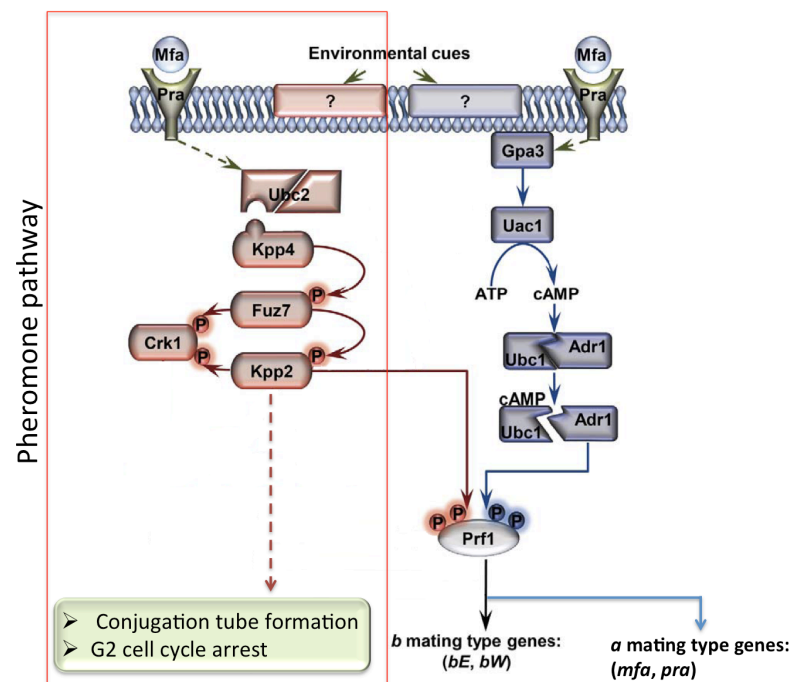
Figure 7: Schematic representation of pheromone pathway and crosstalk with PKA pathway (Adapted from Elías-Villalobos et al., 2011)**.** Pheromone (Mfa) binding to receptor (Pra) along with the environmental cues sensed by unknown receptors (represented by question marks) leads to the activation of the MAPK and cAMP pathways. The MAPK cascade is composed of Kpp4 (MAPKKK), Fuz7 (MAPKK) and Kpp2 (MAPK), and the alternative MAP kinase, Crk1. Once both pathways have been activated, the downstream transcription factor Prf1 becomes transcriptionally and post-translationally activated and the expression of a and b mating-type are induced. Uac1 encodes adenylyl cyclase enzyme, which is required to produce cAMP. Ubc1 is the regulatory subunit of PKA and Adr1 the catalytic subunit of PKA.

4.4. Cell cycle arrest triggered by bW/bE heterodimer

As previously described, to become pathogenic, *U. maydis* requires mating of compatible haploid sporidia which result in the pathogenic dikaryotic filaments, capable of extending through the plant surface. Such filaments grow

unipolar and are arrested in the G2 phase of the cell cycle. Haploid cells that grow by budding can be cultured in both liquid and solid culture, and easily manipulated in the laboratory, whereas dikaryotic filament does not grow in liquid culture. However, establishment of dikaryotic filament can be monitored on charcoal agar-plates. Mixed cultures of haploids carrying different a and b alleles produce long, straight, unbranched filaments with two nuclei apparently arrested at the tip of the cell (Puhalla, 1968; Rowell, 1955).

Haploid solopathogenic strains, which are able to infect plants without a mating partner, have been engineered through manipulation of b mating-type genes (Banuett and Herskowitz, 1994). This methodology overcame the difficulties associated with manipulation of the dikaryotic filaments. Ectopic and inducible expression of the compatible b subunits controlled by regulable promoters lead to the formation of a monokaryotic filament in liquid culture. This can mimic the dikaryotic counterpart regarding filamentous growth and apparent cell cycle arrest. Mielnichuk and colleagues (2009) found that infectious hyphae produced after the expression of compatible b proteins showed a single nucleus with 2C DNA content surrounded by an intact nuclear envelope and a defined cytoplasmatic array of microtubules, demonstrating the occurrence of cell cycle arrest in G2 phase. They also found that this b-induced cell cycle arrest is mediated by the accumulation of the phosphorylated inactive form of Cdk1. Interference with this inhibitory phosphorylation either through downregulation of the kinase Wee1 (responsible for this phosphorylation) or expression of a Cdk1 allele refractory to inhibitory phosphorylation, resulted in filaments that had no cell cycle arrested. Accumulation of phosphorylated Cdk1 upon b-factor production was due to the inactivation of the Cdc25 phosphatase by the Bmh1, a 14-3-3 protein that retains Cdc25 in the cytoplasm. Cytoplasmic retention of Cdc25 requires the previous phosphorylation of their 14-3-3 binding sites. Surprisingly, Mielnichuk and colleagues (2009) found that Chk1, a kinase involved in DNA damage response, is responsible for Cdc25 phosphorylation. However, they pointed out that Chk1 was transiently activated during the formation of the infective hypha. Considering that b-induced cell cycle arrest can be sustained for a long period of time, it has been hypothesized that additional factors are required to sustain a long-term cell cycle arrest (Pérez-Martín, 2012).
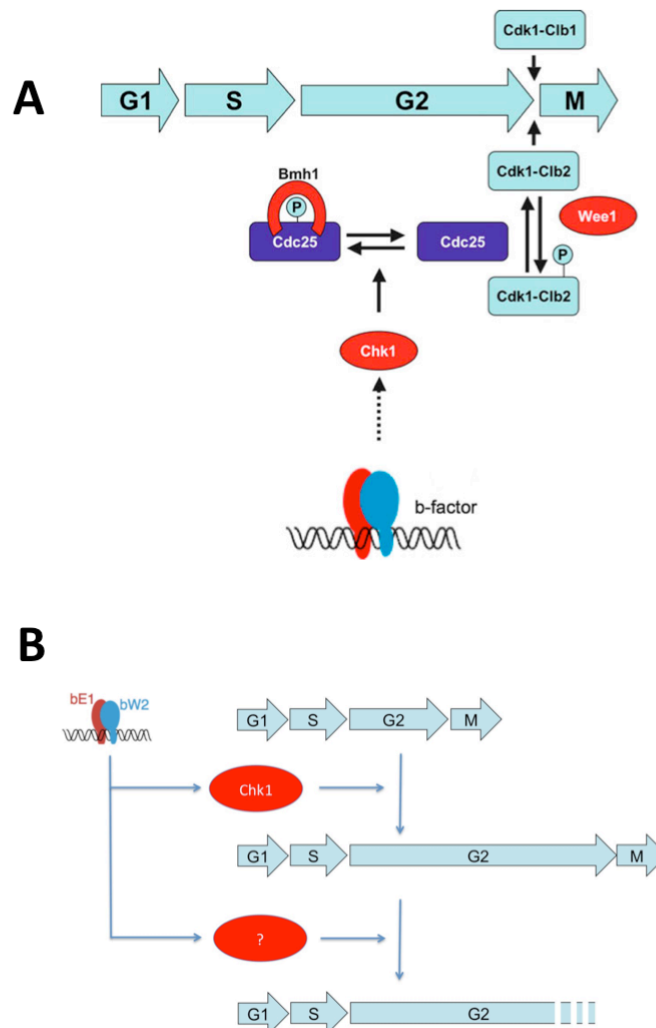
Figure 8: b-induced cell cycle arrest. (A) Cdk1-Clb1 and Cdk1-Clb2 complexes control G2/M transition. Cdk1/Clb2 activity is modulated by inhibitory phosphorylation of Cdk1 via Wee1 kinase. Upon induction of b-factor, Chk1 gets activated and retains Cdc25 in the cytoplasm, leading to cell cycle arrest in G2 **(B)** Scheme showing the hypothesis in which Chk1 triggers the G2 cell cycle arrest upon b-factor formation and additional factors are recruited for sustaining a long cell cycle arrest.

5. Aim of the study

Pathogenic development of the maize smut fungus *Ustilago maydis* is tightly linked to sexual differentiation and is accompanied by numerous morphological transitions associated to an accurate control of the cell cycle. This makes this fungus an excellent model to identify cell-cycle target genes that play essential causative roles in fungal virulence. Since in most situations, fungicides are not effective in controlling the disease if the pathogen has already entered (infected) the plant tissues, the disease should be prevented during the early stages of plant infection. In *U. maydis* two crucial development decisions are taken on the plant surface before the fungus penetrate the plant tissue. The first one takes place when yeast-like haploid sporidia of *Ustilago maydis* sense pheromone secreted by compatible partners. Cells arrest cell cycle, which allows them to initiate sexual development and form conjugation tubes in order to mate. The second step is the formation of the dikaryotic hyphae, which relies on a dual process that involves both a specific G2 cell cycle arrest and the activation of a strong polar growth (Perez-Martin and Castillo-Lluva, 2008). Therefore unravelling the molecular mechanisms involved in mating and formation of the infective filament (before the fungus enter the plant) will be crucial in the rational design of antifungal. We aim to elucidate the mechanism behind these stops in cell cycle in order to uncouple cycle arrest from the rest of processes during filament formation to unravel the consequences in the infective process.

Materials & Methods

1. Strains and plasmids

U. maydis strains used in this study are listed in the table 1, in which the genotype, the origin and the reference for each one are indicated.

Table 1: *U. maydis* strains used in this study

Strain	Genotype	Progenitor	Reference
FB1	*a1b1*	521×518	(Banuett and Herskowitz, 1989)
FB2	*a2b2*	521×518	(Banuett and Herskowitz, 1989)
AB33	*a2 P_{nar1}:bW2 P_{nar1}:bE1*	FB2	(Brachmann et al., 2001)
AB34	*a2 P_{nar1}:bE2 P_{nar1}:bW2*	FB2	(Bölker et al., 1995a)
SG200	*a1 mfa2 bE1bW2*	FB1	This study
UMS52	*a1b1 hsl1-3GFP*	FB1	This study
MUM1	*a1b1 hsl1Δ*	FB1	Mielnichuk
UMS59	*a1b1 hsl1Δ clb2-3GFP*	MUM1	This study
UMS60	*a1b1 hsl1Δ cut11-Cherry NLS-3GFP*	MUM1	This study
UMS61	*a1b1 hsl1Δ P_{nar1}:wee1*	MUM1	This study
UMP112	*a2 P_{nar1}:bW2 P_{nar1}:bE1 P_{dik6}: NLS-3GFP*	AB33	P-Martín
UMS65	*a2 P_{nar1}:bW2 P_{nar1}:bE1 hdp1Δ*	AB33	This study
UMS76	*a2 P_{nar1}:bW2 P_{nar1}:bE1 P_{dik6}: NLS-3GFP hsl1^{tef1}*	UMP112	This study
UMP121	*a2 P_{nar1}:bW2 P_{nar1}:bE1 P_{dik6}: NLS-3GFP chk1Δ*	UMP112	This study
UMS120	*a2 P_{nar1}:bW2 P_{nar1}:bE1 P_{dik6}: NLS-3GFP chk1Δ P_{tef1}:hsl1*	UMS76	This study
UMS127	*a2b2 P_{dik6}: NLS-3GFP*	FB2	This study
UMP129	*a2b2 chk1Δ*	FB2	(Mielnichuk et al., 2009)
UMS128	*a2b2 chk1Δ P_{dik6}: NLS-3GFP*	UMP129	This study
UMS130	*a1 mfa2 bE1bW2 hsl1^{tef1}*	SG200	This study
UMS126	*a1 mfa2 bE1bW2 chk1Δ*	SG200	This study

UMS131	*a1 mfa2 bE1bW2 chk1Δ hsl1^{tef1}*	UMS126	This study
UMS132	*a1 mfa2 bW2 bE1 P_{um01779}:GFP*	SG200	This study
UMS143	*a1 mfa2 bE1bW2 hsl1^{tef1} P_{um01779}:GFP*	UMS130	This study
UMS129	*a1 mfa2 bE1bW2 chk1Δ P_{um01779}:GFP*	UMS126	This study
UMS137	*a1 mfa2 bE1bW2 chk1Δ hsl1^{tef1} P_{um01779}:GFP*	UMS131	This study
UMS190	*a1 mfa2 bE1bW2 P_{um01779}:GFP cherry*	UMS132	This study
UMS191	*a1 mfa2 bE1bW2 chk1Δ hsl1^{tef1} P_{um01779}:GFP cherry*	UMS137	This study
UMS145	*a1 mfa2 bE1bW2 P_{um01779}:GFP P_{crg1}: fuz7^{DD}*	UMS132	This study
UMS154	*a1 mfa2 bE1bW2 chk1Δ hsl1^{tef1} P_{um01779}:GFP P_{crg1}: fuz^{DD}*	UMS137	This study
UMN4	*a1b1 fuz7^{DD crg1}*	FB1	Flor-Parra
UMS1	*a1b1 fuz7^{DD} cut11-Cherry NLS-3GFP*	UMN4	This study
UMS26	*a1b1 fuz7^{DD} kpp2Δ*	UMN4	This study
UMS28	*a1b1 fuz7^{DD} prf1Δ*	UMN4	This study
UMS12	*a1b1 fuz7^{DD} cut11-Cherry NLS-3GFP kpp2Δ*	UMS1	This study
UMS13	*a1b1 fuz7^{DD} cut11-Cherry NLS-3GFP prf1Δ*	UMS1	This study
UMS3	*a1b1 fuz7^{DD crg1} cut11-Cherry NLS-3GFP P_{crg1}: cdk1-myc*	UMS1	This study
UMS5	*a1b1 fuz7^{DD crg1} cut11-Cherry NLS-3GFP Pcrg1: cdk1^{AF}-myc*	UMS1	This study
UMS15	*a1b1 fuz7^{DD crg1} cut11-Cherry NLS-3GFP wee1^{nar1}*	UMS1	This study
UMS46	*a1b1 fuz7^{DDcrg1}*	FB1	This study
UMS51	*a1b1 fuz7^{DDcrg1} cut11-Cherry NLS-3GFP*	UMS46	This study
UMS73	*a1b1 fuz7^{DD crg1} cut11-Cherry NLS-3GFP hsl1^{tef1}*	UMS51	This study

UMS175	*a1b1 fuz7$^{DD\ crg1}$ cut11-Cherry NLS-3GFP hsl1^{tef1} chk1Δ*	UMS73	This study
UMS125	*a1b1 fuz7$^{DD\ crg1}$ cut11-Cherry NLS-3GFP crk1Δ*	UMS1	This study
UMS151	*a1b1 P$_{crg1}$:pcl12*	FB1	This study
UMS144	*a1b1 fuz7^{DD} cut11-Cherry NLS-3GFP pcl12Δ*	UMS1	This study
UMS169	*a1b1 cut11-Cherry NLS-3GFP*	FB1	This study
UMS179	*a1b1 cut11-Cherry NLS-3GFP P$_{crg1}$:pcl12*	UMS169	This study
UMS162	*a1b1 crk1Δ P$_{crg1}$:pcl12*	UMC38	This study
UMS176	*a1b1 crk1Δ P$_{crg1}$:pcl12 cut11-Cherry NLS-3GFP*	UMS162	This study
UMS183	*a1b1 P$_{crg1}$:pcl12 crk1-myc*	UMS151	This study
UMS185	*a1b1 P$_{crg1}$:pcl12 crk1^{AAA}-myc*	UMS151	This study
UMS184	*a1b1 P$_{crg1}$:pcl12 crk1^{AEF}-myc*	UMS151	This study
UMP244	*a1b1 P$_{crg1}$:pcl12 crk1-myc cut11-Cherry NLS-3GFP*	UMS183	This study
UMP246	*a1b1 P$_{crg1}$:pcl12 crk1^{AAA}-myc cut11-Cherry NLS-3GFP*	UMS185	This study
UMP245	*a1b1 P$_{crg1}$:pcl12 crk1^{AEF}-myc cut11-Cherry NLS-3GFP*	UMS184	This study
UMS186	*a1b1 cdk5^{ts} P$_{crg1}$:pcl12 cut11-Cherry NLS-3GFP*	SONU150	This study
UMS187	*a1b1 fuz7^{DD} cut11-Cherry NLS-3GFP crk1-myc* (Hyg^R)	UMS1	This study
UMS188	*a1b1 fuz7^{DD} cut11-Cherry NLS-3GFP crk1^{AAA}-myc* (Hyg^R)	UMS1	This study
UMS189	*a1b1 fuz7^{DD} cut11-Cherry NLS-3GFP crk1^{AEF}-myc* (Hyg^R)	UMS1	This study
UMP248	*a1b1 pcl12^{crg1}*	FB1	This study
UMP249	*a1b1 pcl12^{crg1} cut11-Cherry NLS-3GFP*	UMP248	This study
UMS198	*a1b1 pcl12^{crg1} P$_{crg1}$:cdk1 cut11-Cherry NLS-3GFP*	UMP249	This study

32

UMS199	*a1b1 pcl12^{crg1} P$_{crg1}$:cdk1^{AF} cut11-Cherry NLS-3GFP*	UMP249	This study
UMS195	*a1b1 cdc25-HA*	FB1	This study
UMS196	*a1b1 fuz7^{DD} cdc25-HA*	UMN4	This study
UMS197	*a1b1 P$_{crg1}$:pcl12 cdc25-HA*	UMS151	This study
UMS200	*a1b1 wee1-HA*	FB1	This study
UMS201	*a1b1 fuz7^{DD} wee1-HA*	UMN4	This study
UMS202	*a1b1 P$_{crg1}$:pcl12 wee1-HA*	UMS151	This study
UMS173	*a1b1 fuz7Δ P$_{crg1}$:pcl12 cut11-Cherry NLS-3GFP*	UMS166	This study
UMS174	*a1b1 kpp2Δ P$_{crg1}$:pcl12 cut11-Cherry NLS-3GFP*	UMS167	This study

2. Growth media and conditions

2.1. General media and conditions

U. maydis strains were grown in yeast peptone (YP), complete medium (CM), or minimal medium with nitrate (MMNO$_3$). Carbon source (glucose (D) or arabinose (A)) were added to the media at a final concentration 1% unless specified. Liquid cultures were incubated at 28ºC with constant shaking at 250 r.p.m and under good conditions of aeration to a measured O.D$_{600}$ = 0.6 – 0.8 (exponential phase). For the mating experiments, strains were crossed on CM-charcoal plates containing CM medium, 2% agar and 1% activated charcoal, and incubated at 22ºC (Holliday, 1974).

For cloning purposes *E. coli* DH5α was grown at 37ºC in LB (Luria Broth) medium (Sambrook et al., 1989) supplemented with ampicillin at 100µg/ml.

2.2. Protoplasts regeneration and transformants selection

The protoplasts were regenerated in regeneration agar containing sucrose as carbon source. Hygromycin B (200 µg/ml), Carboxin (2 µg/ml), Nourseothricin (150 µg/ml), G418 (500 µg/ml) or Phleomycin (5 µg/ml) were used as antibiotic for the selection of transformant cells. Regeneration plates

were made with two agar layers in which the lower layer has double concentration of antibiotic and the top layer has only regeneration agar.

2.3. Inducible and constitutive promoters in *U. maydis*

For controlled expression of genes, the inducible promoter P_{crg1}, which is activated in presence of arabinose and repressed in the presence of glucose, and the inducible promoter P_{nar1}, which is activated in the presence of nitrate and repressed with ammonium found in CM or YP media were used. To perform induction experiments, cells were first grown in non-inductor medium until a cell density of OD_{600} ~ 0.6, washed three times with sterile water and then transferred to induction medium. To perform repression experiments, cells were grown in $MMNO_3$ until exponential phase and then were transferred to a repressive medium. Another inducible promoter used was P_{dik6}, which is activated in the presence of the bW-bE heterodimer (Flor-Parra et al., 2006b). For constitutive expression of genes, the P_{tef1} promoter was used.

3. Genetic methodology

3.1. Cloning and restriction mapping

E. coli plasmid DNA extraction, DNA restriction enzyme digestions, alkaline-phosphatase treatment and electrophoretic analysis were performed as described by Ausubel and colleagues (1997). Restriction enzymes were provided by New England Biolabs. Ligations were carried out using T4 DNA Ligase from Roche. DNA fragment isolation from TAE electrophoresis gels was done according to QIAGEN QIAquick Gel Extraction Kit. *E. coli* competent cells were transformed with either purified plasmids or ligation mixes by the heat shock method (Hanahan, 1983).

3.2. PCR reaction

PCR amplification was performed in a thermocycler machine. Mix and PCR program were adjusted in function of the DNA polymerase used. The elongation time was set according to the size of the amplified fragment and the

annealing temperature according to the oligonucleotides used. DNA polymerases used in this study were: Taq (own production), Expand Long Template (from Roche), Pwo (from Roche) and Velocity (from Roche). Reaction mix had 500nM of each oligonucleotide, 10ng DNA, 200µM of each dNTP, 5µl of 10x buffer and one unit of polymerase per 50µl of reaction volume. In high fidelity amplifications Pwo, Expand Long Template and Velocity DNA polymerases were used whereas for all other amplifications Taq was used.

3.3. Genomic DNA extraction

U. maydis genomic DNA was isolated by the glass bead method as described by Hoffman and Winston (1987) with a few modifications. Firstly, cells were grown overnight until they reached an $O.D_{600} \sim 0,8 - 1$ and then 1,5ml of the culture was spun down at 14000rpm for 2 minutes. After discarding the supernatant 500µl of lysis buffer (10mM Tris-HCl pH 8, 1mM EDTA, 100mM NaCl, 1% SDS and 2% Triton) and 500µl of buffered Phenol were added together with glass beads (Sigma). Cells were smashed in a Hybaid ribolyser set at speed 6 for 30". After lysis, the upper layer was transferred into a new eppendorf tube and 400 µl of isopropanol were added to precipitate DNA. Finally, after being centrifugated and air dried, DNA was resuspended in 50µl of distilled water by incubation at 70ºC with shaking for 10 minutes.

3.4. *U. maydis* transformation

U. maydis transformation was performed as described by Schulz and colleagues (1990). Log-phase cells (50 ml of culture at $O.D_{600} \sim 0.7 - 0.8$) were washed once with SCS buffer (20 mM sodium citrate [pH 5.8] –1M sorbitol buffer). Protoplasts were induced by resuspending the cells in 2 ml of the same buffer containing Novozyme328 (6mg/ml), and incubated with gently shaking at room temperature for 10-15 min (until cells became round). Following procedures were performed at 4ºC. The resulting protoplasts were centrifuged at 2500 r.p.m. for 5 min, washed twice with SCS buffer and once with STC buffer (10 mM Tris-HCl [pH 7.5]–1M $CaCl_2$–1M sorbitol buffer). Subsequently, the protoplasts were resuspended in 500 µl of STC buffer and stored in 50 µl

aliquots at -80ºC. All the solutions were prepared in Milli-Q water. The transformation was done on ice by first incubating 50µl protoplast suspension with 1µl heparin and 5 µl of linear DNA. After 40 min, 500 µl of STC containing 40% polyethylene glycol was added, and the sample was incubated for an additional 30 min on ice. Finally, the protoplasts were spread on two freshly prepared regeneration agar plates and grown at 28ºC until colonies formed.

4. Gene expression analysis

4.1. RNA extraction, cDNA synthesis and quantitative Real-Time PCR

Total RNA was extracted with acidic phenol solution followed by a chloroform: isoamyl alcohol (24:1) solution. After the extraction, the RNA was cleaned using the High Pure RNA Isolation Kit (Roche Diagnostics GmbH) and its content quantified with a NanoVue Plus spectrophotometer (GE Healthcare). For qRT- PCR, cDNA was synthesised using the High Capacity cDNA Reverse Transcription Kit (Applied Biosystems) employing 1 µg total RNA per sample. qRT-PCR was performed using the SsoAdvanced Universal SYBR Green Supermix (BioRad) in a CFX96 Real-Time PCR system (BioRad). The *U. maydis tub1* (*um01221*) gene was used as reference. Reaction conditions were as follows: 3 min 95ºC followed by 40 cycles of 10 sec 95ºC/10 sec 60ºC/30 sec 72ºC.

5. Protein analysis methods

5.1. Protein extraction

The cells from 5 ml cultures were collected, washed in the same volume of water and immediately resuspended in 1 ml of trichloroacetic acid (TCA) 20%. Then, the cells were centrifuged, the supernatant was removed and the biomass was weighed. Subsequently the pellets obtained were resuspended in 100 µl of TCA 20% and glass beads were added to rupture the cells in a FastPrep. Three pulses were given for 15 sec each and the tubes kept on ice for 1 min between runs. The cell lysate was collected, the glass beads were

washed with 200 µl of 5% TCA and the whole cell lysate was centrifuged for 5 min at 3000 rpm. After this, the supernatant was taken off and the pellet from sample with less biomass was resuspended in 100 µl of 2X Laemmli buffer (100mM Tris.HCl pH 6.8, 4% SDS, 200mM DTT, 20% glicerol and traces of bromophenol blue). The remaining samples were resuspended in 2X Laemmli buffer amount proportional to their biomass to equal the amount of protein present in all samples. Once resuspended the pellet with corresponding volume, half of this volume was added of Tris 2M and the samples were boiled for 5 min. Finally the samples were centrifuged at 13200 rpm for 5 min and the supernatants were collected into new tubes and frozen at -80ºC.

5.2. Western blotting

Protein extracts were separated on 4–15% Mini-PROTEAN® TGX™ precast polyacrylamide gels from Bio-Rad and run on Tris–HCl/Glycine/SDS (50mM/400mM/0.02%) running buffer with constant amperage. The proteins were transfered to an Inmobilon-P membrane (Milipore) using a Trans-Blot Turbo Transfer System also from Bio-Rad. The transfer was done at 0.2 mA for 30 min on transfer buffer (48mM Tris-HCl pH 7.5, 39mM glycine, 0.0375% SDS, and 20% metanol). The membrane was blocked for 1 hour with 10% milk in PBST. Primary antibody was followed by a secondary antibody conjugated to horseradish peroxidase and immunoreactive proteins were visualized using a chemiluminescent susbtrate. The chemiluminescent signal was detected using film developer (Kodak M35, X-Omat Processor).

5.3. Stripping for reprobing western blots

The primary and secondary antibodies were removed from the western blot membrane by stripping. The membrane was incubated with shaking at room temperature for 30 minutes in previously heated to 50ºC stripping buffer (2% SDS, 100 mM beta-mercaptoetanol, 50 mM Tris, pH 6.8). After incubation, the membrane was rinsed 3 times in PBST and finally blocked and blotted as normal.

6. Fluorescence-activated cell sorting (FACS)

Analysis of the cellular DNA content by flow cytometry was done according to the protocol described by Garrido and Perez-Martin (2003). Briefly, cells were fixed with 70% ethanol and then were treated with 0.025mg/ml RNAse A and 1mg/ml Proteinase K. Finally the samples were incubated with 16μg/ml propidium iodide to stain the DNA and were subsequently analysed with a Coulter XL machine.

7. Microscopy

Images were obtained using a Nikon Eclipse 90i fluorescence microscope with a Hamamatsu Orca-ER camera driven by Metamorph (Universal Imaging, Downingtown, PA). Images were further processed with Adobe Photoshop CS or ImageJ software.

7.1. Nuclear and septa visualization

U. maydis nuclear observation was done with strains that carried a *NLS-GFP* sequence or by staining the nucleus with a DAPI (4',6'-diamidino-2-phenylindole) solution prepared on PBS (Garcia-Muse et al., 2003a). Samples were prepared by air-drying 2μl of the culture on the microscope slide and later adding 1μl from a 1μg/ml DAPI solution. For the observation of the nuclear membrane a *cut11-Cherry* endogenous fusion was introduced in the cells (Perez-Martin, 2009).

Cell wall and septum were visualized after staining with calcofluor white. For the staining, cells ere mixed with calcofluor (0.2 mg/ml) directly on a coverslip.

7.2. *U. maydis* staining in planta

Chlorazole Black E (CBE) staining was performed as described (Brachmann et al., 2003). Infected leaf tissue was harvested from maize plants 1 to 9 dpi and cleared in ethanol overnight. The next day sample was washed in water before being treat with 10% KOH at 90% for 3–4 h. Samples were then

washed with water, incubated in CBE staining solution (0.03% Chlorazole Black E in a 1:1:1 solution of water, lactic acid and glycerol) at 60ºC overnight, and destained in 50% glycerol for at least one day.

8. Plant infections

Cultures of compatible strains were grown overnight in liquid medium. Cells were diluted to O.D.: 1 with water (around 10^7 cells/ml) and similar volumes of compatible strains were mixed (except for solopathogenic strains). The cells were centrifuged and resuspended with water in ½ of initial volume (i.e. to have around 10^7 cells/ml). Finally, 14-day-old maize plants (*Zea mays*) of the variety Early Golden Bantam (Olds seeds) were injected with 1 ml of cell suspension (around 10^7 cells per plant).

Pathogenic development of wild type and mutant strains was assayed as described (Kamper et al., 2006).

9. Analysis of appressoria

The *in vitro* system for inducing filaments and appressoria in *U. maydis* was applied as described previously (Mendoza-Mendoza et al., 2009). SG200AM and derivatives were grown in YEPSL (0.4% yeast extract, 0.4% peptone, and 2% sucrose) at 28ºC to an O.D$_{600}$ of 0.6 to 0.8. The cells were washed with water, resuspended in 2% YEPSL to an O.D$_{600}$ of 0.1 and supplemented with 100 mM 16-hydroxyhexadecanoic acid (Sigma-Aldrich). To quantify appressoria, cells were sprayed on ParafilmM and incubated at 100% humidity at 28ºC. After 16 h – 20 h the Parafilm M samples were rinsed with water and stained with calcofluor to visualize fungal cells. Using fluorescence microscopy, filaments expressing the AM1 marker that is expressed in cells forming appressoria were visualized by their GFP fluorescence, and the ratio of appressoria to filamentous cells was determined.

10. *Ustilago maydis* strains constructs

Plasmid pGEM-T easy (Promega) was used for subcloning and sequencing of genomic fragments and fragments generated by PCR. Sequencing of fragments generated by PCR was performed by DNA sequencing services at the University of Salamanca and analysed with standard bioinformatic tools (ApE-a plasmid editor and Stryder). pJET1.2/blunt (Thermo Scientific) was also used for subcloning. Gene replacement into the corresponding loci was verified by diagnostic PCR and in some cases also by RT-PCR.

To generate the different strains, the constructs detailed below were used to transform protoplasts. The integration of the plasmids into the corresponding loci by homologous recombination was verified by diagnostic PCR. Oligonucleotides used to perform the constructs appear on the figures in black and those used to check the correct insertion in red. Oligos are detailed in table 3.

10.1. Deletions

Deletion of each gene was performed using PCR-based gene targeting (Brachmann et al., 2004). Briefly, a pair of DNA fragments flanking the corresponding kinase ORF were amplified and ligated to antibiotic resistance cassettes via *Sfi*I sites. The 5′ and 3′ fragments were amplified with specific oligonucleotide pairs using FB1 genomic DNA. Each flanking fragment was about 1 kb in length.
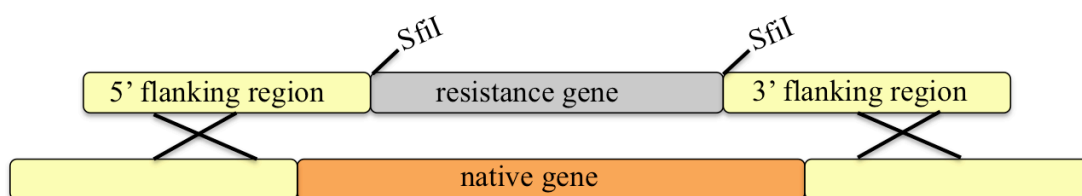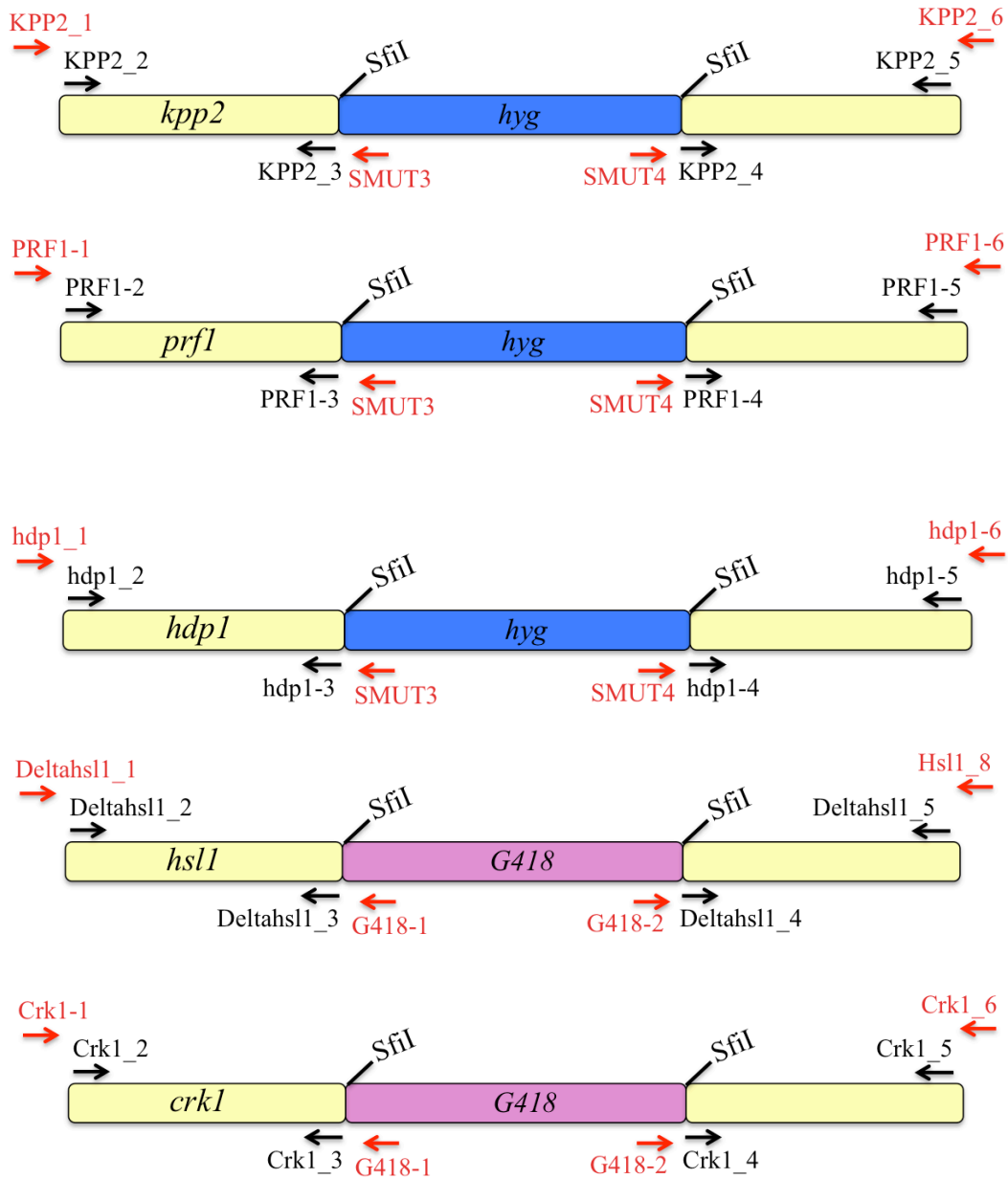
Figure 9: Schematic representation of the deletion cassettes of *kpp2*, *prf1*, *hdp1*, *hsl1*, *crk1* genes.

10.2. Construction of Hsl1-3GFP protein fusion

To construct the *hsl1-3GFP* allele, a 1-kb C-terminal fragment of *hsl1* ORF excluding the stop codon with the primer set hsl1_2/hsl1_3, and a 1-kb flanking downstream region of *hsl1* with the primer set hsl1_4 /hsl1_5 were amplified. Both fragments were digested with SfiI and ligated to the 3GFP-hyg

41

cassete isolated as SfiI fragment from plasmid pMF5-3n. The ligation product was cloned into pGEM-T yielding phsl1-3gfp-hyg. This plasmid was digested with PacI and introduced by homologous recombination into the *U. maydis* genome. Transformants were checked by PCR using the primers hsl1_1 and GFP1 for the left border (~1.1 kb fragment) and hsl1_6 and SMUT4 for the right border (~1.1 kb fragment).

10.3. Substitution of the *hsl1* native promoter by the P*tef1* constitutive promoter

To generate the plasmid pPtef1hsl1, two fragments were amplified from genomic DNA. The left flank, a *hsl1* promoter fragment, was obtained using primers Hsl1Ptef_2 and Hsl1Ptef_3 and the right flank, a N-terminal fragment, using primer combination Hsl1Ptef_4 and Hsl1Ptef_5. The PCR N-terminal fragment was cloned into pGEMT-T and sequenced for accuracy. The plasmid was digested with NdeI and KpnI and the left flank with KpnI and EcoRI. The two fragments were ligated into the NdeI and EcorI sites of pCU3 plasmid. The resulting plasmid was digested with KpnI and integrated by homologous recombination into the *hsl1* locus. To check the correct insertion, Hsl1Ptef_1 and Cbx2 for left border (~1.5 kb) and Hsl1Ptef_6 and Ptef for right border (~1.3 kb) were used.

10.4. AM appressorium-marker strains

To generate strains AM, which carry an appressorium-specific GFP-reporter construct in the *carboxine* locus, the upstream region of the um01779 gene was amplified using the um01779SfiI and um01779NdeI primers. The PCR amplified fragment of ~1.2 kb was cloned into pGEM-T and sequenced. The resulting plasmid was digested with NdeI and SfiI, and ligated to a NdeI-SfiI fragment of pCU3 containing 3GFP Cbx^R. The plasmid pCU3SfiIum01779NdeI was linearized with SspI prior to transformation of *U. maydis* strain SG200 and its derivatives. Transformants were checked by their carboxine resistance and by PCR amplification with um01779SfiI and gfp-1 primers (PCR product of ~1.3 kb).

10.5. pRU11 *fuz*^{DD} Nat^R

The *nourseothricin* (Nat) gene was obtained by digestion of the pUMa262 plasmid with NotI enzyme and inserted into pRU11fuz-1 NotI site in opposite direction of *crg1* promoter. The resulting plasmid was cut with SspI and integrated by homologous recombination into the *carboxine locus*. The transformants were checked by their nourseothricin resistance and with the primer set pcrg1/Fuz7 4 (PCR product of ~0.8 kb).

10.6. T7-Pcl12 protein fusion overexpression

The pcl12 expression vector was constructed by amplifying the entire *pcl12* ORF in two separated fragments. For amplification of the first fragment (~0.6 kb) in which the ATG start codon was exchanged with a BamHI site, T7pcl12_A1 and T7ORFpcl12_2 primers were used. For amplification of second fragment (~1 kb), which includes STOP codon, T7ORFpcl12_3 and T7ORFpcl12_4 primers were used. PCR products were cloned into pGEM-T and sequenced. The end of the first fragment possesses an overlap to the beginning of the second fragment, an EcorV restriction site, which allows them to ligate and originate entire ORF. The plasmid was digested with BamHI and EcoRI and *pcl12* ORF was ligated to a 7.8 kb BamHI-EcoRI fragment of pRU11T7. Pcl12 is in the same translational phase as T7 epitope via BamHI and under the control of P*crg1*. The resulting plasmid PRU11T7ORFpcl12 was digested with SspI and introduced by homologous recombination into the *carboxine* locus. Transformants were checked by their carboxine resistance and by PCR amplification with pcrg1 and T7ORFpcl12_4 primers (PCR product of ~1.7 kb).

10.7. *crk1-myc*, *crk1*^{AF}*-myc* and *crk1*^{AAA}*-myc* alleles under control of their own gene promoter

Plasmids pRU11-Crk1AEFmyc and pRU11-Crk1AAAmyc contain mutant *crk1*^{AAA} and *crk1*^{AEF} alleles, respectively, each tagged with three copies of the

myc *epitope*. These plasmids were digested with NdeI. Following treatment with T4 DNA polymerase to create blunt ends, were cut with AflIII. Obtained fragments of 3.7 kb were ligated to a ApaI (blunt ended)-AflIII fragment of 7.2 kb, containing the terminator region of *crk1*, from pCrk1-3GFP-hyg. Resulting plasmids pCrk1AEFmyc-hyg and pCrk1AAAmyc-hyg were cut with AhdI and PacI and introduced by homologous recombination into the *crk1* locus of *U. maydis*. CRK1-6/SMUT4 primer set was used to check right border and IMEA / HA/myc primer set to check left border. PCR product obtained from left border (4.1 kb) was digested with EcoRI to check whether *crk1* harbours the *AF* point mutations, resulting in three fragments of 2.6 kb, 1.2 kb and 0.4 kb. PCR product from left border was digested with SacII (2.3 kb and 1.8 kb) and XhoI (2.6 kb, 0.8 kb, 0 .38 kb, 0.35 kb and 0.083 kb) to check whether *crk1* harbours the *AA* point mutations. Transformants, whose left and right borders were amplified by PCR but did not harbour point mutations, were selected as control (*crk1-myc* allele).

Table 3: Oligos used for constructs and check colonies.

Name	Sequence 5'-3'
Bleo1	GTGTCCGGTGCATTTCGCCTTCTCGGCG
Bleo2	AAACCTCGAAATCATTCCTACTAAGAT
CBX1	TCTGGGTTTCGCGAGAGATCTCACAGAGCA
CBX2	AATTGCACAGATCAAGAAGGACATGGCCGT
Pnar	GGTGAATAGTGAGAACAGTCTCGATCACTCTG
SMUT3	ATTCACGTTTTGTAGCACACGACTCACATC
SMUT4	CACCACCCAATCGACGCGGAAGGCAACCCA
GFP1	ACGCTGAACTTGTGGCCGTTTACGTCG
CRG1	GAGATCACGACACCGCGAGGTTTGCGGTGA
PTEF-1	GGCGCAAGAAAATTTTTCTCTGGTTCTG
G418-1	GCTCGGTACGGGTACATCGGATCTGCCGGC
G418-2	CTTGAGAAGGTTTTGGGACGCTCGAAGGCT
DIK6-1	AAGCATATATACCCGGCCTTCTTGCTC
HA/MYC	TCGCAAGACCGGCAACAGGATTCAATCTTA
Cherry123-2	TGATCACTTGTACAGCTCGTCCATGCCGCG
KPP2-1	AGATGCCCATCATCCACAGCGAATCCT
KPP2-2	ACTTAATTAATAGTGCAGGCTTGAAGCCGAAAGATTC

KPP2-3	GGTGGCCATCTAGGCCCTTGGTTGGGTCTTTCTAGCCAGATAG
KPP2-4	ATAGGCCTGAGTGGCCTCTTGCGCCGATTTCTGCCGAATTCGCT
KPP2-5	TGTTAATTAAGCCTCAACTCTAAGGCGACTGTCGGAC
KPP2-6	GAGTCGCTCTTCATTCGACGACCTTCG
PRF1-1	GCAAAGCTTTGCAGTCGTTCGCAAGCC
PRF1-2	ACTTAATTAATTGGTGTAACTAAGTTAGCGCAGATCT
PRF1-3	GGTGGCCATCTAGGCCGGTGAGCACGACTTTGCCTTAGAAGCA
PRF1-4	ATAGGCCTGAGTGGCCTTGTCTTTCACACAAATCTCCTTTTTC
PRF1-5	TGTTAATTAAATTGTGTTGGATGAGTATAAACGATCG
PRF1-6	AGGTGGTGCTTCGGGCCGCGAACCACT
hdp1_1	CTCTAGCGTGCGGTAACCCCCCTGTGT
hdp1_2	ACTTAATTAAAGCGTTGATGACCAACATAGCCATTCA
hdp1_3	GGTGGCCATCTAGGCCTTTCAACTCGCTTGATCGCAGCAACGG
hdp1_4	ATAGGCCTGAGTGGCCCTCACTCTGCCGTGTTGGCAACGCAGC
hdp1_5	TGTTAATTAAGCAGTGGTTGAAGAGGTACTGGGATCA
hdp1_6	AAGCGCAACCGCATCGACAAGCCTATT
hsl1_1	TTGCTCCTTTGGCACTGACGGACAAGT
hsl1_2	ACTTAATTAAGGTTCGAAGCGCACGATCTGGCACTGA
hsl1_3	GGTGGCCGCGTTGGCCATGATAGCCGAGCCAAGGTCGAGCATC
hsl1_4	ATAGGCCTGAGTGGCCGCTCGGAGCTTGTCCTCATGTCACTCT
hsl1_5	TGTTAATTAACTTCCGAAACAGAAAGAAACCATCACA
hsl1_6	CTCGTCACTTGTCGGCGCAAGCCGTGT
Crk1-1	AAATCGTGAATCGTGAAACATGAATCA
Crk1-2	ACTTAATTAATCCATTGGATTGGCATAATCACACATC
Crk1-3	GGTGGCCATCTAGGCCGGCGGCAGGCAAGCGCAACACGTCGTG
Crk1-4	ATAGGCCTGAGTGGCCTCATCGATGATCTCGCATTCTACCTTC
Crk1-5	TGTTAATTAAAGATAGAAGATGAGTGGGGCGCCGAGC
Crk1-6	TTCGGTTTCGGACGATCGGATCAAGTT
CRK1-6	CTCGAGTCTTCATCGACGGTTAAAGTGCGA
IMEA	GCTCATTAGCAACTTGCTTTTTAACTTGAT
Hsl1Ptef_1	TTTCAGTAGCACCAATACTTGGAATAC
Hsl1Ptef_2	ACCGGTACCTTCCGACACGCAGCTTAACTAGGCTGG
Hsl1Ptef_3	GGTGAATTCGTGTGTAGTCAACGTTGGCAAACGCGA
Hsl1Ptef_4	ACCCATATGTCTTCCTCGCAACGCCCCGTGGTG
Hsl1Ptef_5	GTTGGTACCTTCCGCTGACGATCTCGGGACTGGCGT
Hsl1Ptef_6	CGGCAGACGTCCGCAGAGAAGCGCGAA

um01779SfiI   CACGGCCCATGCGGCCCTCGAGCCTCGTCCCT

um01779NdeI   GACCATATGCTTGAGCGAAGGTTTACCTTGAG

T7pcl12_A1   ACCGGATCCGCTACCACCGTCGCTTCTACATACACT

T7pcl12_A2   TTGGAATTCTCAGCGGCTTCCGTCGACATCCTGCACAAG

T7ORFpcl12_2   GTAGATATCGTCACAACTGCTCTTGCTAGCGATCAA

T7ORFpcl12_3   GACGATATCTACTCGAACAAGAGCTGGGCCATCGTG

T7ORFpcl12_4   TTGGAATTCTCACGACCTCCAGCTGTAAGGTTGCAG

Fuz7DD-check   ACCTATCTCTTTTATCTGTGCCGCCCGTAA

Fuz7 4   TGTACCAACAAAGTCTGCTGCAATGTCGTTGATGAGCTC

hsl1-8 new   GTCATCGTATGATTCACGACTCGCTCG

hsl1-17 new   TTGATCTGTCATCCGTTTCATAACTTG

orfhsl1-3B   TTCTTCCAAGAGATCGCCGACGAGCTC

Deltahsl1_1   CTGGTCCTGGCAAGCACAAGACGAGCT

Deltahsl1_2   ACTTAATTAAACGAGAAAGCTGTGCTGTTTGCAATGT

Deltahsl1_3   GGTGGCCATCTAGGCCGATCGAAGCTCTGCCCAAAGCTCCAGA

Deltahsl1_4   ATAGGCCTGAGTGGCCGCTCGGAGCTTGTCCTCATGTCACTCT

Deltahsl1_5   TGTTAATTAAGAGGTGAACCCCTTCGACTTTCTTCCC

Table 4: Oligos used for quantitative RT-PCR.

Name	Sequence 5'-3'
TUB RT1	CGA GAT GAC CTT CTC GTC GT
TUB RT2	AAC ATC ACC ACG GTA CAG CA
Crk1 RT 1	CGC AAG CAA CGA AAC TAT CA
Crk1 RT 2	CTA CTT CCA GCA AGC GTT CC
CLB1_RT_1	CGA TCT CAC AAA CGC CAA C
CLB1_RT_2	ATG TAG AAG CCG AGG TGG TG
CLB2_RT_1	GTG ACA AGG TCA CGC ATC AG
CLB2_RT_2	TTG CCA GAT GAC TTG TGG AG
WEE1_RT_1	CAC ATG CCT ACC ACA ACT CG
WEE1_RT_2	CGA AGA AAA GGC ATG AGA GC
CDC25_RT_1	AGC ACC ACC ACC AAT ACC TC
CDC25_RT_2	GAG ACC ATG AGG ACG CGT AT
HSL1_RT_1	ATC ACG CTT CAC AAC GAC AG
HSL1_RT_2	CTC CCT CTC TAG ACG CGA TG

46

PLK_RT_1	CAC CAT TGC TTC AAA ACA GC
PLK_RT_2	AGG TGG CAG GGT AGG TTT CT
BMH1_RT_1	ACA TCC TCG ACG TTT TGG AC
BMH1_RT_2	GCG AGG TAT CGG TGG TAG TC
HDP1 RT 1	CAG GAG CAG GAG ATT GCT CT
HDP1 RT 2	GAA ACA CCA AGT TGG AAG C
Cln1 RT1	GAT TTT GGC ACG CTT CAT TT
Cln1 RT2	CTT GAA GGT TCT CCC AGA CG
Pcl4 RT 1	GTT CCT CGA CGA CCA CAC TT
Pcl4 RT 2	GAG CCA AAA TTC GAT CTC CA

Results

b-induced G2 cell cycle arrest in *Ustilago maydis*

1. The induction of the expression of *b* genes resulted in specific down-regulation of the gene encoding the Nim1-like kinase Hsl1

Previous research in *U. maydis* has shown that efficient cell cycle arrest during the infective filament formation requires the cooperation of elements from the DNA Damage Response (DDR) cascade, such as the kinase Chk1 and its upstream activating kinase Atr1 (de Sena-Tomas et al., 2011; Mielnichuk et al., 2009; Perez-Martin, 2009). During the early stages of formation of the infective hypha, the Chk1 kinase is activated for a short period of time, resulting in a transient G2 cell cycle arrest (Mielnichuk et al., 2009).

We hypothesized that the activation of the DDR cascade provides a time frame during which additional mechanisms are recruited to sustain a long-term cell cycle arrest. Our rationale was that the additional elements required for sustained cell cycle arrest during the formation of the infective filament might be cell cycle regulatory genes, whose transcriptional levels may be affected by the b-dependent transcriptional program. However, caution should be exercised when analyzing the expression of cell cycle genes because the transcription of cell cycle genes is linked to an active cell cycle, and then down-regulation of these genes could be merely a consequence and not a cause of the b-induced cell cycle arrest.

To overcome this problem, we analyzed the expression of genes encoding G2/M regulators in conditions of *b*-expression and non-arrested cell cycle. To achieve this, we took advantage of a *U. maydis* strain that expresses simultaneously the genes encoding the b-factor as well as an ectopic Cdk1 allele refractory to inhibitory phosphorylation at Tyr15 (*cdk1^{AF}*), the ultimate cause of the b-induced G2 cell cycle arrest (Mielnichuk et al., 2009; Sgarlata and Perez-Martin, 2005b). In this strain, in spite of the activation of the b-dependent transcriptional program, the cell cycle is not arrested (Garcia et al., 2009).

To express the b-factor, we used the haploid *U. maydis* strains AB33 and AB34 that harbor the compatible *bE1* and *bW2* and non-compatible *bE1* and *bW1* genes respectively, both under the control of the nitrate-inducible *nar1* promoter (Brachmann et al., 2001). Induction of *bE1/bW2* in the compatible

strain growing in medium with nitrate results in a filament that resembles the infectious hypha formed after fusion of compatible haploid cells. The *cdk1* alleles (mutant and wild type as a control) were also expressed under the *nar1* promoter, to induce both classes of genes (the b-factor encoding genes and *cdk1* alleles) simultaneously.
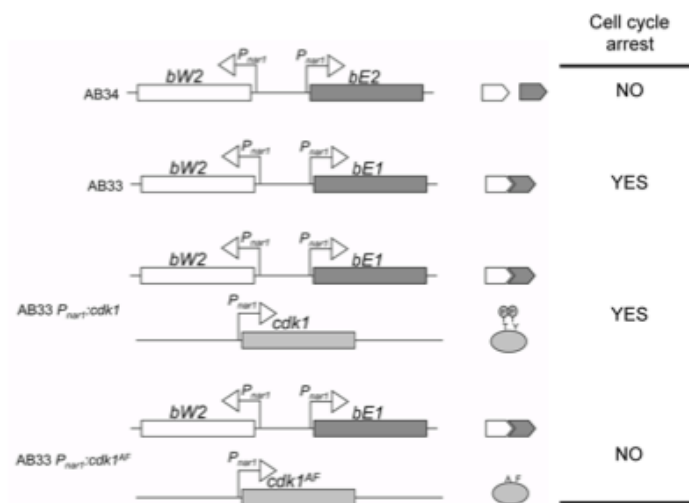

Figure 10: Scheme showing the constructions inserted in order to generate AB34, AB33, UMC19 (AB33 *P$_{nar1}$:cdk1*) and UMC20 (AB33 *P$_{nar1}$:cdk1^{AF}*) strains and their expected cell cycle outcome.

We included in our transcriptional analysis well characterized *U. maydis* G2/M regulatory genes such as the B-cyclins *clb1* and *clb2* (Garcia-Muse et al., 2004), the *wee1* kinase (Sgarlata and Perez-Martin, 2005b), and the *cdc25* phosphatase (Sgarlata and Perez-Martin, 2005a). We also included genes putatively encoding G2/M regulators, whose transcriptional levels were altered upon b-expression in a recent wide-genome transcriptomic analysis (Heimel et al., 2010). These regulators included um03234.2, encoding a homolog to the Polo kinase, and renamed Plk1, as well as um03928, encoding a Nim1-like kinase, and renamed Hsl1.

We found that for all the analysed genes, the levels of mRNA decreased upon *b*-induced cell cycle arrest. However, in general, this decrease seems to be a consequence of the cell cycle arrest: interference with the *b*-induced cell cycle arrest upon expression of the *cdk1^{AF}* allele prevented the decrease in the mRNA levels in all but one case (Fig. 11). The only exception was observed for *hsl1*, the gene encoding a putative Nim1-like kinase. In this case, the levels of

mRNA decreased upon b-factor expression, regardless of whether cell cycle was or not arrested. Therefore, we considered that *hsl1* could be a prime candidate for our study.
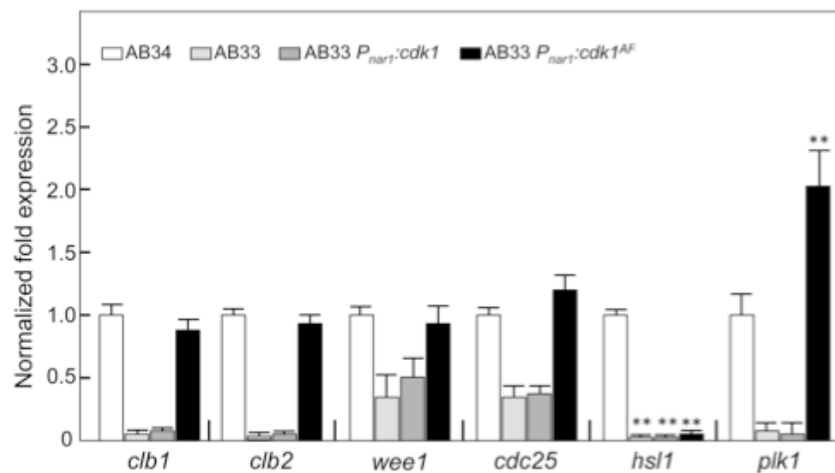

Figure 11: Quantitative real time-PCR for the indicated genes in the different strains. RNA was isolated after 6 hours of induction of *nar1* promoter. As internal control the expression of *tub1* (encoding Tubulin α) was used. Values are referred to the expression of each gene in AB34. Each column represents the mean value of four independent biological replicates. Error bars represent the SD; **p<0.01 based on a two-tailed Student´s *t*-test to control sample (AB34).

2. The Hsl1 kinase is a G2/M cell cycle regulator in *U. maydis*

The Nim1 family of kinases is composed of several serine/threonine kinases that act as negative regulators of Wee1, the mitotic inhibitor responsible for the Cdk1 inhibitory phosphorylation. In *S. cerevisiae*, this family is composed of three kinases, Hsl1, Kcc4 and Gin4 (Barral et al., 1999), whereas in *S. pombe* this family is composed of two members, Nim1/Cdr1 and Cdr2 (Coleman et al., 1993; Feilotter et al., 1991; Kanoh and Russell, 1998; Wu and Russell, 1993). A sequence similarity search using the annotated genome of *U. maydis* indicated that Hsl1 seems to be the single component of this family (Fig. 12).
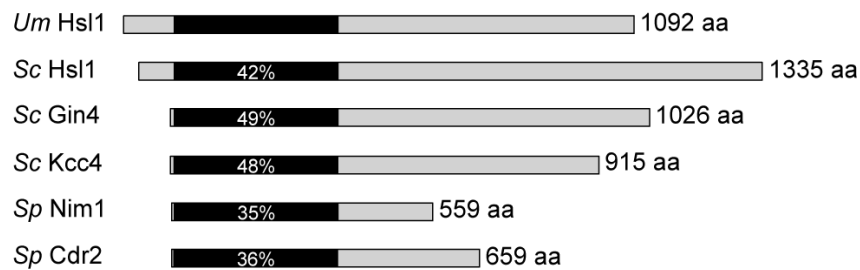
Figure 12: Alignment of *U. maydis* Hsl1 and orthologs from *S. cerevisae* and *S. pombe.*

The preliminary characterization of Hsl1 in *U. maydis* had been performed previously in the laboratory and indicated that mutant cells of *hsl1* are more elongated than wild type cells as it can be observed in the figure 13.
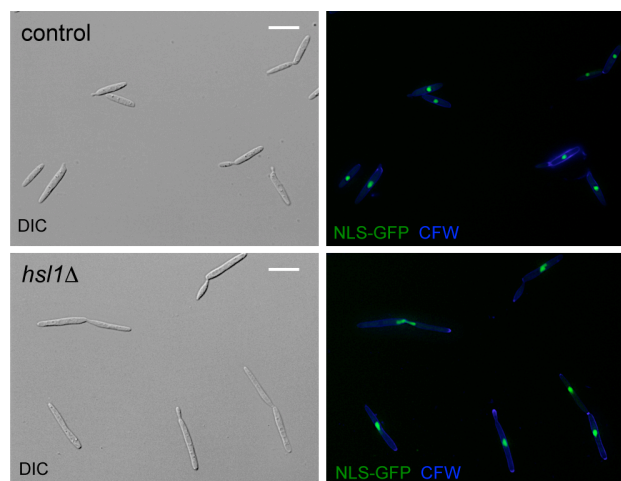

Figure 13: Cell morphology of control (UMI194) and *hsl1*Δ (UMS60) cells during exponential growth in CMD liquid cultures. Cells carried a constitutively expressed NLS-GFP reporter to detect nuclei and were stained with Calcofluor White (CFW) to detect septa. Scale bars: 15 µm.

It was also found that for some proportion of the population (variable, depending on growth conditions), cell separation was delayed resulting in cell chains composed of two or three cells. The elongated cell phenotype in *U. maydis* has been related to an enlargement of the G2 phase (Pérez-Martín and Castillo-Lluva, 2008). To address whether this was the case in *hsl1*Δ mutants, the DNA content of wild type and *hsl1*Δ mutant cells was studied using FACS analysis. Since in *U. maydis* the length of the different cell cycle phases is adapted to nutritional conditions (Garrido and Perez-Martin, 2003), three

different growth media were used. Control cells growing in minimal medium (MMD) showed a prominent peak at G1 (1C DNA content), which decreased as the quality of the medium increased (from complete medium, CMD, to rich medium, YPD). Interestingly, *hsl1Δ* mutant cells showed an unaltered pattern in all media, consisting in an accumulation of cells carrying a 2C DNA content. In *S. pombe*, the absence of Cdr2, one of the Nim1-lke kinases, also resulted in lack of cell cycle adaptation to nutritional conditions, defect that is exacerbated in the double *nim1* and *cdr2* mutant (Kanoh and Russell, 1998).

We investigated the localisation of Hsl1 in *U. maydis*. For this purpose, an N-terminal triple fusion of GFP to Hsl1 was generated. The resulting strain, UMS52, was grown in CMD until mid-exponential growth. Cells had a wild type appearance indicating that the fusion protein was functional. We found that, as it was described for Nim1-like kinases in *S. cerevisiae*, in *U. maydis* an Hsl1 locates at the bud neck, which is consistent with roles in cell separation (Fig. 14).
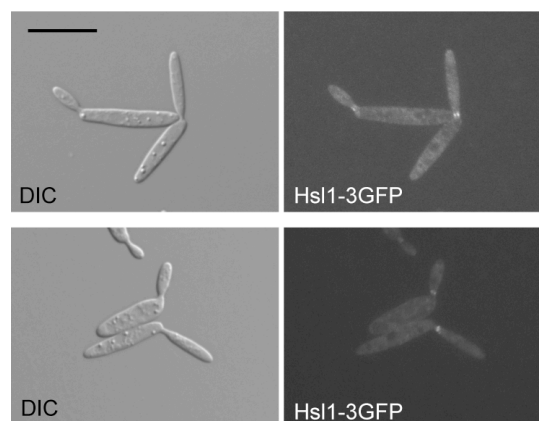

Figure 14: Hsl1 localizes to the bud neck. Wild type cells carrying a Hsl1-3GFP protein fusion. Scale bar: 15 µm.

Although the accumulation of cells with 2C DNA content in the *hsl1Δ* strain can be consistent with an increase of cells in G2 phase, it is worth mentioning that this strain showed cell separation defects; therefore, a part of the 2C population could be doublets of G1 cells. To circumvent this problem we took advantage of previous studies showing that the mitotic cyclin Clb2 is synthesized during G2 phase and degraded at anaphase, providing a reliable marker of G2 phase (Carbo and Perez-Martin, 2010). Wild type and *hsl1Δ* cells carrying a *clb2-GFP* fusion at its native locus were scored as being in G2 phase

or not, based on the presence or absence of a nuclear GFP signal, respectively. We have observed a dramatic increase in the number of cells showing Clb2-GFP signal in the *hsl1Δ* mutant strain with respect to the wild type strain (Fig. 15). Therefore we can conclude that the absence of Hsl1 leads to an increase of cells in G2 phase.
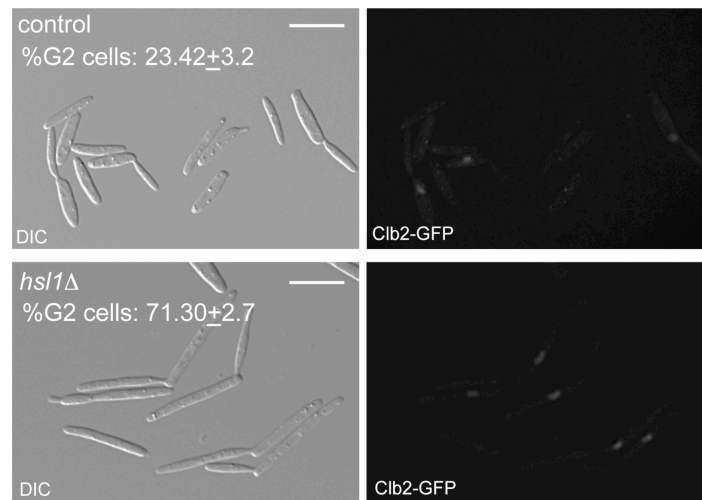

Figure 15: Control (UMA88) and *hsl1Δ* (UMS59) cells expressing the G2 marker Clb2-GFP. Cells were incubated in CMD until mid-exponential phase. The numbers at the corner indicate the percentage of cells in G2 phase as scored for the presence of Clb2-GFP signal (100 cells per experiment, 2 independent experiments). Scale bars: 20 μm.

Nim1-like kinases are negative regulators of Wee1 kinase in *S. cerevisiae* (McMillan et al., 1999; McMillan et al., 2002) as well as in *S. pombe* (Coleman et al., 1993; Wu and Russell, 1993). Since Wee1 acts as a mitotic inhibitor in cells lacking these kinases, the G2/M transition is delayed resulting in an prolongation of G2 phase and as a consequence a cell elongation phenotype. These effects can be suppressed by mutations that disable the Wee1 kinase (Barral et al., 1999; Kanoh and Russell, 1998). We have observed that in a similar way, down-regulation of *wee1* expression using a conditional *wee1^nar1* allele (Wee1 is essential in *U. maydis*) suppressed the cell elongation phenotype of *hsl1Δ* cells (Fig. 16). In *S. cerevisiae*, the Nim1 family of kinases collaborates through a still unclear mechanism to the degradation of Swe1 (Sia et al., 1998; McMillan et al., 2002; King et al., 2012). In contrast in *S. pombe,*

Nim1 and Cdr2 kinases seem not to affect the protein levels of Wee1 but they inhibit its activity (Coleman et al., 1993; Wu and Russell, 1993; Kanoh and Russell, 1998). We have found that for *U. maydis* the absence of Hsl1 resulted in a increase in the levels of Cdk1 inhibitory phosphorylation. However, the levels of Wee1 protein in these mutant cells seemed to be similar to those observed in control cells (Fig. 17). Also, consistent with a role of *U. maydis* Hsl1 as a Wee1 negative regulator, previous results indicated that the levels of Cdk1 inhibitory phosphorylation are higher in *hsl1*Δ cells (Fig. 18).

In summary, our data reinforces Hsl1 as a *bona fide* Nim1-like kinase, thus acting as a G2/M regulator.

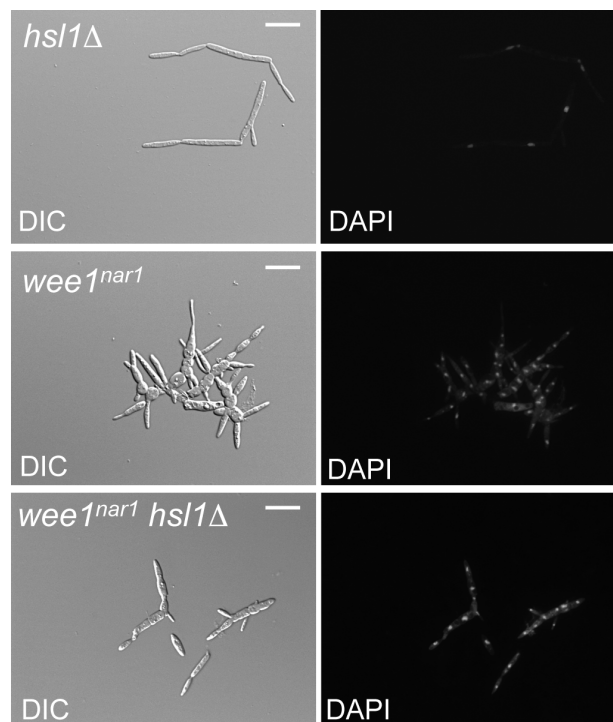**Figure 16: Epistatic analysis of *hsl1* and *wee1*.** The single mutant *hsl1*Δ (MUM1) and *wee1*^nar1^ (UMC23) as well as the double *hsl1*Δ *wee1*^nar1^ (UMS61) mutant strains were grown in restrictive conditions to allow *nar1* expression (YPD) for 8 h. Note that the phenotype of the double mutant in these conditions is similar to the phenotype of the *wee1*^nar1^ cells. Scale bar: 15 μm.
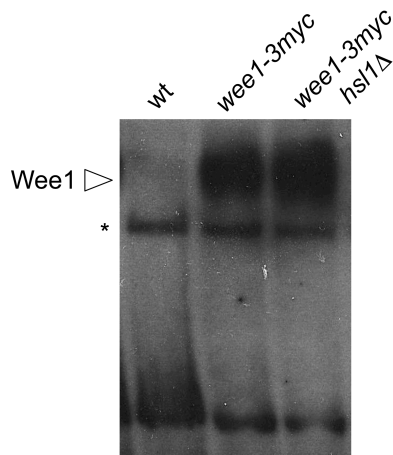
Figure 17: Levels of Wee1 in *hsl1Δ* mutants. FB1 (wt) cells and derivatives carrying the allele *wee1-3myc* were grown in CMD until mid-exponential phase. Whole cell extracts from these cultures were obtained and submitted to Western blotting with antimyc antibodies. The star symbol indicates a non-specific band.
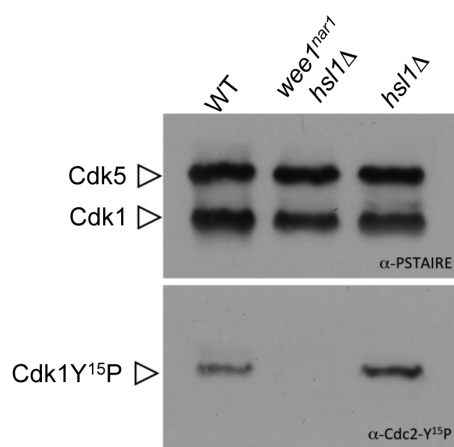

Figure 18: Tyrosine phosphorylation of Cdk1 in cells lacking Hsl1. Protein extracts from the strains indicated (FB1: wt; UMS61: *hsl1*D *wee1^{nar1}*; MUM1: *hsl1Δ*) were obtained after 8 h of incubation in YPD media. A similar amount of protein (around 150 µg) was submitted to Western blotting with antiphospho-Cdc2 (Tyr15). The membrane was then stripped and probed with anti-PSTAIRE antibodies, which recognizes Cdk1 as well as Cdk5, a second CDK from *U. maydis*.

3. *hsl1* down-regulation and Chk1 activation collaborate in b-induced cell cycle arrest

The previous results indicated that the down-regulation of *hsl1* mRNA levels seems to be an effect of the induction of the transcriptional *b*-program and not a consequence of the cell cycle arrest. In addition, the deletion of *hsl1* in haploid cells growing in axenic conditions produced a G2 cell cycle delay. These results fitted in our initial reasoning by which additional mechanisms are recruited to sustain a long-term cell cycle arrest during the infective filament formation, and these mechanisms are most likely related to b-dependent transcriptional changes of regulatory genes needed for G2/M transition. In consequence, we wondered whether the down-regulation of *hsl1* expression upon *b*-induction is responsible for the observed cell cycle arrest.

The b factor seems to activate a cascade of transcriptional regulators downstream (Heimel et al., 2010; Pérez-Martín, 2012). A previous study has

found that Rbf1, a transcriptional regulator located immediately downstream of b-factor, is required for *hsl1 b*-dependent down-regulation as well as for *b*-induced cell cycle arrest (Heimel et al., 2010). Moreover, inactivation of Rbf1 resulted in no filament formation. As previously reported (Heimel et al., 2010), we found that in a wild type strain overexpressing *rbf1,* the *hsl1* mRNA levels were dramatically decreased (Fig. 19A). We sought for two additional regulators that were located downstream of Rbf1: Biz1 –a previously characterized transcription factor (Flor-Parra et al., 2006a)– and Hdp1 –an homeodomain-containing protein. We ectopically overexpressed the genes encoding the regulators Biz1 and Hdp1 in a wild type strain. We have found that while *biz1* overexpression had no effect on *hsl1* mRNA levels, overexpression of *hdp1* resulted in a down-regulation of *hsl1* (Fig. 19A). However, we observed that in a strain ectopically expressing the b-factor but lacking *hdp1*, the *hsl1* mRNA levels were still downregulated (Fig. 19B). All these data gathered suggest that additional layers of complexity, including redundant pathways, are responsible for the *hsl1* down-regulation.
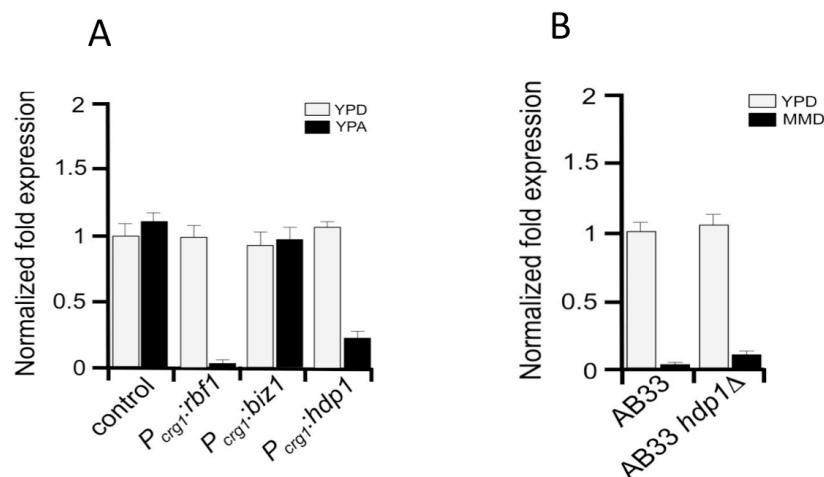

Figure 19: Hdp1 is sufficient but not necessary to down-regulate *hsl1* expression: (A) overexpression of *rbf1*, and *hdp1* but not *biz1* results in lower levels of *hsl1* mRNA. FB1 cells (control) were transformed with an integrative plasmid carrying the *rbf1*, *biz1* or *hdp1* genes under the control of *crg1* promoter. The plasmids were integrated at the *cbx1* locus. The resulting strains were grown in YPD (repressive conditions for *crg1* expression) or YPA (induction conditions for *crg1* expression) for 8 hours. The expression of *hsl1* in FB1 cells (control) growing in YPD was used as a reference to calculate the normalized fold expression. As internal control, the expression of *tub1* (encoding Tubulin α) was used. **(B)** Hdp1 seems to be dispensable

for b-mediated down-regulation of *hsl1* expression. AB33 cells and its derivative lacking the *hdp1* gene (UMS65) were grown for 6 hours in YPD (no expression of *b* genes) or MMD (expression of *b* genes). The expression of *hsl1* in AB33 cells (control) growing in YPD was used as a reference to calculate the normalized fold expression. As internal control, the expression of *tub1* (encoding Tubulin α) was used.

Since our attempt to prevent the downregulation of *hsl1* by removing downstream transcription factor was unsuccessful, we opted to circumvent the down-regulation of *hsl1* by exchanging the native *hsl1* promoter with the *tef1* promoter (which renders the *hsl1^{tef1}* allele). This promoter was selected because its expression was refractory to inhibition by the b-dependent transcriptional program and it was able to produce roughly similar transcriptional levels as the native *hsl1* promoter does in minimal medium as well (Fig. 20).

To address the effect of sustained transcription of *hsl1* mRNA during the induction of the infective filament, we introduced the *hsl1^{tef1}* allele into the UMP112 strain. This strain is derived from AB33 and it carries a GFP fusion to a nuclear localization signal under control of the *dik6* promoter. Because the expression of *dik6* promoter is dependent on an active b heterodimer (Brachmann et al., 2001), this strain allowed us the use of the nuclear fluorescence as a marker of the release of cell cycle arrest (counting the nuclear content of the filaments) as well as a surrogated marker of the ability of the different mutants to respond to the *b*-program. In addition, to analyse the possible joint contribution on cell cycle arrest of *hsl1* down-regulation and the activation of the DDR pathway, we have also combined the *hsl1^{tef1}* allele with the deletion of *chk1*. In first place, we observed that for filaments carrying the *hsl1^{tef1}* allele, the content of *hsl1* mRNA was maintained at a high level upon b-factor induction (Fig. 20), bypassing the above described b-dependent transcriptional down-regulation. Secondly, we have found no difference in the proportion of cells responding to b-factor in the different mutant backgrounds. Even at short times upon induction of *b* expression (4 h), almost the whole cell population showed nuclear fluorescence, indicating that there were no interferences with the *b*-induced transcriptional program.
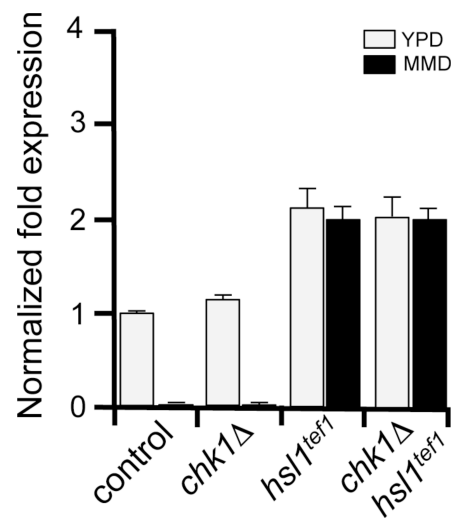
Figure 20: Bypassing *hsl1* down-regulation upon induction of the b-transcriptional program. The *hsl1* locus was exchanged with a transgene in which *hsl1* is under the control of *tef1* promoter. As a consequence, *hsl1^{tef1}* is expressed in a constitutive manner regardless the b program is active (MMD) or not (YPD). Strains UMP112 (control), UMP121 (*chk1Δ*), UMS76 (*hsl1^{tef1}*), and UMS120 (*chk1Δ, hsl1^{tef1}*) were used. The expression of *hsl1* in UMP112 cells (control) growing in YPD was used as a reference to calculate the normalized fold expression. RNA was isolated after 6 hours of induction of *nar1* promoter. As internal control, the expression of *tub1* (encoding Tubulin α) was used.

Unexpectedly, we have found that sustained levels of *hsl1* mRNA alone seem to have no effect on the cell cycle arrest during filament induction. No differences between control (UMP112) filaments and filaments carrying the *hsl1^{tef1}* allele alone were found regarding nuclear content (Fig. 21A). In contrast, as previously reported (Garcia et al, 2009), in the *chk1* mutant filaments it was possible to observe two and, less frequently, three nuclei, indicating that they were able to divide once, and rarely twice, and that eventually they arrested their cell cycle. Strikingly, in combination with the absence of Chk1, the presence of the *hsl1^{tef1}* allele precluded the b-dependent permanent cell cycle arrest. In the double mutant (*chk1Δ hsl1^{tef1}*) strain, we have observed that the filaments carried several nuclei (Fig. 21). Moreover, these nuclei were separated by the presence of septa, indicating that the release from cell cycle arrest was complete, resulting in cell division after each cell cycle. As a consequence, the morphology of the mutant filament was different from the control cell cycle-arrested filament and, it resembles the growth of a filamentous fungus.

In summary, our results indicate that two individual mechanisms act in concert to specifically establish immediate and sustained arrest upon b-induction during the formation of the infective filament in *U. maydis*.
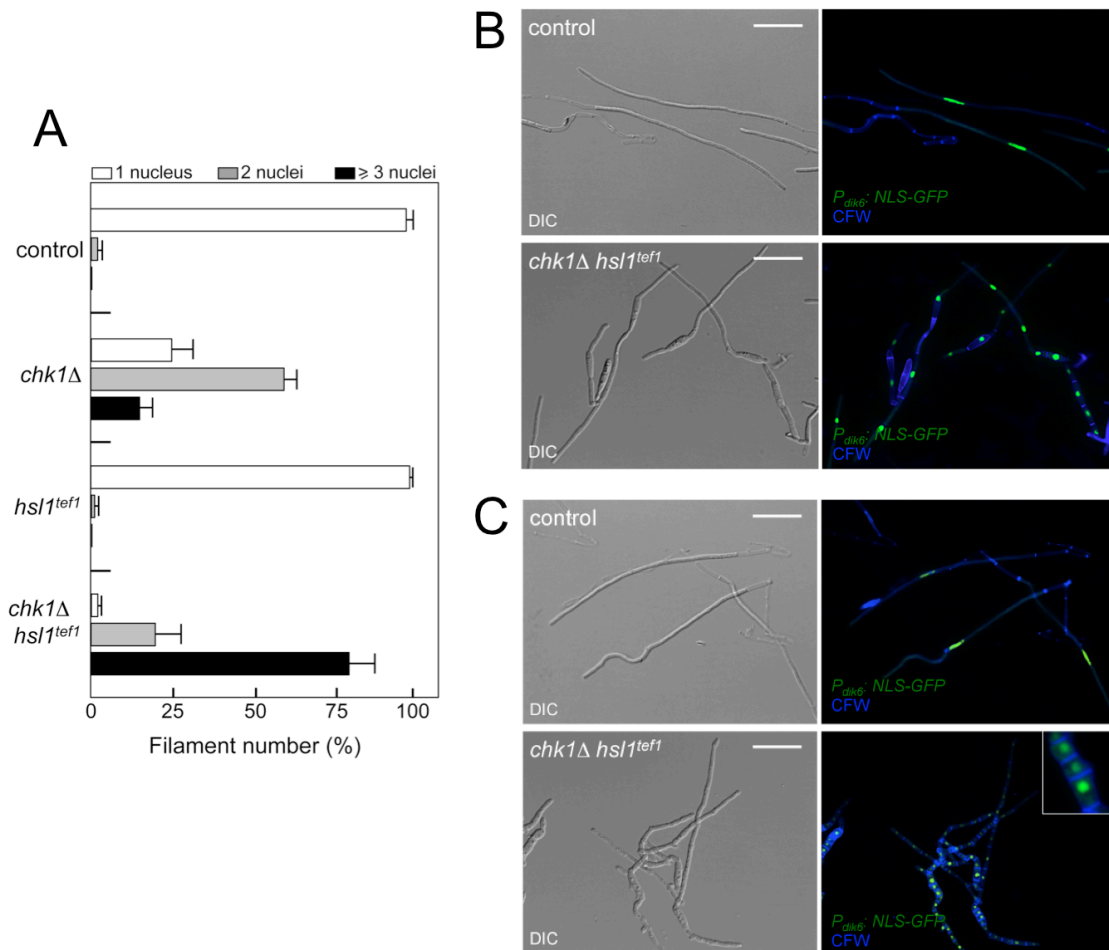

Figure 21: *hsl1* down-regulation and Chk1 activation collaborate in b-induced cell cycle arrest. (A) AB33-derived strains carrying the P_{dik6}:*NLS-GFP* transgene and carrying the indicated mutations (control, UMP112; *chk1Δ*, UMP121; *hsl1^tef1^*, UMS76; *chk1Δ hsl1^tef1^*, UMS120) were incubated in inducing conditions (MMD) for 8 hours. Filaments were sorted as carrying 1, 2 or 3 and more nuclei. The graph shows the result from two independent experiments, counting more than 100 filaments each. Means and SDs are shown. **(B)** Cell images of control (UMP112) and a derived strain lacking the *chk1* gene and carrying the *hsl1^tef1^* allele (UMS120) incubated for 8 h in inducing conditions (MMD). Strains carried an NLS-GFP fusion under control of the b-dependent *dik6* promoter to detect the nucleus. Cultures were stained with CFW to detect septa. Bar = 20 mm. **(C)** As in C, but after 16 hours of incubation. Note that filaments in the double mutant were composed of cell compartments carrying one nucleus each and separated by septa (inset). Scale bar: 20 mm.

4. The strains unable to arrest the cell cycle were severely impaired in virulence

To address the consequences of a defective cell cycle arrest during corn infection by *U. maydis*, we constructed compatible haploid strains (i.e. *a1b1* and *a2b2* mating types) carrying the *hsl1^{tef1}* allele, alone or in combination with the *chk1Δ* allele. Mixtures of compatible strains carrying different mutant combinations (wild type, *hsl1^{tef1}*, *chk1Δ*, and *hsl1^{tef1} chk1Δ*) were used to infect seven-day-old maize seedlings by stem injection. Disease symptoms were scored 14 days after infection according to severity (Kamper et al., 2006) (Fig. 22A). We have found that the infection with strains unable to arrest permanently the cell cycle (*hsl1^{tef1} chk1Δ*) results in a dramatic loss of virulence (Fig. 22). The most severe symptoms detectable in plants inoculated with *hsl1^{tef1} chk1Δ* crosses were small chlorotic spots. Only two plants out of 67 developed further symptoms (in one of them we observed ligula swelling whereas in the other plants only small tumours on the injected leaf were observed). In contrast, all plants inoculated with wild type crosses showed tumour formation. Strains carrying a *chk1* deletion alone were less efficient infecting plants and never produced large tumours, as described before (Garcia et al., 2009), whereas the virulence of strains carrying the *hsl1^{tef1}* allele alone was slightly less severe than control strains .
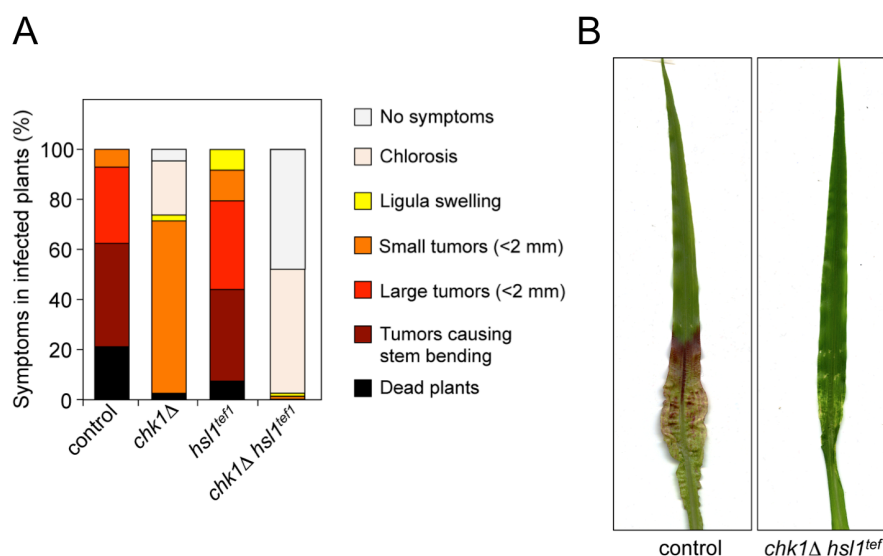
Figure 22: The deletion of *chk1* and constitutive expression of *hsl1* affects the pathogenicity (A) Disease symptoms caused by the indicated crosses were scored 14 days after infection of 7-day-old maize seedlings. The strains used in each cross were FB1xFB2 (control); UMP122xUMP129 (*chk1*Δ); UMS122xUMS124 (*hsl1^{tef1}*) and UMS123xUMS125 (*chk1*Δ, *hsl1^{tef1}*). Based on the severity of symptoms observed on each plant, symptoms were grouped into color-coded categories according to previous report (Kamper et al., 2006) depicted on the right side of graph. Two independent experiments were carried out and the average values are expressed as percentage of the total number of infected plants (n: > 50 plants). **(B)** Photographs of representative leaves 14 days after infection with the indicated strains.

In *U. maydis* virulence and sexual development are intricately interconnected. A prerequisite for generating the infectious stage is the mating of two compatible haploid cells to form, after cell fusion, the infective dikaryotic filament. Since the mating process also involves a transient cell cycle arrest (Garcia-Muse et al., 2003b) we wondered whether the observed dramatic virulence defects in *hsl1^{tef1} chk1*Δ strains were caused simply by the inability to mate. To address this question, we have analysed the presence of b-dependent filaments in crosses of compatible haploid strains on charcoal-containing plates. To distinguish the b-induced filaments from the cell population background (frequently enriched in aberrant elongated cells) we have used haploid strains carrying the above described *P$_{dik6}$:NLS-GFP* fusion. In this way, only the filaments carrying fluorescent nuclei can be attributed to be the result of a mating process. We have observed that wild type crosses led to white fuzzy colonies. Microscopic analysis of these colonies showed the formation of b-dependent filaments, which presented two fluorescent nuclei. In contrast, the *hsl1^{tef1} chk1*Δ mutant crosses showed an obvious impaired fuzzy response (Fig. 23A). However, we observed filaments with several fluorescent nuclei (Fig. 23B) indicating that although attenuated in filament formation, the *hsl1^{tef1} chk1*Δ strains were able to mate.
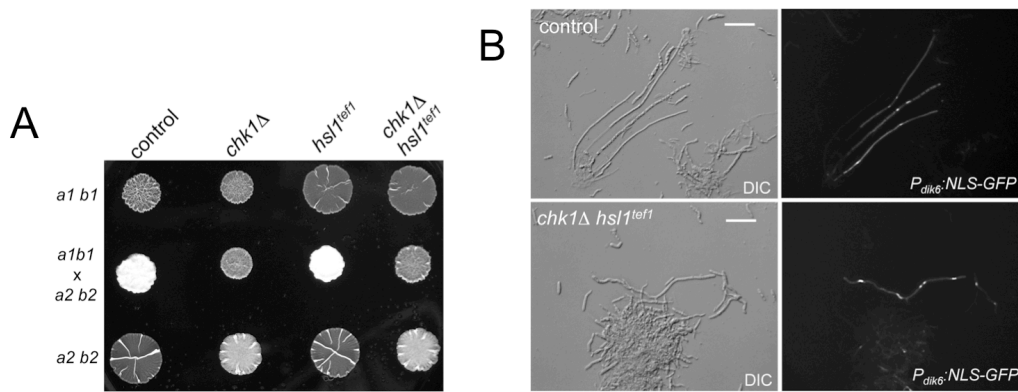
Figure 23: The deletion of *chk1* and constitutive expression of *hsl1* attenuates but does not abolish mating. (A) Crosses of control as well as single and double mutants strains carrying compatible mating types (*a1 b1* and *a2 b2*) in charcoal-containing agar plates. The strains used in each cross were FB1xFB2 (control); UMP122xUMP129 (*chk1∆*); UMS122xUMS124 (*hsl1^tef1^*) and UMS123xUMS125 (*chk1∆, hsl1^tef1^*). **(B)** Compatible strains carrying a NLS-GFP fusion under control of the b-factor-dependent *dik6* promoter were scrapped from agar surface, mounted on microscopy slides and epifluorescence was observed. Control cross was done with UMP182 and FB2 strains; *chk1∆ hsl1^tef1^* cross was done with UMS127 and UMS125 strains. Left panels show DIC images of cells and right panels show fluorescence in GFP channel. Scale bar: 25 mm.

To discard that the lack of virulence of the *hsl1^tef1^ chk1∆* strain was a consequence of impaired mating, we have constructed a double *hsl1^tef1^ chk1∆* mutant in the SG200 genetic background. The SG200 strain is engineered to express both pheromone genes and encodes an active bE1/bW2 heterodimer, what makes it able to infect plants without mating (Bölker et al., 1995a) (Bolker et al., 1995). We have infected plants with the SG200 strain as well as the double *hsl1^tef1^ chk1∆* mutant as above. Encouragingly, we have found that the double mutant was totally unable to infect plants (Fig. 24), discarding mating defects as the reason for the lack of virulence in strains unable to arrest the cell cycle.
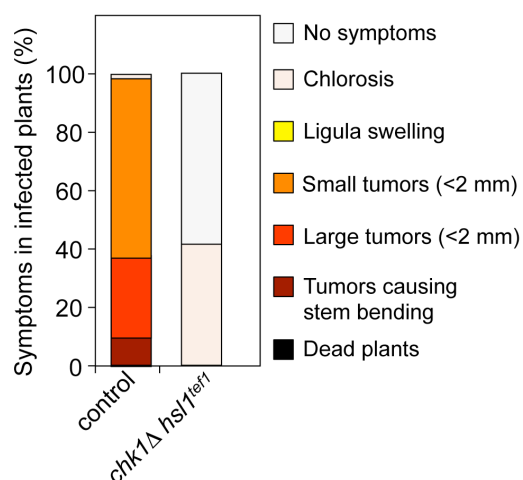
Figure 24: The inability of *chk1*Δ hsl1^tef1 mutant to infect is not due to defects in mating. Disease symptoms caused by the solopathogenic SG200 (control) strain and UMS131 (*chk1*Δ, *hsl1^tef1*) were scored 14 days after infection. Symptoms were grouped into color-coded categories. Two independent experiments were carried out and the average values are expressed as percentage of the total number of infected plants (n: > 50 plants).

5. The cell cycle arrest seems to be required for appressorium formation

To address the step at which the cell cycle arrest-defective strains were impaired during the pathogenic development, we have investigated the presence of fungal material around the puncture in leaves inoculated with the double mutant cross. We have found no evidence of mutant fungal cells inside the plant tissue. Similar experiment performed with wild type crosses showed fungal hyphae inside the plant tissue (Fig. 25). This result suggests that the mutant cells were defective in cuticle penetration and/or subsequent colonization of the plant tissue.
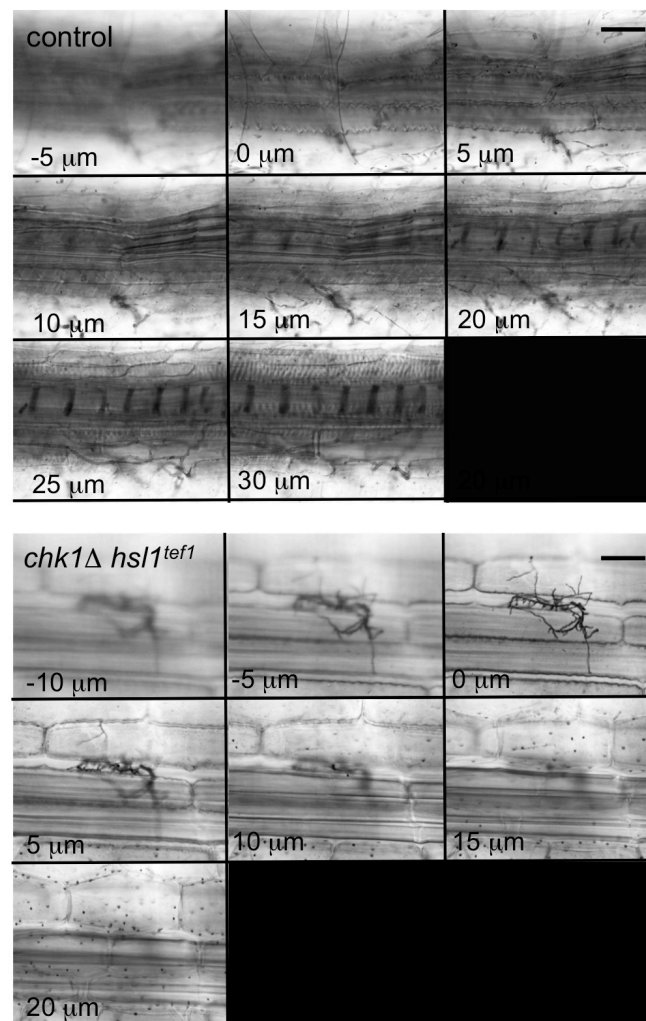
Figure 25: Double *hsl1^tef1* *chk1Δ* mutant is unable to penetrate the plant cuticle. Series of z axis projections showing the infection of wild type (FB1xFB2) (upper panel) and mutant (UMS123xUMS125) (bottom panel) crosses. Corn leaves showing symptoms (chlorotic areas in the case of mutant crosses) were collected at day 5 after infection and fungal material was visualized by staining with Chlorazole Black. Note the presence of fungal material inside the plant tissue in control infections and its absence in mutant infections. Scale bar: 25 mm.

The appressorium formation is a requisite for plant penetration, and therefore we decided to look for the presence of appressoria on leaves infected with the double *hsl1^tef1* *chk1Δ* mutant. To facilitate the localization of appressoria, first we have introduced the AM1 reporter into control (wild type) and double mutant combination produced in the SG200 genetic background. The AM1 reporter is a transcriptional GFP fusion with the promoter from the

gene encoding um10779. This marker shows GFP expression exclusively in those tip cells of filaments that differentiate an appressorium (Mendoza-Mendoza et al., 2009). The leaves were also stained with calcofluor white (CFW) to detect fungal filaments, as well as to distinguish appressorium formation, which is preceded by formation of a characteristic crook-like structure that frequently accumulates CFW (Snetselaar and Mims, 1993). By using this approach we have easily found appressoria in wild type infections, but we have rarely detected appressoria in the double mutant strain (Fig. 26). We take this as evidence that in the absence of a cell cycle arrest, the *U. maydis* infective filaments were unable to induce apressorium formation, and thereby were unable to infect plants.
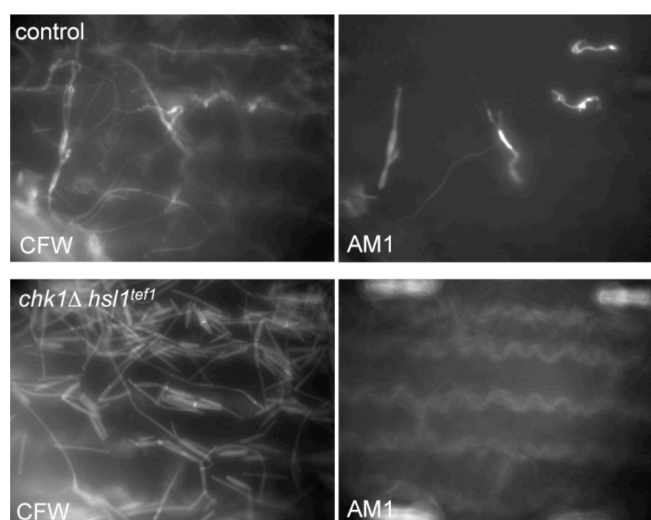
Figure 26: Appressoria formation *in vivo*. Microscopy images of colonized leaf tissue 18 hours after infection with the indicated strains. Fungal material on the leaf surface was stained with calcofluor white (CFW) and expression of the appressorium-specific promoter P*um01779* fused to GFP (AM1) was monitored.

To allow the quantitative comparison of appressoria formation, we co-infected plants with equal numbers of SG200 AM1 tagged with constitutively expressed genes for cherry fluorescent protein (UMS190) and SG200 *chk1∆hsl1*^*tef1* AM1 cells (UMS137) in one case (upper panel) or SG200 AM1 (UMS132) and SG200 *chk1∆hsl1*^*tef1* AM1 tagged with constitutively expressed genes for cherry fluorescent protein cells (UMS191) in other case (bottom panel). After 1 day, expression of AM1 (GFP fluorescence) was scored with respect to specific cherry fluorescence. A decrease in the frequency of appressorium formation was observed in SG200 *chk1∆hsl1*^*tef1* AM1 cells,

regardless of the presence or not of the cherry fluorescence marker (Fig. 27). Fungal material on the leaf surface was stained with calcofluor white (CFW).
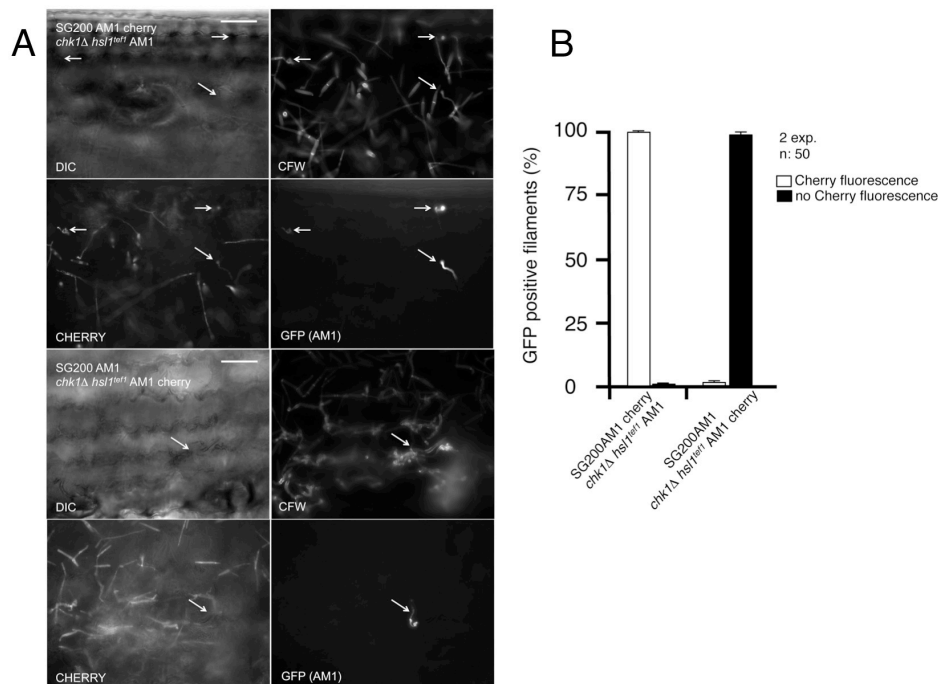
Figure 27: Quantification of appressoria formation *in vivo*. Scale bar: 25 μm.

We also used established *in vitro* conditions to induce appressoria formation in *U. maydis* (Mendoza-Mendoza et al., 2009). We spread wild type and mutant strains carrying the AM1 reporter on an artificial hydrophobic surface in the presence of long-chain hydroxy fatty acids. After 20 hours of incubation, we scored the proportion of filaments (stained with CFW) showing GFP fluorescence (i.e. adopting the appressorium differentiation program). We have found that both wild type and single mutants were able to produce appressoria at a ratio comparable to those found in other studies for these *in vitro* conditions (Berndt et al., 2010; Freitag et al., 2011; Lanver et al., 2010; Mendoza-Mendoza et al., 2009). However in the *hsl1^tef1^ chk1Δ* strain we rarely found GFP positive filaments (Fig. 28).

Figure 28: Appressorium formation requires cell cycle arrest. (A) Appressoria formation on a hydrophobic surface in the presence of hydroxy-fatty acids. Strains used carried the ap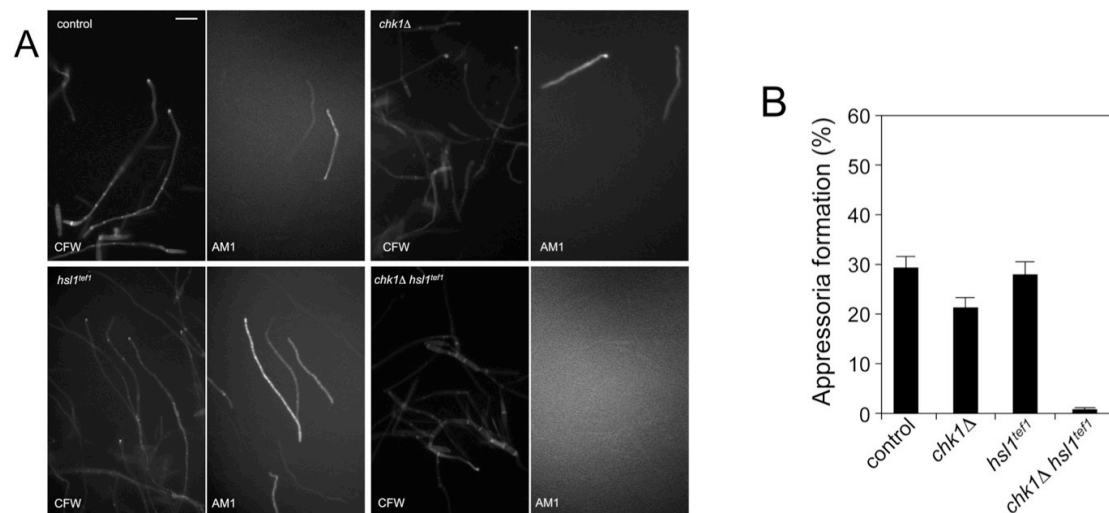pressorium-specific AM1 reporter as well as the indicated mutations: UMS132 (control); UMS129 (*chk1Δ*); UMS143 (*hsl1^tef1*); and UMS137 (*chk1Δ, hsl1^tef1*). Cells were sprayed on Parafilm M in the presence of 100 mM 16-hydroxyhexadecanoic acid. After 20 h cells were stained with Calcofluor white (CFW), and analyzed for AM1 marker expression (AM1). The images represent the overlay of both signals. Scale bar: 20 mm. **(B)** Quantification of appressoria formation in the different mutants. At least 100 filaments per experiment were counted and the percentage of filaments producing appressorium was noted. The average percentage was determined from two independent experiments.

We were interested in studying at which step the cell cycle arrest affects the ability to produce the appressorium. Activation of the program that produces the appressorium in *U. maydis* involves the sensing of at least two different plant-derived stimuli: a hydrophobic surface and hydroxyl fatty acids. It has been proposed that this signals are sensed, among other elements, by two membrane proteins related to *S. cerevisiae* Sho1p and Msb2p (Lanver et al., 2010), and transmitted by the same MAPK cascade that mediates the pheromone signalling (Mendoza-Mendoza et al., 2009). Mutants lacking these elements or those unable to process the surface receptors correctly (i. e. showing defects in glycosylation), are severely impaired in their capacity to produce appressoria and subsequently show dramatic defects in virulence (Fernandez-Alvarez et al., 2012; Lanver et al., 2010). Cell cycle regulation could affect the transmission pathway or it could interfere with elements downstream the signalling cascade. To address whether the cell cycle arrest is affecting the ability to transmit the signal, we have introduced in the strains (mutant and wild

type) carrying the AM1 reporter a construction that expresses the *fuz7^{DD}* allele, encoding a hyperactive version of the pheromone cascade MAPK kinase (Muller et al., 2003) under the control of *crg1* promoter. In this way we bypassed the requirement of the signal transmission upstream the last step, the activation of the MAP kinase (Kpp2) by its cognate MAPK kinase (Fuz7). We have found that even in conditions of high levels of activation of the MAPK cascade, the cell cycle arrest was required for appressorium formation (Fig. 29). These results strongly suggest that the putative targets of the signal emanating from cell cycle arrest are downstream the MAPK cascade.
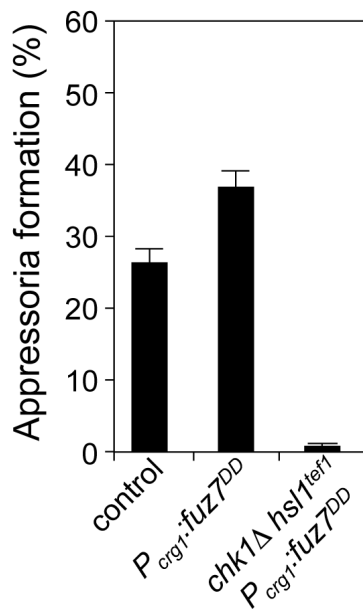
Figure 29: Overactivation of MAPK cascade does not bypass the cell cycle arrest signal. UMS132 (control) as well as the double mutant derivative (UMS137) were transformed with a construction expressing under the control of *crg1* promoter the hyperactivated Fuz7DD MAPKK resulting in UMS145 (P_{crg1}:*fuz7^{DD}*) and UMS154 (*chk1Δ*, *hsl1^{tef1}* P_{crg1}:*fuz7^{DD}*). All strains were pre-grown until mid-exponential phase in CMD, and then washed twice and re-suspended in CMA (2% arabinose) to induce P_{crg1}: *fuz7^{DD}* prior to spraying on Parafilm M. After 20 h cells were stained with Calcofluor white and analysed for appressoria-like structures showing GFP fluorescence. At least 100 filaments were counted and the bars represent the average percentage of two independent experiments.

Pheromone-induced G2 cell cycle arrest in *Ustilago maydis*

Studies in fission and budding yeasts showed that exposure of cells to pheromone of opposite mating type leads to a cell cycle arrest. As a consequence, cells synchronize their cell cycle at the same phase before fusion and grow towards the mating partner in a polarized way, giving rise to the mating structures. In our laboratory, previous work showed that *U. maydis* cells upon pheromone exposure also arrest the cell cycle. However, in contrast to fission and budding yeasts, which arrest the cell cycle in G1, *U. maydis* cells arrest their cell cycle in G2 upon exposure to pheromones (Garcia-Muse et al., 2003).

The mechanism of G2 arrest in *U. maydis* is yet to be characterized. As in budding and fission yeasts, in *U. maydis* a common conserved MAP kinase pathway transduces the pheromone signal from membrane-located pheromone receptors, and the integrity of this pathway is required for the induction of the cell cycle arrest (García-Muse et al., 2004; Garcia-Muse et al., 2003b; Muller et al., 2003). However, no downstream effectors of this pathway specifically required for cell cycle arrest have been characterized so far. In this section we will describe our attempts to characterize the mechanism behind the pheromone-induced cell cycle arrest in *U. maydis.*

1. Expression of the constitutively active *fuz7*[DD] allele mimics the pheromone-induced G2 cell cycle arrest

Pheromone response in *U. maydis* requires starvation conditions since genes encoding the receptors as well as pheromone precursors are not expressed in the presence of nutrients. Because the absence of nutrients may also affect cell cycle regulation, we decided to use conditions that mimic the pheromone addition by conditional expression of an activated version of the MAPKK of the pheromone-response pathway (Muller et al., 2003). For that, we took advantage of a strain in which the *fuz7* endogenous locus, encoding the MAPKK of the pheromone-response pathway, was exchanged with a constitutively active allele termed *fuz7*[DD] (Muller et al., 2003) that mimics an activated MAPK kinase. The expression of this *fuz7*[DD] is under the control of *crg1* promoter (*fuz7*[DD crg1]), which is induced by arabinose and repressed by glucose. Previous results have indicated that *fuz7*[DD crg1] cells grown in presence

of arabinose form structures that resemble the conjugation tubes. These structures are the typical response upon pheromone recognition in *U. maydis* (Spellig et al., 1994). Thus we were able to mimic the addition of pheromone simply by changing the carbon source (Fig. 30).
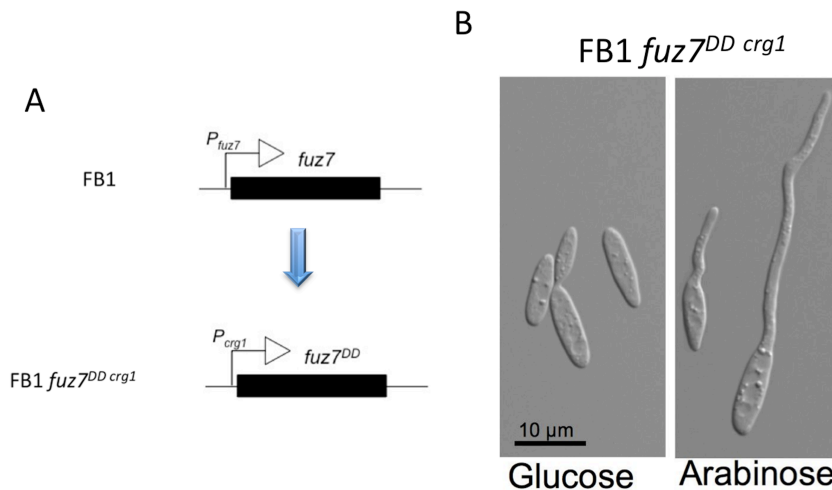

Figure 30: Expression of *fuz7^{DD}* mimics the response to pheromone. (A) The endogenous locus of *fuz7*, in the wild type strain FB1, was exchanged by the allele *fuz7^{DD}*, which is under the control of the regulatable *crg1* promoter, resulting in the strain UMN4. **(B)** Cell morphology of *fuz7^{DDcrg1}* growing in CMD (glucose) and in CMA (arabinose). Note that while *fuz7^{DD}* in CMD is repressed and the cells divide by budding, in CMA is expressed leading to the formation of structures resembling conjugation tubes.

To validate the described pheromone-dependent G2 cell cycle arrest in the strain *fuz7$^{DD\ crg1}$*, an analysis of its cellular DNA content by flow cytometry was performed. Control and *fuz7$^{DD\ crg1}$* cell samples grown on CMD (repression of *crg1*) and CMA (expression of *crg1*) were analysed after 0, 3, 6 and 9 h of incubation. We have found that *fuz7$^{DD\ crg1}$* cells gown in arabinose-containing medium accumulated 2C DNA content indicating that they are either in G2 phase or in mitosis. Because *U. maydis* undergoes an open-like mitosis –the nuclear envelope disassembles in mitosis (Straube et al., 2005)–, the G2 phase can be distinguished from early mitosis by the integrity of the nuclear membrane. Therefore, to distinguish between G2 and early mitosis stages, a *fuz7$^{DD\ crg1}$* strain carrying a Cut11-Cherry fusion protein (Cut11 is a component of the nuclear membrane and it has been used as a nuclear membrane marker (Pérez-Martín, 2009)) and a GFP-nuclear localization signal fusion was generated resulting in UMS1 strain. Cells expressing *fuz7^{DD}* showed a single nucleus per cell with an intact nuclear membrane (Fig. 31). Taken together,

these results showed that the expression of *fuz7DD* triggers a G2 cell cycle arrest equivalent to the previously obtained upon addition of pheromone.
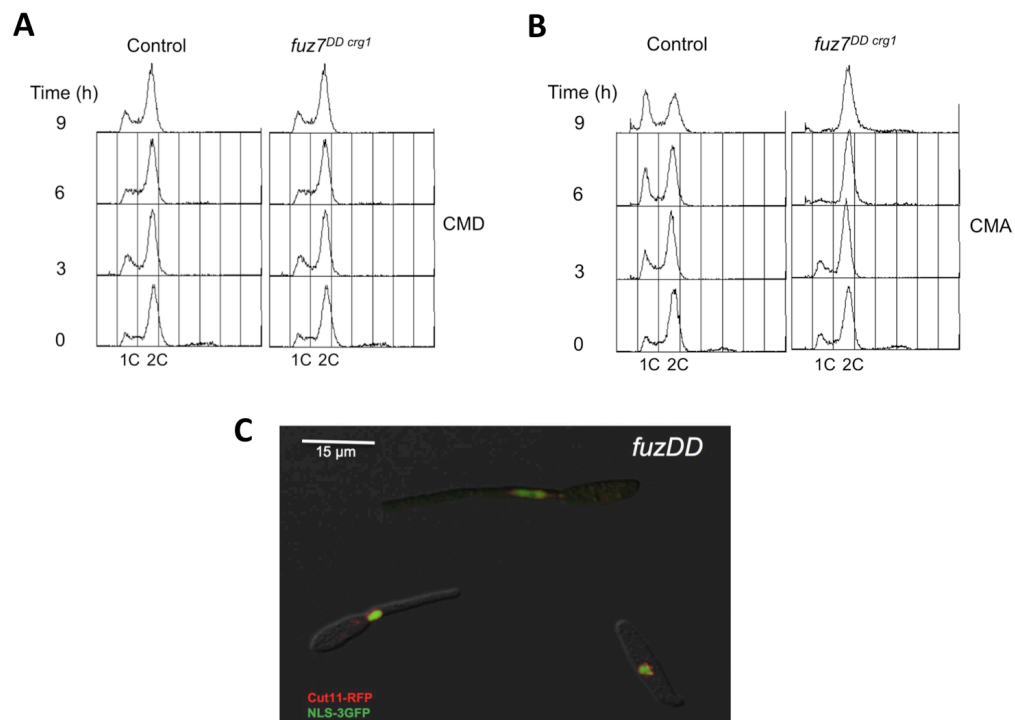

Figure 31: The induction of *fuz7DD* leads to a G2 cell cycle arrest. (A) FACS analysis of control (FB1) and FB1 *fuz7DD crg1* (UMN4) strains grown under non-expressing (CMD) and **(B)** expressing *fuz7DD* conditions (CMA). After 9 hours of *fuz7DD* expression, FB1 *fuz7DDcrg1* showed an accumulation of 2C DNA containing cells. **(C)** Microscopic analysis of cells after activation of *fuz7DD*. Cells carrying a Cut11-Cherry and a NLS-3GFP fusions were grown in CMA media to induce *fuz7DD* expression, thus leading to the formation of structures similar to conjugation tubes. Only single nuclei with intact nuclear membrane were observed. Scale bar: 15µm.

To further validation of our experimental system, we sought to prove that the observed cell cycle arrest was dependent on components located downstream of Fuz7 in the pheromone cascade. In *U. maydis* the pheromone signal is transmitted via a MAPK module constituted by the hierarchical kinases Kpp4 (MAP3K), Fuz7 (MAP2K) and Kpp2 (MAPK) (Muller et al., 2003) that are activated sequentially by phosphorylation. Downstream of the MAPK module, has been described to act Prf1, a HMG (high-mobility-group) domain transcription factor, necessary for transcription of *a* and *b* mating type genes upon binding to pheromone response elements located upstream of these genes (Hartmann et al., 1996), but dispensable for cell cycle arrest and conjugative tube formation (Muller et al., 2003). To analyse whether Kpp2, the

MAPK next in line to Fuz7, and Prf1 were required for the cell cycle arrest induced by *fuz^DD* expression, deletion alleles in these genes were introduced in the UMS1 strain giving rise to the strains FB1*fuz7^{DD\ crg1}\ kpp2*Δ (UMS26) and FB1*fuz7^{DD\ crg1}prf1*Δ (UMS28). The nuclear DNA content of these strains was analysed by flow cytometry, and a microscopic analysis was performed. The deletion of *kpp2* led to cells unable to form conjugation tubes and arrest cell cycle, showing identical morphology to cells in non-inducing conditions (CMD). The deletion of *prf1* neither abolished the morphological transition induced by f*uz7^{DD}*, as already previously reported (Muller et al., 2003), nor affected cell cycle arrest (Fig. 32).

All these results showed that the controlled expression of *fuz7^{DD}* faithfully mimics the pheromone response with respect to the observed G2 cell cycle arrest.
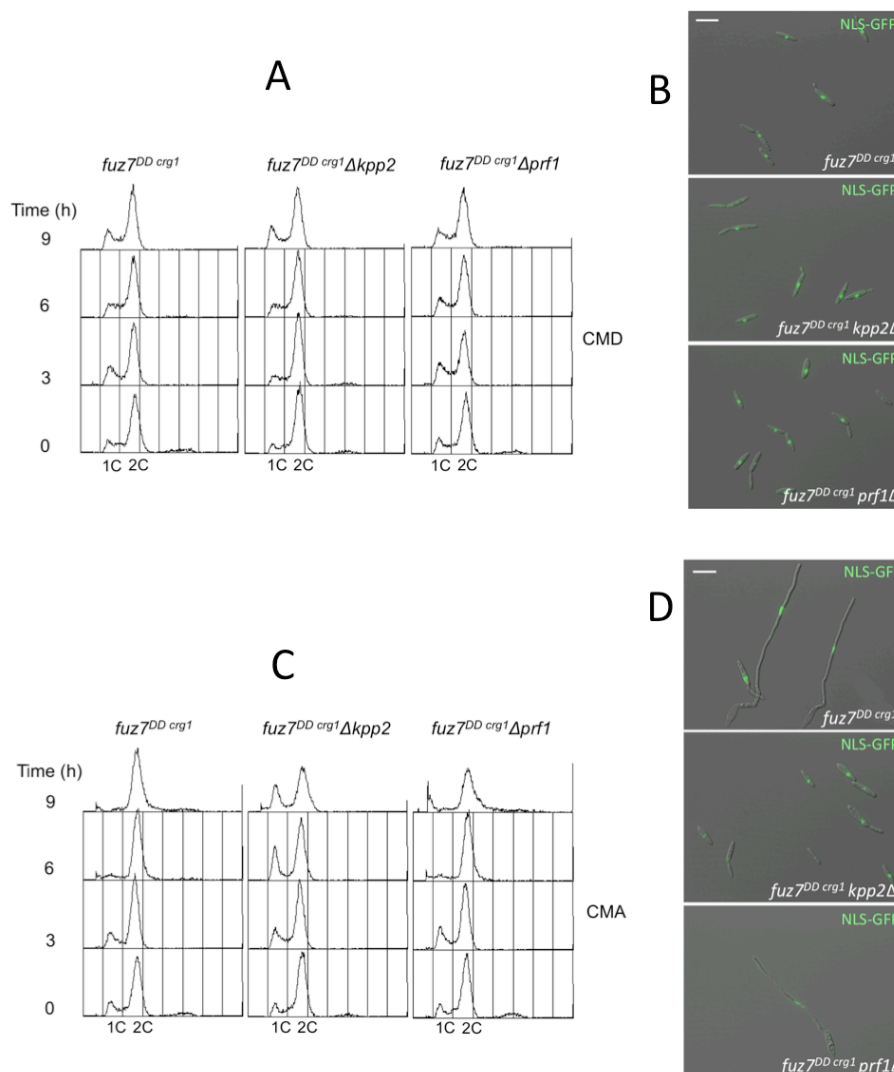
Figure 32: *kpp2* **deletion abolishes conjugation tube formation and** *fuz7^{DD}*-**mediated G2 cell cycle arrest, whereas** *prf1* **deletion does not. (A)** FACS analysis of indicated strains grown under *fuz7^{DD}* non-inducing conditions in CMD. The FACS profiles observed were similar for all strains. **(B)** Microscopic analysis of indicated strains. Cells were grown in CMD until mid-exponential phase. **(C)** FACS analysis of strains grown under *fuz7^{DD}* inducing conditions in CMA. For FB1*fuz7$^{DD\ crg1}$* and FB1*fuz7$^{DD\ crg1}$ prf1Δ* only cells with a 2C-DNA content were observed after 9 hours of induction, whereas for FB1*fuz7$^{DD\ crg1}$ kpp2Δ*, cells with 1C-DNA and 2C-DNA content were observed. **(D)** Cell morphology of indicated strains incubated in CMA. Scale bar: 15µm.

2. Inhibitory phosphorylation of Cdk1 is required for *fuz7^{DD}*-induced G2 cell cycle arrest

Cyclin-dependent kinases (CDKs) control the progression of the cells through the cell cycle in eukaryotes. In *U. maydis* the G2/mitosis transition was described to be controlled through inhibitory phosphorylation of the catalytic subunit of the its mitotic CDK (Cdk1) by the Wee1 kinase (Sgarlata and Perez-Martin, 2005b)(Sgarlata and Perez-Martin, 2005). The Cdk1 kinase contains conserved residues that are targets of inhibitory phosphorylation by Wee1 kinase. To investigate the influence of this phosphorylation in the G2 cell cycle arrest induced by the expression of *fuz7^{DD}* we used a mutant allele, *cdk1^{AF}*, in which the putative inhibitory phosphorylation sites in Cdk1 were replaced with residues that cannot be phosphorylated (Thr^{14} to Ala and Tyr^{15} to Phe) (Sgarlata and Perez-Martin, 2005). Because a continuous expression of this allele is deleterious to the cells, we introduced an ectopic copy of the mutant *cdk1^{AF}* allele under the control of *crg1* promoter in the UMS1 strain. This way *cdk1^{AF}* and *fuz7^{DD}* are simultaneously expressed. As a control, we introduced an ectopic copy of the wild type *cdk1* also under the control of *crg1* promoter. To follow the induction of the ectopic copies of the Cdk1 alleles, these were tagged with 3xMyc to distinguish the levels of protein produced by the endogenous locus from the ectopically expressed alleles (Fig. 33A and 33B). We have found that while a strain expressing an additional copy of the wild type *cdk1* allele produces conjugation tubes that are indistinguishable from those obtained for *fuz7$^{DD\ crg1}$* control strain, cells expressing the Cdk1 version refractory to inhibitory phosphorylation carried several nuclei, indicating that they were not cell cycle arrested (Fig. 33C and 33D). These findings indicated

that inhibitory phosphorylation of Cdk1 plays a pivotal role in the *fuz7^{DD}*-induced G2 cell cycle arrest.
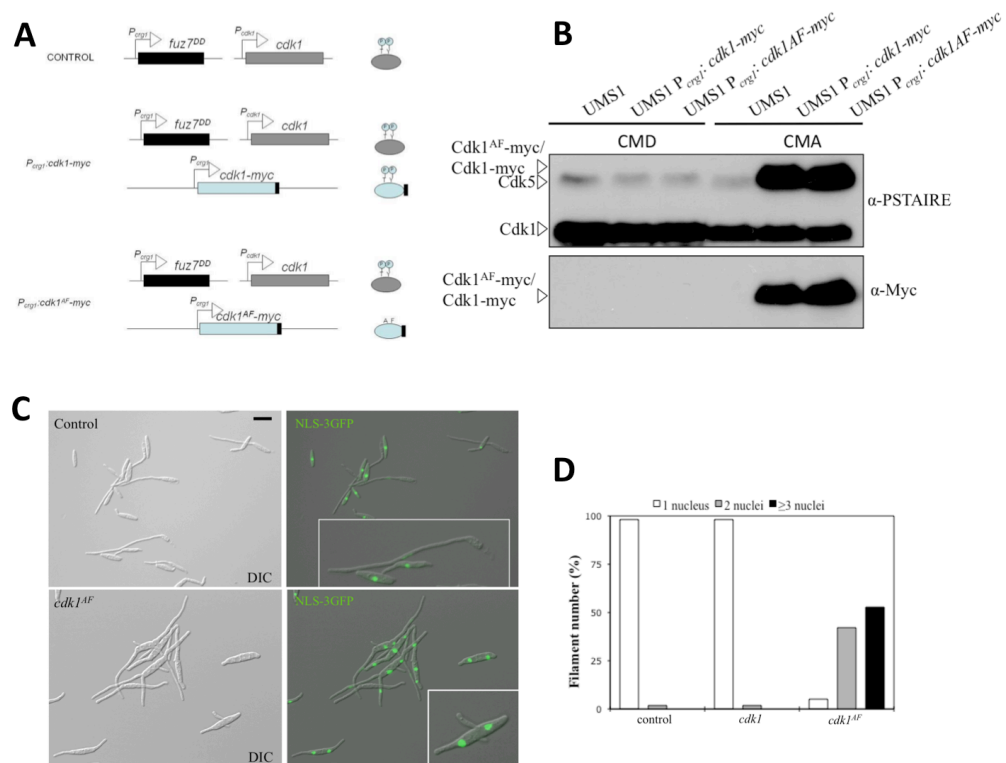

Figure 33: Cdk1 refractory to inhibitory phosphorylation affects the number of nuclei in filaments induced by *fuz7^{DD}* (A) Scheme showing the constructions inserted in the strains used. **(B)** Levels of Cdk1 in the indicated strains. In addition to endogenous *cdk1* wild type allele, UMS1 P$_{crg1}$:*cdk1*-myc and UMS1 P$_{crg1}$:*cdk1^{AF}*-myc strains carry an ectopic extra copy of a *cdk1*-myc or *cdk1^{AF}*-myc allele under the control of *crg1* promoter. **(C)** Microscopic pictures FB1*fuz7^{DDcrg1}* (control) and FB1*fuz7^{DD}* ^{crg1}P$_{crg1}$: *cdk1^{AF}*. Cells carry a NLS-3GFP fusion to visualize the nuclei **(D)** Quantification of cells carrying single, two and three or more nuclei after induction of *fuz7^{DD}*. In *cdk1^{AF}* mutant, the frequency of cells with more than one nucleus was drastically increased. Scale bar: 15µm.

Cdk1 inhibitory phosphorylation during vegetative growth depends on the activity of Wee1 kinase (Sgarlata and Perez-Martin, 2005b). Furthermore, this essential kinase has been demonstrated to be necessary for b-factor-induced cell cycle arrest (Garcia et al., 2009). To investigate whether Wee1 is also required for the *fuz7^{DD}*-induced cell cycle arrest, we introduced the conditional allele *wee1^{nar1}* in the UMS1 strain. This allele allows the expression of *wee1* in minimal medium containing nitrate as a nitrogen source (MM-NO$_3$), whereas it

is downregulated in either complete medium or rich medium. When *fuz7^{DDcrg1}wee1^{nar1}* conditional cells were grown in repressive conditions (CMA), multinucleated conjugative tubes were observed. In similar grown conditions, *fuz7^{DDcrg1}* cells showed conjugative tubes carrying a single nucleus, indicating that Wee1 was necessary for the *fuz7^{DD}* induced cell cycle arrest (Fig. 34).
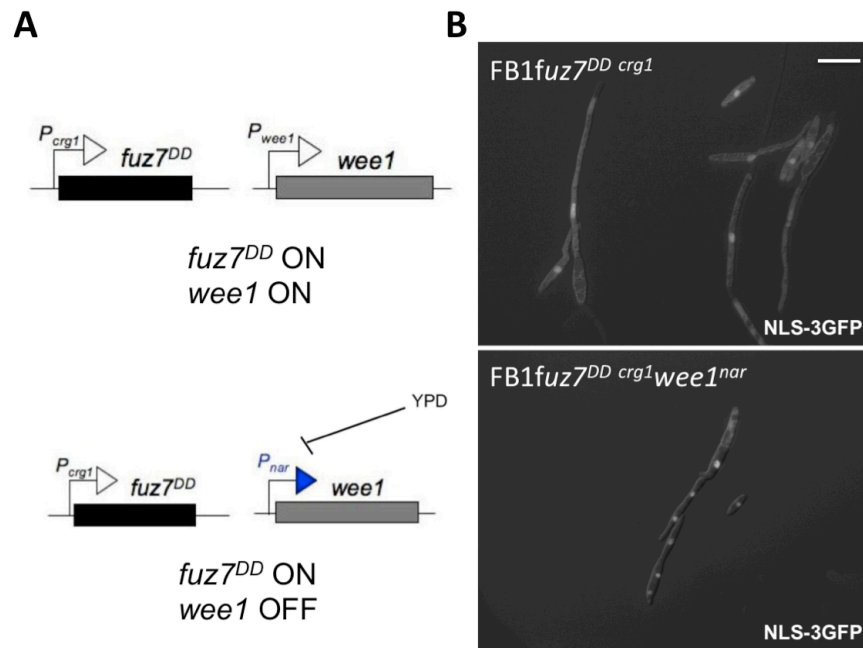
Figure 34: Wee1 is required for *fuz7^{DD}*-induced cell cycle arrest. (A) Scheme showing the constructions inserted in the the strains used in panel B. **(B)** Microscopic pictures of UMS1 (FB1*fuz7^{DDcrg1}*) and UMS1-derived strain carrying a conditional *wee1^{nar1}* allele after incubation under expression conditions of *fuz7^{DD}* and repression conditions of *wee1*. Strains carry a NLS-3GFP fusion to visualize the nuclei. Scale bar: 15μm.

3. Pheromone and b factor use distinct mechanisms to arrest cell cycle

We hypothesized that the pheromone MAPK pathway activation may produce altered transcription of genes that are important for the cell cycle progression. In fact, a previously described genome-wide analysis of the *U. maydis* transcriptome upon pheromone response showed that several cell cycle genes were altered (Zarnack et al., 2008). However, as we have reasoned for the analysis of the b-dependent cell cycle arrest, it would be difficult to conclude from this analysis whether the changes in the levels of these genes are a cause

or a consequence of the pheromone-induced cell cycle arrest. Therefore, we have employed a similar strategy to that described previously for transcriptional analysis upon b-expression. We used the strain that expresses *fuz7^DD* and an ectopic Cdk1 allele refractory to inhibitory phosphorylation (*cdk1^AF*) at same time to distinguish carefully between genes which expression was specifically altered by *fuz7^DD*, regardless of the of an inactive cell cycle. Similarly to the transcriptional analysis carried out in response to bE1/bW2 activation, we have found that the levels of mRNA of all analysed genes decreased after *fuz7^DD* induction. In the same way, uncoupling the activity of *fuz7^DD* from cell cycle arrest by preventing the Wee1-mediated inactivation of Cdk1 identified *hsl1* as the only transcript that was still dramatically *fuz7^DD* repressed in the absence of cell cycle block (Fig. 35).

These findings prompted us to wonder whether *fuz7^DD*- and b-induction would trigger identical mechanism to arrest the cell cycle at G2 phase. The b-dependent cell cycle arrest in *U. maydis* is based on at least two distinct mechanisms involving Hsl1 and Chk1 to modulate the G2/M transition. Therefore, we have constructed a UMS1 strain carrying the deletion *chk1* allele as well as the *hsl1^tef1* allele, both described in previous sections. Strikingly, this strain was able to produce conjugative tubes that were cell cycle arrested as the control strain (Fig. 36). In summary these results indicated that although b-dependent cell cycle arrest and pheromone-dependent cell cycle arrest share the same final target (inhibitory phosphorylation of the Cdk1), the genetic circuitry involved in this down regulation seems to be distinct.
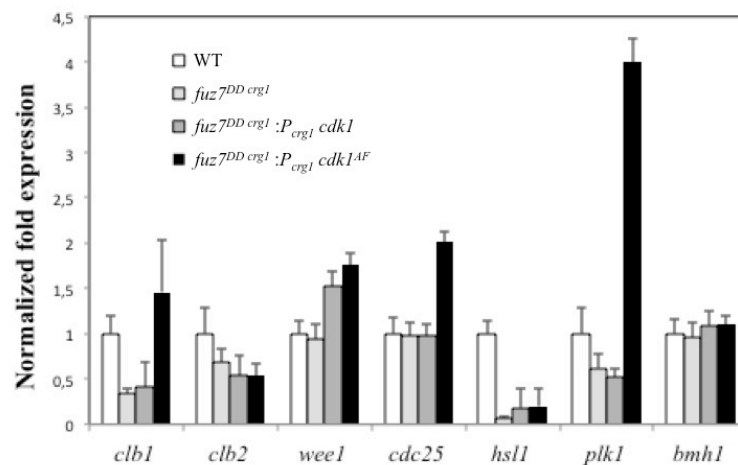
Figure 35: Quantitative real time-PCR for the indicated genes in the different strains. RNA was isolated after 6 hours of induction of *crg1* promoter. As internal control the expression of *tub1* (encoding Tubulin α) was used. Values are referred to the expression of each gene in FB1 (WT). Each column represents the mean value of four independent biological replicates.
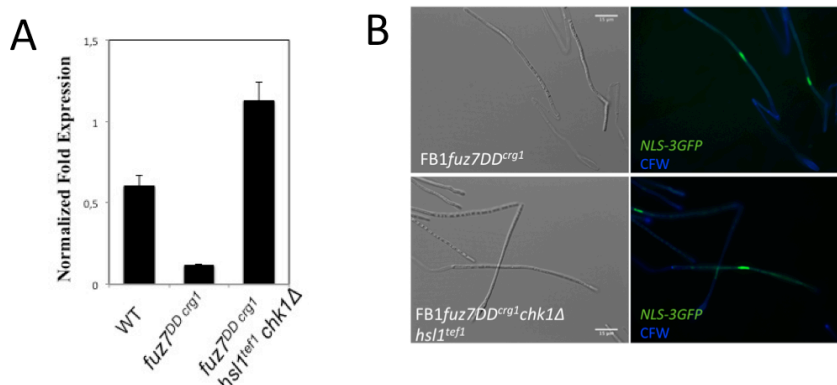

Figure 36: *chk1* deletion and overexpression of *hsl1* do not affect *fuz7^{DD}*-induced G2 cell cycle arrest. (A) The *hsl1* locus was exchanged with a transgene in which *hsl1* is under the control of *tef1* promoter. As a consequence, *hsl1^{tef1}* is expressed in a constitutive manner and bypasses *hsl1* downregulation upon *fuz^{DD}* induction. Strains FB1 (WT), UMS1 (*fuz7$^{DD\ crg1}$*) and UMS175 (*fuz7$^{DD\ crg1}$ hsl1^{tef1} Δchk1*) were used. The expression of *hsl1* in FB1 cells (WT) growing in CMA was used as a reference to calculate the normalized fold expression. RNA was isolated after 6 hours of induction of *crg1* promoter. As internal control, the expression of *tub1* (encoding Tubulin α) was used. **(B)** Microscopic analysis of conjugation tubes from UMS1 (*fuz7^{DDcrg1}*) and UMS175 (*fuz7^{DDcrg1} hsl1^{tef1} Δchk1*) strains. Cells were grown in CMA overnight to induce *fuz7^{DD}* expression. Only single nucleus was observed in both strains. Scale bar: 15μm.

4. The levels of the Cdc25 phosphatase decrease upon *fuz7^{DD}* induction

The Cdc25 phosphatase promotes entry into mitosis by removing the Cdk1 inhibitory phosphorylation. Sequestration in the cytoplasm of the Cdc25 phosphatase upon Chk1 phosphorylation was reported to be one of the reasons for the increase of the inhibitory phosphorylation in b-induced cell cycle arrest (Garcia et al, 2009). However, we have found that the mechanism of *fuz7^{DD}*-induced cell cycle arrest is different from the one induced by the b-factor. The full understanding of Cdk1 inhibitory phosphorylation will therefore require elucidation of the mechanisms that regulate Wee1 and Cdc25. Quantitative RT-PCT data indicated that the levels of *wee1* and *cdc25* are not significantly

altered upon *fuz7^{DD}* induction. Hence, we decided to study the Wee1 and Cdc25 protein levels. For this, *fuz7^{DDcrg1}* cells carrying either a *cdc25-HA* or a *wee1-HA* allele were grown on *fuz7^{DD}*-inducing conditions and samples were taken every two hours. We observed that upon *fuz7^{DD}* induction, while the levels of Wee1 protein seem to remain relatively unaltered (Fig. A), the levels of Cdc25 seem to be decreased (Fig. B) suggesting this as a likely cause of the G2 cell cycle arrest. The change to a new medium (CMA) also affected the control cells (FB1) as demonstrated by the levels of Cdc25 that also decreased, although not at the low levels reached by *fuz7^{DD}* strain.
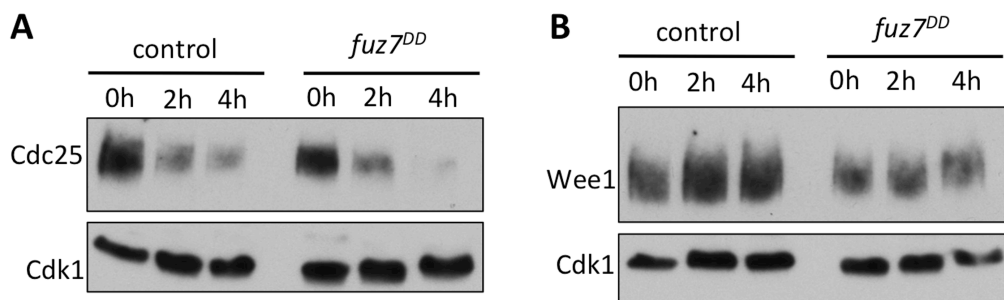

Figure 37: Levels of Cdc25 protein seem to be decreased upon *pcl12* activation. Protein extracts of FB1*wee1-HA* (control), FB1P_{crg1}:*pcl12 wee1-HA,* FB1*cdc25-HA* (control), FB1P_{crg1}:*pcl12 cdc25-HA* grown in CMD (0 hours) and in inducing conditions (CM medium with arabinose and raphinose) at 2 and 4 hours were separated by SDS-PAGE. Immunoblots were incubated successively with anti-HP antibody and anti-PSTAIRE, which recognizes Cdk1. Cdk1 was used as loading control since mitotic CDK levels are constant throughout the cell cycle.

5. The Cdk5-Pcl12 complex is required for pheromone-dependent cell cycle arrest

Previous results from the laboratory showed that in response to b-induction, a gene encoding a cyclin called Pcl12 was specifically induced. This cyclin interacts with Cdk5, an essential cyclin-dependent kinase. The Cdk5-Pcl12 complex was required for appropriated polar growth of the b-dependent filament, although no effect during the b-dependent cell cycle arrest was observed (Flor-Parra et al., 2007). Interestingly, during the course of this study it was noted that cells defective in Pcl12 showed defects during the cell cycle arrest in mating, suggesting a role of Pcl12 in pheromone-dependent cell cycle arrest. Therefore we decided analyse more carefully this observation.

First we have observed, using RT-PCR, that *pcl12* transcription was also induced upon activation of the pheromone MAPK cascade (Fig. 38). We also disrupted *pcl12* in the UMS1 strain. We have found that the absence of *pcl12* resulted in a severe delay in the formation of conjugation tube in comparison to the control cells (Fig. 39A) indicating that as it was observed with b-dependent filaments, Pcl12 was required for appropriated polar growth. Additionally, we have also found effects on the cell cycle. While control cells led to long mononucleated filaments in which only the tip portion was filled with cytoplasm, cells lacking *pcl12* were not cell cycle arrested and contained several cellular compartments each with a single nucleus (Fig. 39B).

Since Pcl12 seems to be a specific cyclin for Cdk5, we decided to investigate if this kinase was also necessary to sustain the cell cycle arrest upon activation of *fuz7^{DD}*. Cdk5 kinase in *U. maydis* is essential and therefore we used a previously described temperature-sensitive mutant allele (*cdk5^{ts}*) (Castillo-Lluva et al, 2007). Cells carrying a *cdk5^{ts}* allele are able to grow at permissive temperature (22ºC), whereas at restrictive temperature (34ºC) are unable to grow. An intermediate temperature (30ºC) allows a residual growth. We analysed the nuclear content in the *fuz7$^{DD\ crg1}$ cdk5^{ts}* filaments. For this, mutant cells and control cells (*fuz7^{DD}*) were grown at permissive temperature (22ºC) until exponential phase. After that, cells were shifted to CMA medium to activate *fuz7^{DD}* and incubated at semi-permissive temperature (30ºC). We have observed that the cells were not cell cycle arrested (Fig. 39).
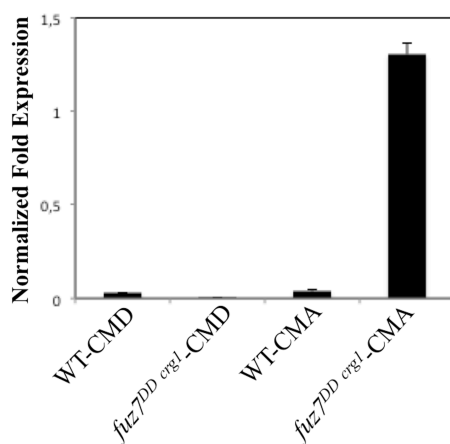
Figure 38: *pcl12* expression is *fuz7^{DD}* dependent. Real-time quantitative RT-PCR analysis of *pcl12* expression in WT (FB1) and *fuz7$^{DD\ crg1}$* (UMS1) grown in CMD and in CMA media. Transcript levels were measured 6 hours after induction. Only *fuz7$^{DD\ crg1}$* cells under induced conditions (CMA) express high levels of *pcl12*. As internal control, the expression of *tub1* (encoding Tubulin α) was used.
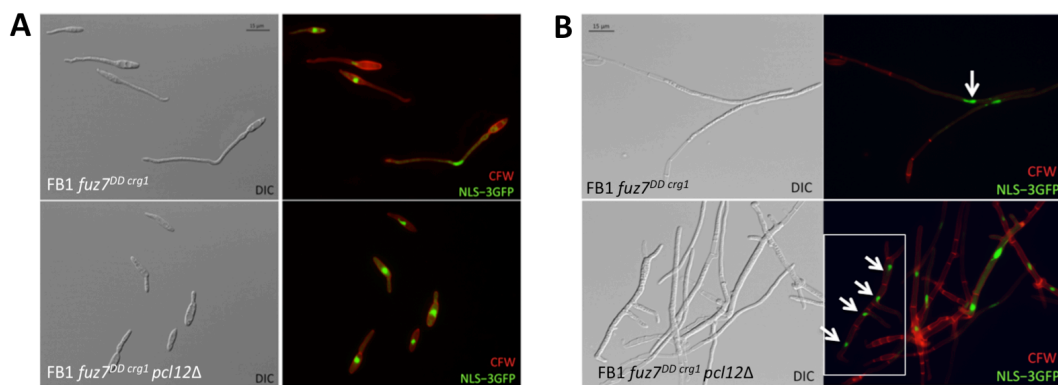
Figure 39: Pcl12 is required for f*uz7^{DD}*-dependent cell cycle arrest. (A) Real-time quantitative RT-PCR analysis of *pcl12* expression in WT (FB1) and *fuz7^{DD crg1}* (UMS1) grown in CMD and in CMA media. Transcript levels were measured 6 hours after induction. Only *fuz7^{DD crg1}* cells under induced conditions (CMA) express high levels of *pcl12*. As internal control, the expression of *tub1* (encoding Tubulin α) was used. **(B)** Microscopic analysis of FB1f*uz7^{DDcrg1}* (UMS1) and its *pcl12*-deletion derivative UMS144 grown in CMA for 8 hours to induce *fuz7^{DD}* expression and **(C)** for 24 hour. *pcl12* deletion delays conjugation tube formation and affects the cell cycle arrest induced by *fuz7^{DD}*. Scale bar: 15μm.

Since Pcl12 seems to be a specific cyclin for Cdk5, we decided to investigate if this kinase was also necessary to sustain the cell cycle arrest upon activation of *fuz7^{DD}*. Cdk5 kinase in *U. maydis* is essential and therefore we used a previously described temperature-sensitive mutant allele (*cdk5^{ts}*) (Castillo-Lluva et al, 2007). Cells carrying a *cdk5^{ts}* allele are able to grow at permissive temperature (22ºC), whereas at restrictive temperature (34ºC) are unable to grow. An intermediate temperature (30ºC) allows a residual growth. We analyzed the nuclear content in the *fuz7^{DD crg1} cdk5^{ts}* filaments. For this, mutant cells and control cells (*fuz7^{DD}*) were grown at permissive temperature (22ºC) until exponential phase. After that, cells were shifted to CMA medium to activate *fuz7^{DD}* and incubated at semi-permissive temperature (30ºC). We have observed that the cells were not cell cycle arrested (Fig. 40).
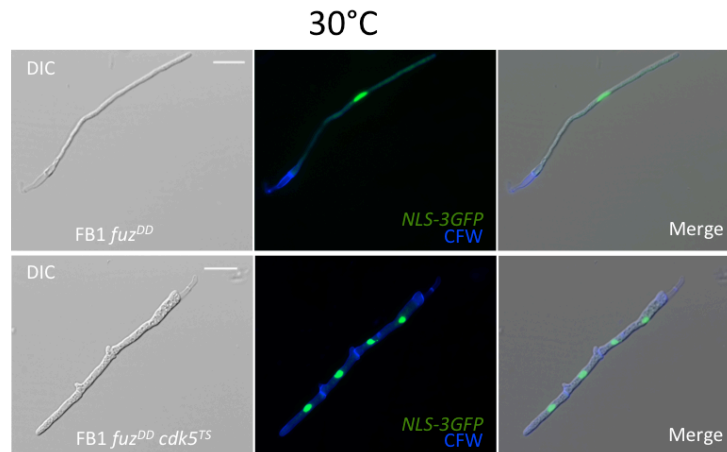
30°C

Figure 40: *fuz7^DD^cdk5^ts^* cells are affected in cell cycle arrest. Cells expressing *fuz7^DD^* arrest at G2 and produce a filament with a single nucleus. However, in *cdk5^ts^* cells, although being able to produce a defective polar growth, upon *fuz7^DD^* activation cell cycle arrest is released giving rise to a filament with several nuclei separated by septa. Scale bar: 15µm.

6. Overexpression of *pcl12* mimics the Fuz7DD-dependent cell cycle arrest

During the characterization of the role of Pcl12 in the b-dependent filament, it was described that the ectopic overexpression of *pcl12* under the control of *crg1* promoter in a wild type haploid strain was enough to induce a cell cycle arrest in G2 that was associated to a strong polar growth (Flor-Parra et al., 2007). We wished to determine whether this ectopic cell cycle arrest was also dependent on Cdk5. We have introduced an allele carrying the *pcl12* gene under the control of *crg1* promoter in a wild type background that carries a NLS-GFP reporter as well as in a similar strain, carrying in addition, the *cdk5^ts^* allele. We have induced the *crg1* promoter in conditions of semipermissive temperature for *cdk5^ts^*. We have found that while cells carrying a wild type *cdk5* allele were cell cycle arrested and produced a strong polar growth, the cells carrying the *cdk5^ts^* allele rarely were able to grow as filaments and the very few observed harboured cell compartments with one nucleus each and separated by septa (Fig. 41). This result indicates that Cdk5 is required for the role of Pcl12 in both promotion of polar growth and cell cycle arrest.

We also analysed whether the Pcl12-Cdk5-dependent cell cycle arrest was dependent on Fuz7 and Kpp2. For that we have ectopically expressed *pcl12* in strains lacking the genes encoding these kinases. Interestingly we

have found that in these conditions neither Fuz7 nor Kpp2 were required for the promotion of cell cycle arrest (Fig. 42).
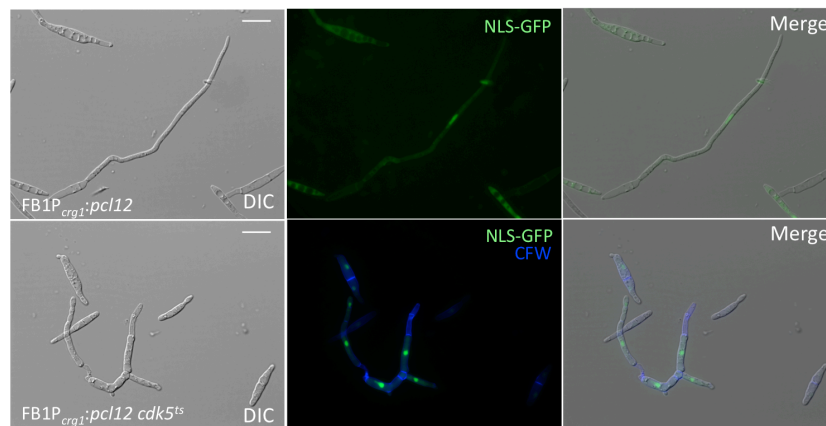
Figure 41: P$_{crg1}$:*pcl12cdk5^{ts}* cells are affected in cell cycle arrest and in filamentous growth. Scale bar: 15µm.
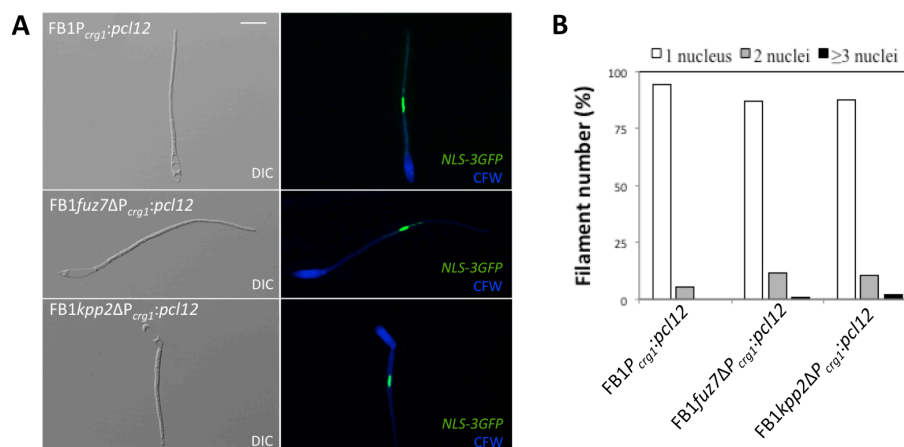
Figure 42: Neither Fuz7 nor Kpp2 are necessary for Pcl12-mediated cell cycle arrest. Scale bar: 15µm.

We decided to study in more detail the arrest triggered by the ectopic *pcl12* overexpression. To avoid the presence of two copies of *pcl12* (one endogenous and the other ectopic) in the same cell, first we have exchanged the endogenous promoter of *pcl12* by the regulatable promoter *crg1*. The corresponding allele, *pcl12^{crg1}*, works as well as the ectopic copy in the promotion of polar growth and cell cycle arrest.

In first place, we wondered whether the cell cycle arrest induced by *pcl12* was dependent on Cdk1 inhibitory phosphorylation as it occurs in cell cycle arrest induced by *fuz7^{DD}*. For that, we have introduced an ectopic copy of the

mutant *cdk1^{AF}* allele under the control of *crg1* promoter in a *pcl12^{crg1}* background. This way *cdk1^{AF}* and *pcl12* were simultaneously expressed. As a control, we introduced an ectopic copy of the wild type *cdk1* also under the control of *crg1* promoter and in a *pcl12^{crg1}* background. Encouragingly we have observed that as it happens in the *fuz7^{DD}*-induced cell cycle arrest, the *pcl12*-induced cell cycle arrest was also dependent on the Cdk1 inhibitory phosphorylation (Fig. 43).

We also sought to analyse the Wee1 and Cdc25 levels upon *pcl12* overexpression. We observed similar results in comparison with alteration of protein levels upon *fuz7^{DD}* induction (Fig. 44). Levels of Cdc25 seemed also to be decreased upon *pcl12* overexpression (Fig. 44A). It is worth to mention that response to *pcl12* induction is more immediate than response to *fuz7^{DD}*. In two hours of induction, it is already observed many *pcl12*-mediated filaments while few and short f*uz7^{DD}*-mediated filaments are observed. This correlates with results obtained from western blot. At two hours of incubation, it seems that Cdc25 protein levels seem to be lower in P$_{crg1}$:*pcl12* cells than in *fuz7^{DD}* cells.
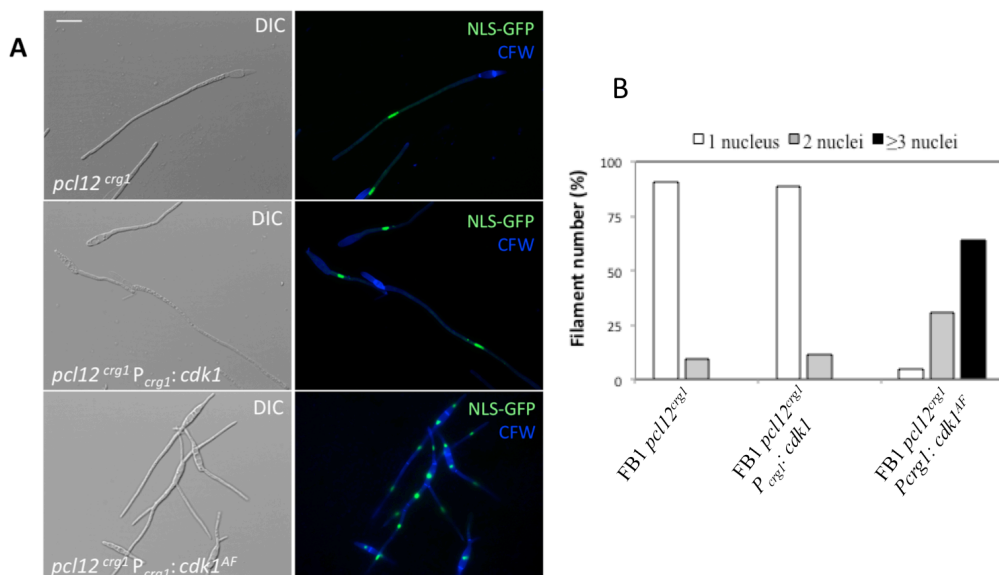
Figure 43: Cdk1 refractory to inhibitory phosphorylation affects the number of nuclei in filaments induced by *pcl12* overexpression. (A) Microscopic pictures of FB1*pcl12^{crg1}* and FB1*pcl1 ^{crg1}*P$_{crg1}$: *cdk1* control strains and FB1*pcl12^{crg1}*P$_{crg1}$: *cdk1^{AF}*. Cells carry a NLS-3GFP fusion to visualize the nuclei **(B)** Quantification of cells carrying single, two and three or more nuclei after induction of *pcl12*. In *cdk1^{AF}* mutant, the frequency of cells with more than one nucleus was drastically increased. Scale bar: 15µm.
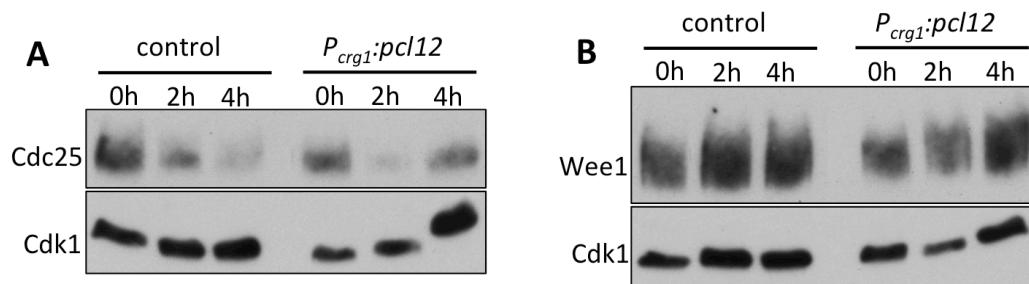
Figure 44: Levels of Cdc25 protein seem to be decreased upon *pcl12* activation. Protein extracts of FB1*wee1-HA* (control), FB1P$_{crg1}$:*pcl12 wee1-HA*, FB1*cdc25-HA* (control), FB1P$_{crg1}$:*pcl12 cdc25-HA* grown in CMD (0 hours) and in inducing conditions (CM medium with arabinose and raphinose) at 2 and 4 hours were separated by SDS-PAGE. Immunoblots were incubated successively with anti-HP antibody and anti-PSTAIRE, which recognizes Cdk1. Cdk1 was used as loading control since mitotic CDK levels are constant throughout the cell cycle.

7. The Ime2-like kinase Crk1 was required for *fuz7^DD^*-dependent cell cycle arrest

The gene *crk1* encodes a protein with sequence similarity to *S. cerevisae* Ime2, which was described to play roles in the induction of *a* locus expression. It was also described that Crk1 has roles in the promotion of polar growth, but its possible involvement in the formation of the conjugative tube was never assessed. Therefore we have deleted the *crk1* gene in strains carrying the *fuz7^DDcrg1^* allele and we have found the formation of filaments carrying several nuclei that were separated by septa (Fig. 45). We have constructed a double *crk1 pcl12* mutant and we have found the same defects, suggesting that for cell cycle arrest both genes work in the same genetic pathway.

Figure 45: Crk1 is necessary for maintaining the cell cycle arrest induced by *fuz7^{DD}* overexpression. (A) Microscopic analysis of UMS1 (FB1*fuz7^{DDcrg1}*), UMS125 (FB1*fuz7^{DDcrg1}crk1Δ*) and FB1*fuz7^{DDcrg1}pcl12Δcrk1Δ* cells grown under *fuz7^{DD}* expression conditions (CMA) for 6 hours **(B)** and for overnight. Scale bar: 15μm.

8. Crk1 was required for Pcl12-dependent cell cycle arrest

pcl12 under the control of arabinose-inducible *crg1* promoter was ectopically expressed in a strain carrying a deletion of the *crk1* gene as well as a nuclear marker (NLS-GFP) to allow the monitoring of the nuclear content. Cells of the resulting *crk1Δ* strains were grown in CMA media in order to induce the expression of *pcl12*. In a coherent way to what it was observed from the genetic search, we have found that this strain, although able to grow in a filamentous way, was not cell cycle arrested. Microscopic investigation revealed that after 8 hours of induction UMS176 cells showed a release of cell cycle arrest, around 50% cells contained two nuclei as it can be observed in the panel A of figure 46. The cultures were grown in CMA medium for longer period (overnight). The control displayed an extensive polarized growth and single nuclei content, and empty sections behind that were separated by septa generated by formation of basal vacuoles as result of a permanent G2 cell cycle arrest. The panel on the right shows a detailed view septa-separated empty sections between cells formed in absence of Crk1. These observations supported a role for Crk1 in cell cycle arrest. It is worth to mention that overexpression of *crk1* did not arrest the cell cycle. Although *crk1*

overexpression induced polar growth, cells carried several nuclei (Fig. 47B). In addition, *crk1* expression levels were not significantly increased upon *fuz7*[DD] activation (Fig. 47A). Thus, while *pcl12* is sufficient and necessary for cell cycle arrest at G2 phase, *crk1* is necessary but not sufficient.

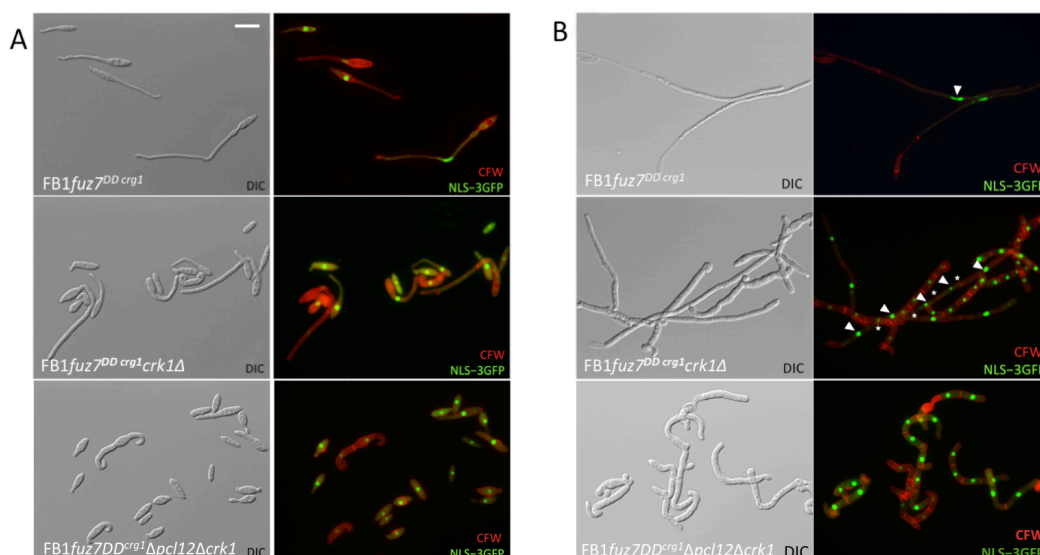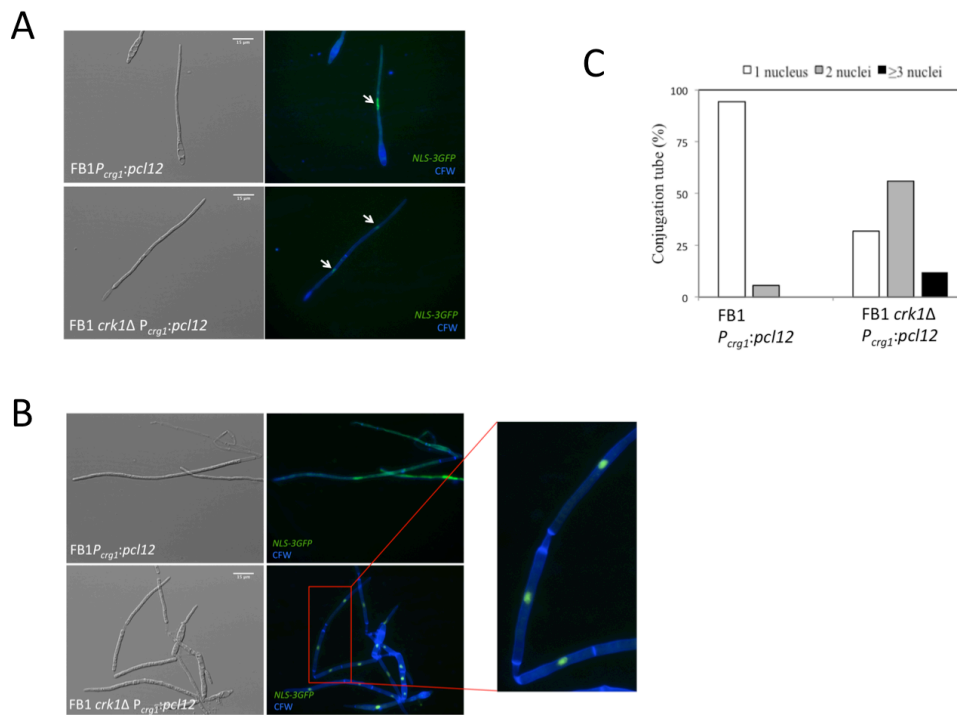**Figure 46: Crk1 is necessary for maintaining the cell cycle arrest induced by *pcl12* overexpression. (A)** Microscopic analysis of UMS170 (P*crg1*:*pcl12*) and UMS176 (*crk1*ΔP*crg1*:*pcl12*) cells grown under *pcl12* expression conditions (CMA) for 8 hours **(B)** and for overnight. Arrows mark the nuclei. **(C)** Quantification of the number of nuclei per filament from each strain after induction of *pcl12*. Scale bar: 15µm.
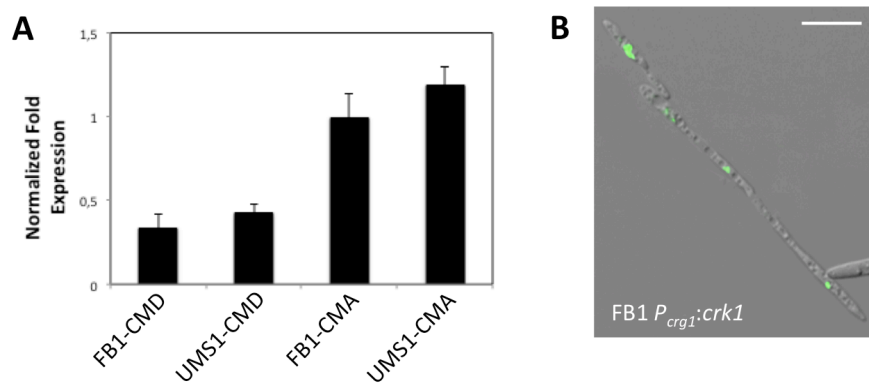
Figure 47: *crk1* expression is not sufficient to sustain cell cycle arrest. (A) Real-time quantitative RT-PCR analysis of *crk1* expression in WT (FB1) and in *fuz7*[DD crg1] (UMS1) grown in CMD and in CMA media. Transcript levels were measured 6 hours

after induction. *crk1* levels were not significantly altered upon *fuz7^{DD}* activation. As internal control, the expression of *tub1* (encoding Tubulin α) was used. **(B)** Microscopic picture of FB1P_{crg1}:*crk1* incubated in CMA to induce *crk1*. Overexpression of *crk1* triggered polar growth but it was not sufficient to induce cell cycle arrest. Nuclei were stained with DAPI. Scale bar: 15μm.

9. MAPKK phosphorylation sites of Crk1 were required to sustain both *fuz7^{DD}*- and *pcl12*-dependent cell cycle arrests

Previous work from our laboratory showed that the ability to promote polar growth by the Crk1 kinase was dependent on Fuz7 and Kpp2. In the first case, it was described that Crk1 has the TXY dual phosphorylation motif characteristic of MAP kinases, and that most likely Fuz7 was able to activate Crk1 by phosphorylation of these residues. In addition two sites of MAPK phosphorylation were described at the C-terminal end of Crk1, and it was suggested that they were the targets of Kpp2. Since Pcl12-dependent cell cycle arrest was dependent on Crk1, and independent on Fuz7 and Kpp2, we wondered whether the phosphorylation of these sites was required to sustain the *pcl12* overexpression-dependent cell cycle arrest. To test this, we generated a mutant of Crk1 unable to accept phosphates at the conserved TEY motif (*crk1^{AEF}*), and other mutant at the two sites at the C-terminal of Crk1 (*crk1^{AAA}*), in a P_{crg1}:*pcl12* background. We observed that while cells expressing the *crk1^{AAA}* allele harboured only one nucleus per filament produced, cells expressing the *crk1^{AEF}* allele harboured many nuclei, showing a similar phenotype to that observed in the absence of Crk1. This result indicated that T-loop phosphorylation but not C-terminal phosphorylation was required for the role played by Crk1 in sustaining cell cycle arrest at G2 phase. Since Fuz7 has been described to phosphorylate Crk1 at T-loop, we postulate that upon pheromone signalling Fuz7 might phosphorylates Crk1 to trigger cell cycle arrest. However, upon *pcl12* overexpression, Fuz7 is not required for the cell cycle arrest. One possibility to explain this result would be the existence of other MAPKK that could replace Fuz7 in its absence. Another possibility would be that the complex Pcl12-Cdk5 phosphorylates Crk1.
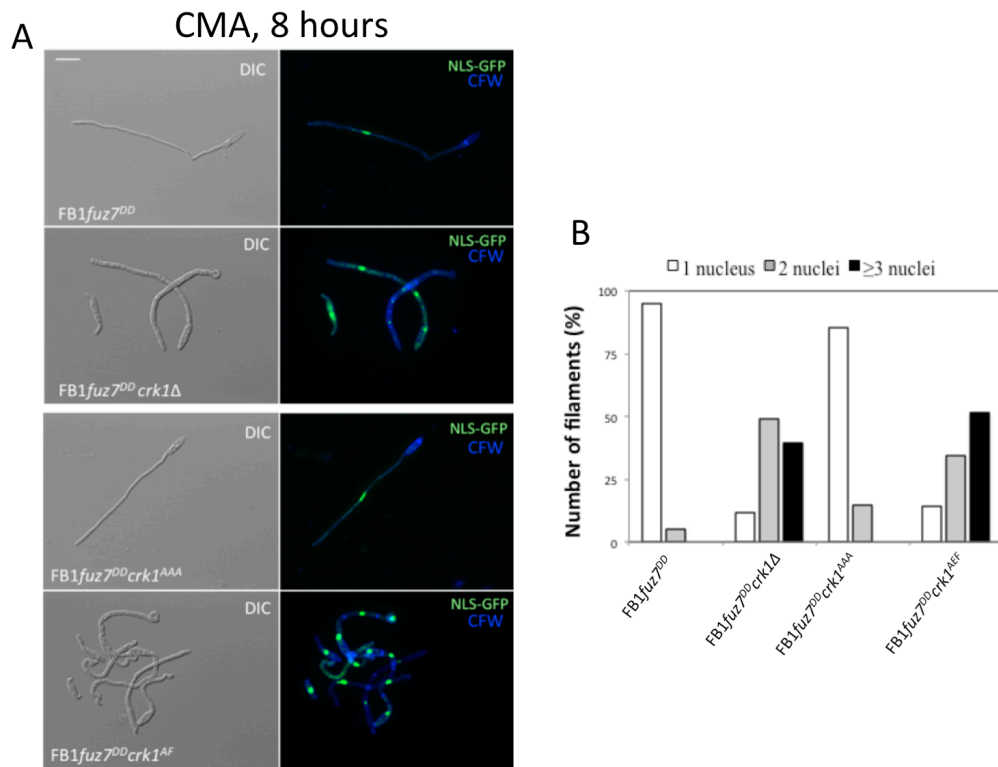
Figure 48: TEY phosphorylation motif is required for the role of Crk1 in sustaining cell cycle arrest mediated by *pcl12* overexpression. (A) Microscopic analysis of filaments from strains FB1*fuz7^{DD}*, FB1*fuz7^{DD}crk1Δ*, FB1*fuz7^{DD}crk1^{AAA}* and FB1*fuz7^{DD}crk1^{AF}*. Cells were incubated in CMA medium for 8 hours to induce *fuz7^{DD}* expression. Cells carry a NLS-3GFP fusion to visualize the nuclei. Scale bar: 15µm. **(B)** Quantification of filaments containing the number of nuclei indicated per filament in control and in *crk1* mutant strains. In *crk1Δ* and *crk1^{AEF}*, the frequency of filaments released from cell cycle arrest is increased.
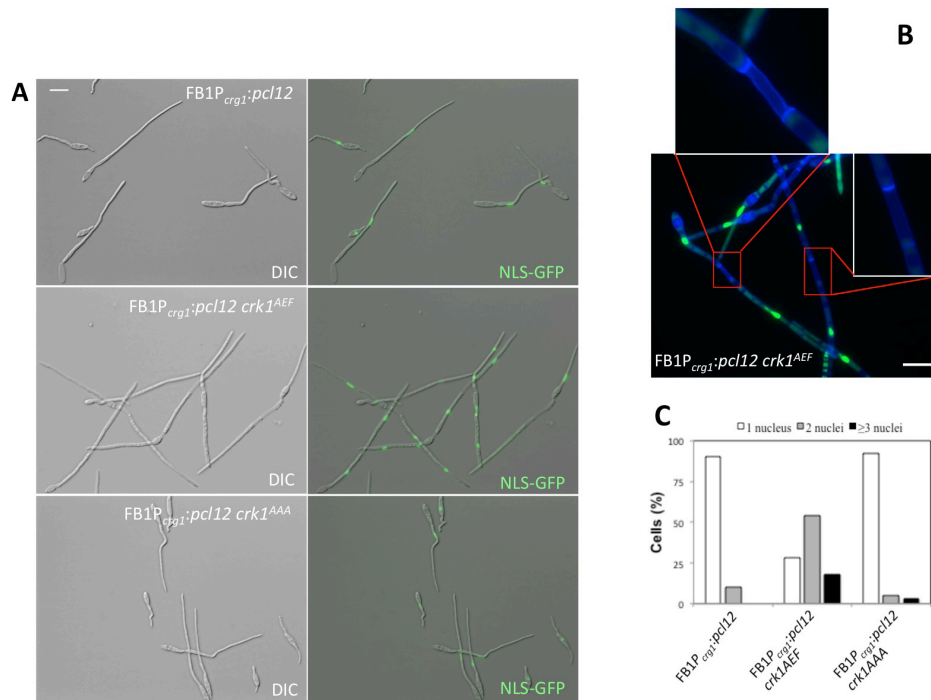
Figure 49: TEY phosphorylation motif is required for the role of Crk1 in sustaining cell cycle arrest mediated by *pcl12* overexpression. (A) Microscopic analysis of filaments from strains FB1P$_{crg1}$:*pcl12*, FB1P$_{crg1}$:*pcl12 crk1*^{AEF} and Fb1P$_{crg1}$:*pcl12 crk1*^{AAA}. Cells were incubated in CMA media for 8 hours to induce pcl12 expression. Scale bar: 15 µm. **(B)** Detailed view of septa-separated empty sections between cells formed in absence of Crk1. **(C)** Quantification of filaments containing the number of nuclei indicated per filament in control and in *crk1* mutant strains after 8 hours of induction. In *crk1*Δ and *crk1*^{AEF}, the frequency of filaments released from cell cycle arrest is increased.

Discussion

In this work, we have studied two cell cycle arrests that occur during formation of the infective filament. We have tried to understand the mechanism behind these sops in cell cycle to uncouple cell cycle arrest from the rest of processes during filament formation. The most important findings will be first discussed separately for each cell cycle arrest, and then we will try to integrate the findings of both arrests.

b-induced G2 cell cycle arrest

It has previously been reported that the activation of the DDR kinase Chk1 confers immediate arrest. This arrest is nevertheless transient as infective filaments defective for Chk1, or its activating kinase Atr1, eventually arrest their cell cycle after one or two nuclear divisions (de Sena-Tomas et al., 2011; Mielnichuk et al., 2009). We hypothesized that during the formation of the infective filament, the activation of the Chk1 kinase induces a transient cell cycle arrest providing a time frame during which additional mechanisms are recruited to sustain a long-term cell cycle arrest. We reasoned that a mechanism could be the down-regulation of some genes encoding elements needed for G2/M transition by the b-dependent transcriptional program. In this study we have found that *hsl1* down-regulation upon b-induction promotes the referred sustained cell cycle arrest.

Hsl1 belongs to the Nim1 family of kinases. In budding and fission yeasts, these kinases were described as positive regulators of G2/M transition, whose inactivation resulted in a prolonged G2 phase (Barral et al., 1999; Feilotter et al., 1991; Kanoh and Russell, 1998). We have found a similar effect in *U. maydis* cells lacking Hsl1 during growth in axenic conditions. The cell cycle target of Nim1 kinases in budding and fission yeasts is the kinase Wee1, and our epistasis analysis suggests that it could be also the case for *U. maydis*. In *S. cerevisae*, the Nim1 family kinases collaborate through a still unclear mechanism to promote degradation of Swe1 (King et al., 2012; McMillan et al., 2002; Sia et al., 1998). In contrast in *S. pombe*, Nim1 and Cdr2 kinases seem not to affect the protein levels of Wee1 but they inhibit its activity (Coleman et al., 1993; Kanoh and Russell, 1998; Wu and Russell, 1993). We have found that for *U. maydis* the absence of Hsl1 resulted in an increase in the levels of

Cdk1 inhibitory phosphorylation. However, the levels of Wee1 protein in these mutant cells seem to be similar to those observed in control cells.

In *S. cerevisae*, Nim 1 like kinases are involved in the "morphogenetic checkpoint" which couples bud formation to the cell division cycle by delaying nuclear division until cells have successfully formed a bud (Lew, 2000; Lew and Reed, 1995). Although it is unknown whether a "morphogenetic checkpoint" is operative in *U. maydis*, we observed defects in cell separation in *hsl1* mutants. In addition, we found that Hsl1 locates at the bud neck, similarly to the *S. cerevisae* orthologs (Barral et al., 1999). In contrast, *S. pombe* Nim1 and Cdr2 have been proposed to be part of the mechanism that coordinates cell size and mitosis (Martin and Berthelot-Grosjean, 2009; Moseley et al., 2009; Pan et al., 2014). This way, these kinases are responsible for adapting the G2/M transition to nutritional conditions (Belenguer et al., 1995; Kanoh and Russell, 1998). It is also unknown whether a similar mechanism is operative in *U. maydis*, but we have found that Hsl1 seems to play a role in the adaptation of the cell cycle to nutritional conditions. In summary, it is likely that in *U. maydis* Hsl1 assumes some of the roles described in budding and fission yeasts.

Regardless of the actual role of Hsl1 during vegetative cell cycle in *U. maydis*, in this study we have examined the relevance of the cell cycle arrest for the infection process. Although sustained *hsl1* expression alone was not sufficient to disable the cell cycle arrest upon b-induction, we have found that in combination with the deletion of *chk1*, the resulting b-dependent filaments were not cell cycle arrested. It is worth noting that a two-step mechanism to promote cells, genotoxic stress induces a G1 arrest that is sustained over a prolonged period of time. The initial process is fast and is mediated by cyclin D1 degradation. At a later stage, p53 activity is required to maintain the arrest. However, the p53 activity is dispensable for G1 arrest during the initial period (Agami and Bernards, 2000). In *U. maydis*, the two independent proposed mechanisms seem to act through the same cell cycle regulatory node: the inhibitory phosphorylation of Cdk1. Chk1 activation results in the inhibition of Cdc25, the phosphatase that removes the inhibitory phosphorylation (Mielnichuk et al., 2009; Sgarlata and Perez-Martin, 2005a), while in the case of down-regulation of Hsl1 we suggest that the Wee1 activity –responsible for the inhibitory phosphorylation of Cdk1– is increased. The imbalance in these

opposing activities (phosphatase and kinase) helps to explain the previously observed accumulation of inhibitory phosphorylation of Cdk1 upon activation of the b-dependent transcriptional program, which is ultimately responsible for the cell cycle arrest in G2 (Mielnichuk et al., 2009a).

Being able to disable the b-dependent cell cycle arrest, we generated double mutant haploid sexually compatible strains enabling us to address the importance of the cell cycle arrest during the infective process in *U. maydis*. These strains were able to mate and to produce infective filaments that were not cell cycle arrested. Importantly, these strains were severely impaired in their virulence. The mutant infective filaments that did not arrest the cell cycle were unable to produce appressoria, either on plant surface or on hydrophobic surface under *in vitro* conditions. The appressorium formation occurs in a localized area of secretion where plant cell-wall degrading enzymes that help the penetration of cuticule (Schirawski et al., 2005) and specific effector proteins required for signalling during infection (Djamei and Kahmann, 2012) are concentrated. Hence appressorium formation is essential during the infective process in *U. maydis*, and mutants affected in this step are severely impaired in virulence (Berndt et al., 2010; Fernandez-Alvarez et al., 2009; Fernandez-Alvarez et al., 2012; Freitag et al., 2011; Lanver et al., 2010). Therefore, it appears that the lack of virulence of non-cell cycle arrested filaments is a consequence of the inability to produce appressoria. The connections between specific cell cycle phases and appressorium formation have been observed in other fungi that produce appressoria markedly different in form and function from the ones produced in *U. maydis*. An example is the appressorium formed by *M. oryzae*. By using inhibitors of DNA replication and conditional mutants in cell cycle regulators, it was found that the regulation point for initiating appressorium development must occur prior to mitosis and depends on a full DNA replication. However, so far no clue has been provided into how the connection between cell cycle and appressorium differentiation is orchestrated at molecular level neither the consequences of uncoupling cell cycle regulation from the appressorium development.

Basal septation in the b-dependent filament has been reported to be important for appressorium formation (Freitag et al., 2011). Because Hsl1 seems to have some role in septation in *U. maydis*, it is worth to point out that

the filaments expressing constitutively *hsl1* alone showed no differences in basal septa formation when compared to control filaments.

We propose a working model to explain the mechanism by which b-factor triggers the cell cycle arrest at G2 phase in order to be able to develop appressorium (Fig. 50). We considered a notion that the putative regulators that activate the appressorium formation could be down-regulated in some way (directly or indirectly) by the activity of the Cdk1-B cyclin complexes. In *U. maydis* there are two Cdk1-B cyclin complexes (García-Muse et al., 2004). The Cdk1-Clb2 complex is the main activator of mitosis entry and it is the target of inhibitory phosphorylation by Wee1 (Sgarlata and Perez-Martin, 2005b). Cdk1-Clb1 in contrast has role both in G1/S and G2/M transitions (Sgarlata and Perez-Martin, 2005b). We propose that in order to produce the appressorium, both complexes should be down-regulated. According to our work model, Cdk1-Clb2 may be repressed through the increase of the inhibitory phosphorylation of the Cdk1 by the two-step mechanism discussed above, whereas the Cdk1-Clb1 complex would be repressed through the transcriptional down-regulation of *clb1* upon binding of Biz1 to its promoter (Flor-Parra et al., 2006). In both cases, the trigger of these down-regulations would be the b-factor acting through distinct regulatory circuits. In this study, we have shown that disabling the machinery involved in the inactivation of Cdk1-Clb2 complex render the fungus unable to produce appressoria. Also, it has previously been reported that *U. maydis* cells in which the *clb1* mRNA levels were kept high, either because they were defective in *biz1* or simply bypassing the repression of *clb1* expression by altering the native promoter, were impaired in appressoria formation (Flor-Parra et al., 2006).

In summary, for the study of b-induced cell cycle arrest in *U. maydis*, we provide clues to understand the interdependent relationship between cell cycle regulation and the program devoted to produce appressoria. Appressorium formation and cell cycle progression seem to be mutually exclusive choices, a principle that could be applied in a broader sense to other fungal systems.
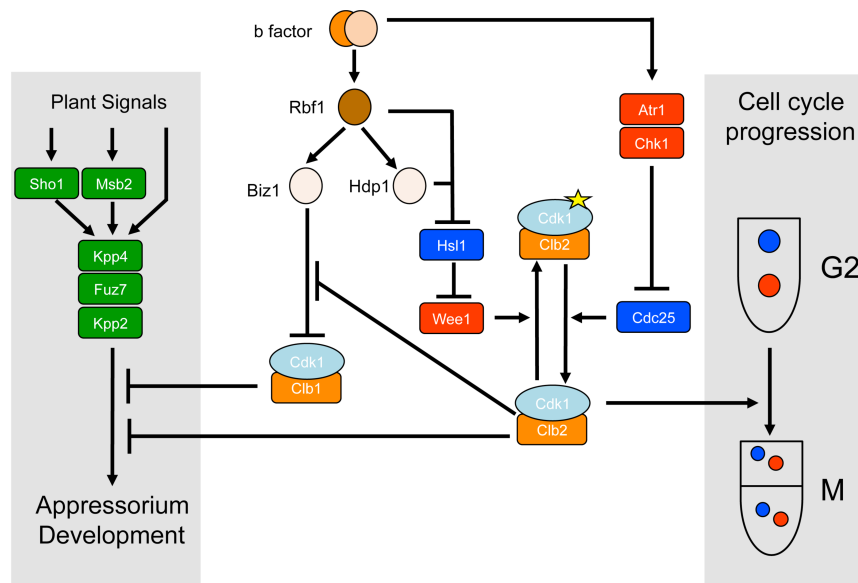
Figure 50. The developmental program required for appressorium formation is incompatible with an active cell cycle. Cdk1-B cyclin complexes inhibit still unidentified targets required for the formation of appressoria. To allow the induction of appressoria during the infective process, the activity of these CDK complexes should be previously down-regulated, which occurs at different levels upon induction of b-factor. Clb1-Cdk1 complexes are down-regulated by the action of Biz1, a transcriptional repressor of *clb1* gene. The Clb2-Cdk1 complexes are repressed by inhibitory phosphorylation of Cdk1 (yellow star), resulting from the up-regulation of the kinase Wee1 (because the b-dependent down-regulation of its negative regulator Hsl1) and down-regulation of the phosphatase Cdc25 (because the activation of the DDR kinases Atr1 and Chk1).

Pheromone-induced G2 cell cycle arrest

Prior to our study, it was established that pheromone signalling through a MAPK pathway induces a cell cycle arrest at G2 phase of the cell cycle (Garcia-Muse et al., 2003). A cell cycle arrest upon pheromone stimulation has also been observed in other fungi as *S. cerevisae* and *S. pombe* ascomycete yeasts (Davey, 1998; Pope et al., 2014). The arrest in the cell cycle progression allows cells to growth in a polarized way, forming conjugation tubes and preparing the fusion between two haploid cells. A major difference in cell cycle arrest mediated by pheromone between *U. maydis* and ascomycetes yeasts is the cell cycle stage at they arrest: ascomycete yeasts at G1 phase and *U. maydis* at G2 phase. This suggests the existence of different mechanisms wiring the pheromone response and the cell cycle between these model yeasts. The

particular cell cycle arrest at G2 phase in *U. maydis* seems to be related to the formation of infective filament that it will be discussed in more detail later. Our focus here was on the elucidation of the mechanism by which pheromone leads to a specific cell cycle arrest at G2 phase. We have found that Pcl12/Cdk5 complex; Crk1 and the apparent degradation of Cdc25 are implicated in the pheromone-induced cell cycle arrest.

While *S. cerevisae* mates spontaneously, sexual differentiation in *U. maydis* is triggered by starvation when compatible mating partners are present as it occurs in *S. pombe*. To bypass nutritional requirements, we used a haploid strain, in which the native allele of the MAPK kinase Fuz7 was replaced by a constitutively active allele of Fuz7 (*fuz7^{DD}*) under the control of a regulatable promoter. This way, we were able to activate the pheromone pathway without starvation conditions and pheromone addition. We have validated this strain for cell cycle arrest at G2 phase. Results obtained with *fuz7^{DD}* strain have indicated that inhibitory phosphorylation of Cdk1 is part of the mechanism of the pheromone-induced G2 cell cycle arrest, as expression of a mutant allele of Cdk1 refractory to inhibitory phosphorylation impaired the cell cycle arrest. This is in agreement with b-induced cell cycle arrest, in which inhibitory phosphorylation of Cdk1 is the last responsible for blocking cell cycle progression (Mielnichuk et al., 2009).

We analysed the transcriptional pattern of cell cycle related genes in response to overactivation of pheromone pathway and found that transcription levels of *hsl1* were decreased. However, either constitutive expression of *hsl1*, which bypassed its downregulation, alone or in combination with absence of Chk1 did not affected cell cycle arrest. Therefore, f*uz7^{DD}* does not take the previously mechanism used by b-factor to inhibit Cdk1. We suspect that the shutdown of *hsl1* expression upon *fuz7^{DD}* activation has to do with the septin collar structure in the neck of the conjugation tube. The structure of the septin collar when cell starts to form the conjugation tube is different from the structure that is assembled when cell makes a bud. Nevertheless, we do not discard the possibility that Hsl1 is also inactivating Wee1 upon *fuz7^{DD}* induction.

A major challenge has been to understand the wiring between pheromone pathway and inhibitory phosphorylation of Cdk1. Our approach was

based on the searching for downstream targets of MAPK pathway with putative roles in cell cycle.

It was established previously that *pcl12*, which encodes for a cyclin that interacts specifically with Cdk5, plays a role in polar growth and virulence (Flor-Parra et al., 2007). This cyclin is upregulated upon *fuz7^{DD}* induction. When *pcl12* is absent, polar growth is impaired and after prolonged incubation cell cycle arrest is also affected. Accordingly, *pcl12* overexpression is sufficient to induce a strong polar growth and cell cycle arrest at G2 phase. On the other hand Cdk5, an essential CDK in *U. maydis*, has been described to have regulatory roles in morphogenesis and polarity. We found that a non-functional Cdk5 (Cdk5ts) abrogates the role of Pcl12 in polar growth and cell cycle arrest. Thus Pcl12 and Cdk5 most probably act together as a complex to trigger cell cycle arrest and polar growth. Moreover, in *fuz7^{DD}* cells with non-functional Cdk5, upon activation of f*uz7^{DD}*, G2 arrest is clearly released. The more severe effect observed with Cdk5ts than with absence of Pcl12 suggests that Cdk5 have additional cell cycle targets, likely through association to other cyclins.

To narrow our search, we characterized the G2 cell cycle arrest mediated by Pcl12. We found that the inhibitory phosphorylation of Cdk1 is also required to sustain Pcl12-mediated cell cycle arrest. Consequently, we tried to determine the molecular mechanism responsible for inhibitory phosphorylation of Cdk1. Cdk1/Clb2 complex in *U. maydis* is held inactive by the phosphorylation placed by the kinase Wee1 (Sgarlata and Perez-Martin, 2005b) and this inhibitory phosphorylation is reverted by the phosphatase Cdc25 (Sgarlata and Perez-Martin, 2005a). Immunoblot analysis of Cdc25 protein obtained from cellular extracts upon *fuz7^{DD}* and *pcl12* overexpression was indicative of an apparent decrease of Cdc25 protein levels. While catalytic domains of Cdc25 proteins are quite conserved, the regulatory regions are more variable. The non-catalytic domain dictates the intracellular localization and turnover of the phosphatases (Boutros et al., 2007). Sequestration in the cytoplasm of the Cdc25 phosphatase is one of the reasons for b-induced arrest (Mielnichuk and Perez-Martin, 2008). However, our results point to an apparent degradation of Cdc25 that could be in part responsible for pheromone-induced cell cycle arrest.

100

Crk1 was originally found in *U. maydis* (Garcia-Muse et al., 2004; Garrido and Perez-Martin, 2003). It is an ortholog of Ime2, which induces meiosis in *S. cerevisae*. In phytopathogenic fungi, Ime2 proteins have been found to be widely conserved and have been considered as a new family of MAPKs (Hamel et al., 2012). In addition, Ime2-related kinases have demonstrated roles in controlling sexual development programs in fungi (Irniger, 2011). Our results highlight a new role of Crk1 in the regulation of cell cycle upon pheromone pathway activation. By using a nonphosphorylatable Crk1 allele, we found that phosphorylation by an upstream kinase is required for the role that Crk1 plays in cell cycle arrest mediated by both Fuz7DD and Pcl12. Interestingly, in *U. maydis*, the MAPK Fuz7 was found to activate Crk1 via phosphorylation of a TXY motif. Since *U. maydis* naturally mates under starvation conditions and Crk1 has been proposed to integrate environmental signals transmitted by the cAMP and MAPK pathways (Garrido and Perez-Martin, 2003), Crk1 could play an important role in taking the developmental decision of differentiating or not into a conjugation tube, process associated to a specific cell cycle arrest. These results could also help to explain why strains lacking Crk1 were impaired in mating in *U. maydis* (Garrido et al., 2004).

Based on the results obtained for *fuz7^DD*-induced cell cycle arrest, we would like to postulate a working model in which two hypotheses are considered to explain how pheromone triggers a cell cycle arrest at G2 phase. In both hypotheses Pcl12 and Crk1 are necessary. Given that overexpression of *pcl12* in the absence of *crk1*, although being able to grow polar, does not sustain a cell cycle arrest and moreover overexpression of *crk1* is not sufficient to sustain the cell cycle arrest led us to think that Pcl12 associated to Cdk5 could activate Crk1 through phosphorylation on its T-loop (Fig. 51). However, upon pheromone MAPK cascade activation in the absence of *crk1* the cell cycle arrest release is much more severe than in the absence of *pcl12*. These results led us to favour the second hypothesis (Fig. 51) in which Pcl12 and Crk1 act in parallel pathways to trigger cell cycle arrest. In this case, either Fuz7 or other MAPK kinase would activate Crk1 upon pheromone signalling. While, in both hypotheses, upon phosphorylation on its T-loop, Crk1 would enter into the nucleus where it would phosphorylate Cdc25 phosphatase targeting it for degradation. According to hypothesis B (Fig. 51) Pcl12-Cdk5 could also

phosphorylates Cdc25. We have performed an assay of affinity purification using TAP-tagged truncated Pcl12 protein and after mass spectrometer analysis an E3-ubiquitin ligase was identified: Hwe1 that belongs to the HECT (E6-AP carboxyl terminus) family of E3 ubiquitin ligases (Bernassola et al., 2008). The absence of Hwe1 released the cell cycle arrest upon both *fuz7^{DD}* and *pcl12* overexpression. Therefore, it would be very tempting to speculate that this ubiquitin ligase recognizes Cdc25 phosphorylated, promoting its degradation. Future work will focus on the characterization of this ubiquitin ligase and on its putative role over Cdc25. Accordingly to both hypotheses, the phosphorylation placed on Cdk1 by Wee1 kinase cannot be removed by Cdc25 phosphatase due its degradation, and consequently inactive Cdk1 is unable to promote progression of cell cycle into mitosis.

In summary, for the pheromone-induced cell cycle arrest, we have found downstream effectors of pheromone pathway required for G2 cell cycle arrest. We have proposed two putative mechanisms by which these effectors are wired with the pheromone pathway and the inhibitory phosphorylation of Cdk1 in order to mediate cell cycle arrest.
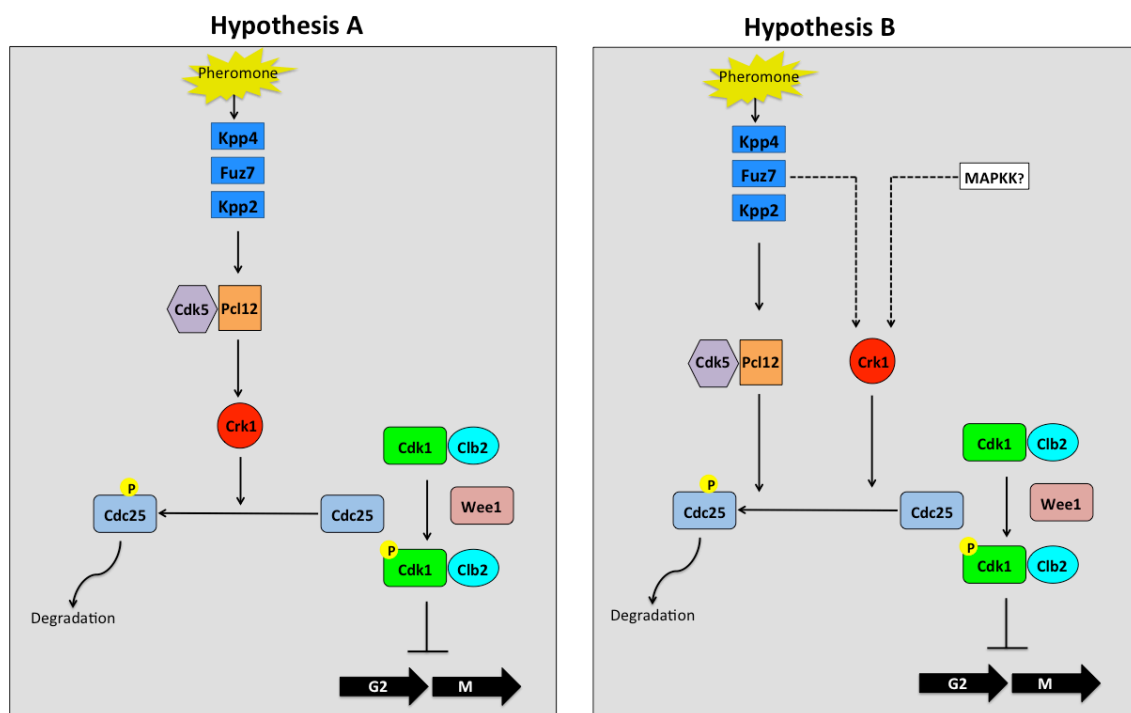

Figure 51: Working model for pheromone-induced cell cycle arrest in *U. maydis*. (Hypothesis A) Upon pheromone cascade activation, pcl12-Cdk5 phosphorylates Crk1, which in turns phosphorylates Cdc25 targeting it for degradation. **(Hypothesis B)**

Upon pheromone cascade induction, activated Crk1 and Pcl12 associated to Cdk5 act in parallel pathways to inactivate Cdc25 phosphatase. In both hypotheses, inhibitory phosphorylation of Cdk1 placed by the kinase Wee1 cannot be reverted and thereby cell cycle is arrested.

Pheromone- and b-induced G2 cell cycle arrests

In this study, we have tried to characterize two cell cycle arrests at G2 phase that happen during sexual development associated to virulence in *U. maydis*. Both arrests are sustained continuously, however the pheromone-induced arrest is controlled by *a* locus and b-induced cell cycle arrest by *b* locus. Importantly, the cell cycle is released only after penetration of the host plant. While pheromone-induced cell cycle arrest seems to be a transient arrest, in which cells still can go back to their vegetative form, depending on the balance between environmental conditions and sexual development costs, b-induced cell cycle arrest is permanent. In this case, cells already have made the development decision of mating and therefore, a more strict control on cell cycle is considered to occur. Concerning cell cycle arrest mediated by pheromone, it was already known to be necessary to synchronize cells before mating in order to the infective filament inherit same DNA content from each cell. Our focus here was on shedding new light on the molecular mechanism by which pheromone arrests cell cycle at G2 phase. For b-induced cell cycle arrest, we found in this study that is necessary to differentiate the appressorium infective structure. This finding was achieved upon being able to uncouple cell cycle from the rest of processes occurring during b-filament development.

As we previously said, in contrast to ascomycete yeasts, the pheromone induces a cell cycle arrest at G2 phase in *U. maydis*. We propose that this is due to the following differentiation process in the sexual cycle of this fungus: the production of an infective filament that undergoes a strong polar growth and a G2 cell cycle arrest. This filament allows *U. maydis* to explore the host plant surface until it differentiates into an appressorium. In this phytopathogen, the cytoskeletal machinery is set up during G2 phase and therefore a prolonged G2 phase will be best suited to support polar growth during infective hyphae formation. Additionally, in *U. maydis*, as it happens in other systems, entry into mitosis demands the recruitment of a large quantity of cytoskeletal elements to

form the mitotic simple (Straube et al., 2005). Therefore it is likely that mitosis and the morphogenetic program responsible for the b-filament and appressorium formation compete for the same cytoskeletal components. If this is the case, it makes sense that cellular controls exist to force these two processes to be incompatible. Interestingly, this sort of incompatibility is akin to developmental processes in metazoans. For example, during the formation of the neural tube in *Ciona* intestinalis embryos, epidermal cells have to change their morphology to fuse each other, requiring for that a massive cytoskeleton remodelling. During this process mitosis is inhibited, lengthening the G2 phase, being the inhibitory phosphorylation of CDK the cell cycle regulatory target (Ogura et al., 2011).

Both pheromone- and b-mediated cell cycle arrests depend on inhibitory phosphorylation of Cdk1. However, the mechanisms used by *a* and *b* locus to inhibit Cdk1 seem to be different. We wish to be able to confirm that degradation of Cdc25 is involved in the pheromone-induced cell cycle arrest. It would be interesting that in one arrest Cdc25 is regulated by a kinase of developmental choices (Crk1) and in other case regulated by a DNA-damage checkpoint kinase (Chk1).

With the findings of this study, we hope to provide clues for futures studies in the connections between cell cycle and development processes in other pathogenic fungi.

Conclusions

1. The expression levels of *hsl1* are downregulated upon b factor induction regardless of cell cycle arrest

2. Hsl1 in *U. maydis* is related to Nim1-like kinases, acting as a negative regulator of Wee1

3. Two distinct mechanisms involving Hsl1 and Chk1 sustain the b-induced G2 cell cycle arrest

4. G2 cell cycle arrest in infective hyphae is important for virulence

5. G2 cell cycle arrest is essential for appressorium formation

6. Pheromone and b factor use distinct mechanisms to arrest cell cycle

7. Pcl12 is sufficient and necessary for cell cycle arrest

8. Crk1 phosphorylation on its TXY loop is necessary for pheromone-induced cell cycle arrest

9. Levels of Cdc25 are apparently decreased upon pheromone induction

Bibliography

Agami, R., and R. Bernards. 2000. Distinct initiation and maintenance mechanisms cooperate to induce G1 cell cycle arrest in response to DNA damage. *Cell*. 102:55-66.

Ausubel, F.M., R. Brent, R.E. Kingston, D.D. Moore, J.G. Seidman, J.A. Smith, and K. Struhl. 1997. Current Protocols in Molecular Biology. Ed. Wiley, New York.

Bachewich, C., and M. Whiteway. 2005. Cyclin Cln3p links G1 progression to hyphal and pseudohyphal development in Candida albicans. *Eukaryot Cell*. 4:95-102.

Banuett, F., and I. Herskowitz. 1989. Different a alleles of Ustilago maydis are necessary for maintenance of filamentous growth but not for meiosis. *Proc Natl Acad Sci U S A*. 86:5878-5882.

Banuett, F., and I. Herskowitz. 1994. Identification of fuz7, a Ustilago maydis MEK/MAPKK homolog required for a-locus-dependent and -independent steps in the fungal life cycle. *Genes Dev*. 8:1367-1378.

Banuett, F., and I. Herskowitz. 1996. Discrete developmental stages during teliospore formation in the corn smut fungus, Ustilago maydis. *Development*. 122:2965-2976.

Barral, Y., M. Parra, S. Bidlingmaier, and M. Snyder. 1999. Nim1-related kinases coordinate cell cycle progression with the organization of the peripheral cytoskeleton in yeast. *Genes Dev*. 13:176-187.

Belenguer, P., L. Pelloquin, V. Baldin, M.L. Oustrin, and B. Ducommun. 1995. The fission yeast Nim1/Cdr1 kinase: a link between nutritional state and cell cycle control. *Prog Cell Cycle Res*. 1:207-214.

Bensen, E.S., A. Clemente-Blanco, K.R. Finley, J. Correa-Bordes, and J. Berman. 2005. The mitotic cyclins Clb2p and Clb4p affect morphogenesis in Candida albicans. *Mol Biol Cell*. 16:3387-3400.

Berman, J. 2006. Morphogenesis and cell cycle progression in Candida albicans. *Current opinion in microbiology*. 9:595-601.

Bernassola, F., M. Karin, A. Ciechanover, and G. Melino. 2008. The HECT family of E3 ubiquitin ligases: multiple players in cancer development. *Cancer Cell*. 14:10-21.

Berndt, P., D. Lanver, and R. Kahmann. 2010. The AGC Ser/Thr kinase Aga1 is essential for appressorium formation and maintenance of the actin

cytoskeleton in the smut fungus Ustilago maydis. *Molecular microbiology*. 78:1484-1499.

Bhaduri, S., and P.M. Pryciak. 2011. Cyclin-specific docking motifs promote phosphorylation of yeast signaling proteins by G1/S Cdk complexes. *Curr Biol*. 21:1615-1623.

Blanco, M.A., A. Sánchez-Díaz, J.M. de Prada, and S. Moreno. 2000. APC[ste9/srw1] promotes degradation of mitotic cyclins in G_1 and is inhibited by cdc2 phosphorylation. *The EMBO journal*. 19:3945-3955.

Bölker, M., H.U. Bohnert, K.H. Braun, J. Gorl, and R. Kahmann. 1995a. Tagging pathogenicity genes in Ustilago maydis by restriction enzyme-mediated integration (REMI). *Mol Gen Genet*. 248:547-552.

Bölker, M., S. Genin, C. Lehmler, and R. Kahmann. 1995b. Genetic regulation of mating and dimorphism in Ustilago maydis. *Canadian journal of botany*. 73:320-325.

Bölker, M., and R. Kahmann. 1993. Sexual pheromones and mating responses in fungi. *Plant Cell*. 5:1461-1469.

Boutros, R., V. Lobjois, and B. Ducommun. 2007. CDC25 phosphatases in cancer cells: key players? Good targets? *Nat Rev Cancer*. 7:495-507.

Brachmann, A., J. Konig, C. Julius, and M. Feldbrugge. 2004. A reverse genetic approach for generating gene replacement mutants in Ustilago maydis. *Mol Genet Genomics*. 272:216-226.

Brachmann, A., J. Schirawski, P. Muller, and R. Kahmann. 2003. An unusual MAP kinase is required for efficient penetration of the plant surface by Ustilago maydis. *The EMBO journal*. 22:2199-2210.

Brachmann, A., G. Weinzierl, J. Kamper, and R. Kahmann. 2001. Identification of genes in the bW/bE regulatory cascade in Ustilago maydis. *Molecular microbiology*. 42:1047-1063.

Brefort, T., G. Doehlemann, A. Mendoza-Mendoza, S. Reissmann, A. Djamei, and R. Kahmann. 2009. Ustilago maydis as a Pathogen. *Annu Rev Phytopathol*. 47:423-445.

Budirahardja, Y., and P. Gönczy. 2009. Coupling the cell cycle to development. *Development*. 136:2861-2872.

Butler, G. 2010. Fungal sex and pathogenesis. *Clin Microbiol Rev*. 23:140-159.

Carbo, N., and J. Perez-Martin. 2010. Activation of the cell wall integrity pathway promotes escape from G2 in the fungus Ustilago maydis. *PLoS Genet*. 6:e1001009.

Coleman, T.R., Z. Tang, and W.G. Dunphy. 1993. Negative regulation of the wee1 protein kinase by direct action of the nim1/cdr1 mitotic inducer. *Cell*. 72:919-929.

Davey, J. 1998. Fusion of a fission yeast. *Yeast*. 14:1529-1566.

Davey, J., and O. Nielsen. 1994. Mutations in cyr1 and pat1 reveal pheromone-induced G1 arrest in the fission yeast Schizosaccharomyces pombe. *Curr Genet*. 26:105-112.

de Sena-Tomas, C., A. Fernandez-Alvarez, W.K. Holloman, and J. Perez-Martin. 2011. The DNA damage response signaling cascade regulates proliferation of the phytopathogenic fungus Ustilago maydis in planta. *Plant Cell*. 23:1654-1665.

Djamei, A., and R. Kahmann. 2012. Ustilago maydis: dissecting the molecular interface between pathogen and plant. *PLoS Pathog*. 8:e1002955.

Elías-Villalobos, A., A. Fernández-Álvarez, and J.I. Ibeas. 2011. The general transcriptional repressor Tup1 is required for dimorphism and virulence in a fungal plant pathogen. *PLoS Pathog*. 7:e1002235.

Feilotter, H., P. Nurse, and P.G. Young. 1991. Genetic and molecular analysis of cdr1/nim1 in Schizosaccharomyces pombe. *Genetics*. 127:309-318.

Feldbrugge, M., J. Kamper, G. Steinberg, and R. Kahmann. 2004. Regulation of mating and pathogenic development in Ustilago maydis. *Curr Opin Microbiol*. 7:666-672.

Fernandez-Alvarez, A., A. Elias-Villalobos, and J.I. Ibeas. 2009. The O-mannosyltransferase PMT4 is essential for normal appressorium formation and penetration in Ustilago maydis. *Plant Cell*. 21:3397-3412.

Fernandez-Alvarez, A., M. Marin-Menguiano, D. Lanver, A. Jimenez-Martin, A. Elias-Villalobos, A.J. Perez-Pulido, R. Kahmann, and J.I. Ibeas. 2012. Identification of O-mannosylated virulence factors in Ustilago maydis. *PLoS Pathog*. 8:e1002563.

Flor-Parra, I., S. Castillo-Lluva, and J. Perez-Martin. 2007. Polar growth in the infectious hyphae of the phytopathogen ustilago maydis depends on a virulence-specific cyclin. *Plant Cell*. 19:3280-3296.

Flor-Parra, I., M. Vranes, J. Kamper, and J. Perez-Martin. 2006. Biz1, a zinc finger protein required for plant invasion by Ustilago maydis, regulates the levels of a mitotic cyclin. *Plant Cell*. 18:2369-2387.

Freitag, J., D. Lanver, C. Bohmer, K.O. Schink, M. Bolker, and B. Sandrock. 2011. Septation of infectious hyphae is critical for appressoria formation and virulence in the smut fungus Ustilago maydis. *PLoS Pathog*. 7:e1002044.

García-Muse, T., G. Steinberg, and J. Perez-Martin. 2004. Characterization of B-type cyclins in the smut fungus Ustilago maydis: roles in morphogenesis and pathogenicity. *Journal of Cell Science*. 117:487-506.

Garcia-Muse, T., G. Steinberg, and J. Perez-Martin. 2003. Pheromone-induced G2 arrest in the phytopathogenic fungus Ustilago maydis. *Eukaryot Cell*. 2:494-500.

Garcia-Muse, T., G. Steinberg, and J. Perez-Martin. 2004. Characterization of B-type cyclins in the smut fungus Ustilago maydis: roles in morphogenesis and pathogenicity. *Journal of cell science*. 117:487-506.

Garrido, E., and J. Perez-Martin. 2003. The crk1 gene encodes an Ime2-related protein that is required for morphogenesis in the plant pathogen Ustilago maydis. *Molecular microbiology*. 47:729-743.

Garrido, E., U. Voss, P. Muller, S. Castillo-Lluva, R. Kahmann, and J. Perez-Martin. 2004. The induction of sexual development and virulence in the smut fungus Ustilago maydis depends on Crk1, a novel MAPK protein. *Genes Dev*. 18:3117-3130.

Gillissen, B., J. Bergemann, C. Sandmann, B. Schroeer, M. Bolker, and R. Kahmann. 1992. A two-component regulatory system for self/non-self recognition in Ustilago maydis. *Cell*. 68:647-657.

Hamel, L.P., M.C. Nicole, S. Duplessis, and B.E. Ellis. 2012. Mitogen-activated protein kinase signaling in plant-interacting fungi: distinct messages from conserved messengers. *Plant Cell*. 24:1327-1351.

Hanahan, D. 1983. Studies on transformation of Escherichia coli with plasmids. *J Mol Biol*. 166:557-580.

Hartmann, H.A., R. Kahmann, and M. Bolker. 1996. The pheromone response factor coordinates filamentous growth and pathogenicity in Ustilago maydis. *The EMBO journal*. 15:1632-1641.

Hazan, I., M. Sepulveda-Becerra, and H. Liu. 2002. Hyphal elongation is regulated independently of cell cycle in Candida albicans. *Mol Biol Cell*. 13:134-145.

Heimel, K., M. Scherer, M. Vranes, R. Wahl, C. Pothiratana, D. Schuler, V. Vincon, F. Finkernagel, I. Flor-Parra, and J. Kamper. 2010. The transcription factor Rbf1 is the master regulator for b-mating type controlled pathogenic development in Ustilago maydis. *PLoS Pathog*. 6:e1001035.

Hindley, C., and A. Philpott. 2012. Co-ordination of cell cycle and differentiation in the developing nervous system. *Biochem J*. 444:375-382.

Hoffman, C.S., and F. Winston. 1987. A ten-minute DNA preparation from yeast efficiently releases autonomous plasmids for transformation of Escherichia coli. *Gene*. 57:267-272.

Holliday, R. 1974. Ustilago maydis. *In* Handbook of Genetics. R.C. King, editor. Plenum Press, New York. 575-595.

Imai, Y., and M. Yamamoto. 1994. The fission yeast mating pheromone P-factor: its molecular structure, gene structure, and ability to induce gene expression and G1 arrest in the mating partner. *Genes Dev*. 8:328-338.

Irniger, S. 2011. The Ime2 protein kinase family in fungi: more duties than just meiosis. *Molecular microbiology*. 80:1-13.

Kamper, J., R. Kahmann, M. Bolker, L.J. Ma, T. Brefort, B.J. Saville, F. Banuett, J.W. Kronstad, S.E. Gold, O. Muller, M.H. Perlin, H.A. Wosten, R. de Vries, J. Ruiz-Herrera, C.G. Reynaga-Pena, K. Snetselaar, M. McCann, J. Perez-Martin, M. Feldbrugge, C.W. Basse, G. Steinberg, J.I. Ibeas, W. Holloman, P. Guzman, M. Farman, J.E. Stajich, R. Sentandreu, J.M. Gonzalez-Prieto, J.C. Kennell, L. Molina, J. Schirawski, A. Mendoza-Mendoza, D. Greilinger, K. Munch, N. Rossel, M. Scherer, M. Vranes, O. Ladendorf, V. Vincon, U. Fuchs, B. Sandrock, S. Meng, E.C. Ho, M.J. Cahill, K.J. Boyce, J. Klose, S.J. Klosterman, H.J. Deelstra, L. Ortiz-Castellanos, W. Li, P. Sanchez-Alonso, P.H. Schreier, I. Hauser-Hahn, M. Vaupel, E. Koopmann, G. Friedrich, H. Voss, T. Schluter, J. Margolis, D. Platt, C. Swimmer, A. Gnirke, F. Chen, V. Vysotskaia, G. Mannhaupt, U. Guldener, M. Munsterkotter, D. Haase, M. Oesterheld, H.W. Mewes, E.W. Mauceli, D. DeCaprio, C.M. Wade, J. Butler, S. Young, D.B. Jaffe,

S. Calvo, C. Nusbaum, J. Galagan, and B.W. Birren. 2006. Insights from the genome of the biotrophic fungal plant pathogen Ustilago maydis. *Nature*. 444:97-101.

Kamper, J., M. Reichmann, T. Romeis, M. Bolker, and R. Kahmann. 1995. Multiallelic recognition: nonself-dependent dimerization of the bE and bW homeodomain proteins in Ustilago maydis. *Cell*. 81:73-83.

Kanoh, J., and P. Russell. 1998. The protein kinase Cdr2, related to Nim1/Cdr1 mitotic inducer, regulates the onset of mitosis in fission yeast. *Mol Biol Cell*. 9:3321-3334.

King, K., M. Jin, and D. Lew. 2012. Roles of Hsl1p and Hsl7p in Swe1p degradation: beyond septin tethering. *Eukaryot Cell*. 11:1496-1502.

Kitamura, K., H. Maekawa, and C. Shimoda. 1998. Fission yeast Ste9, a homolog of Hct1/Cdh1 and Fizzy-related, is a novel negative regulator of cell cycle progression during G1-phase. *Mol Biol Cell*. 9:1065-1080.

Kõivomägi, M., E. Valk, R. Venta, A. Iofik, M. Lepiku, D.O. Morgan, and M. Loog. 2011. Dynamics of Cdk1 substrate specificity during the cell cycle. *Mol Cell*. 42:610-623.

Lanver, D., A. Mendoza-Mendoza, A. Brachmann, and R. Kahmann. 2010. Sho1 and Msb2-related proteins regulate appressorium development in the smut fungus Ustilago maydis. *Plant Cell*. 22:2085-2101.

Lew, D.J. 2000. Cell-cycle checkpoints that ensure coordination between nuclear and cytoplasmic events in Saccharomyces cerevisiae. *Curr Opin Genet Dev*. 10:47-53.

Lew, D.J., and S.I. Reed. 1995. A cell cycle checkpoint monitors cell morphogenesis in budding yeast. *J Cell Biol*. 129:739-749.

Loeb, J.D., M. Sepulveda-Becerra, I. Hazan, and H. Liu. 1999. A G1 cyclin is necessary for maintenance of filamentous growth in Candida albicans. *Molecular and cellular biology*. 19:4019-4027.

Martin, S.G., and M. Berthelot-Grosjean. 2009. Polar gradients of the DYRK-family kinase Pom1 couple cell length with the cell cycle. *Nature*. 459:852-856.

Martínez-Espinoza, A.D., M.D. García-Pedrajas, and S.E. Gold. 2002. The Ustilaginales as plant pests and model systems. *Fungal Genet Biol*. 35:1-20.

McMillan, J.N., M.S. Longtine, R.A. Sia, C.L. Theesfeld, E.S. Bardes, J.R. Pringle, and D.J. Lew. 1999. The morphogenesis checkpoint in Saccharomyces cerevisiae: cell cycle control of Swe1p degradation by Hsl1p and Hsl7p. *Molecular and cellular biology*. 19:6929-6939.

McMillan, J.N., C.L. Theesfeld, J.C. Harrison, E.S. Bardes, and D.J. Lew. 2002. Determinants of Swe1p degradation in Saccharomyces cerevisiae. *Mol Biol Cell*. 13:3560-3575.

Mendoza-Mendoza, A., P. Berndt, A. Djamei, C. Weise, U. Linne, M. Marahiel, M. Vranes, J. Kamper, and R. Kahmann. 2009. Physical-chemical plant-derived signals induce differentiation in Ustilago maydis. *Molecular microbiology*. 71:895-911.

Mielnichuk, N., and J. Perez-Martin. 2008. 14-3-3 regulates the G2/M transition in the basidiomycete Ustilago maydis. *Fungal Genet Biol*. 45:1206-1215.

Mielnichuk, N., C. Sgarlata, and J. Perez-Martin. 2009. A role for the DNA-damage checkpoint kinase Chk1 in the virulence program of the fungus Ustilago maydis. *Journal of cell science*. 122:4130-4140.

Moreno, S., and P. Nurse. 1994. Regulation of progression through the G1 phase of the cell cycle by the rum1+ gene. *Nature*. 367:236-242.

Morrow, C.A., and J.A. Fraser. 2009. Sexual reproduction and dimorphism in the pathogenic basidiomycetes. *FEMS Yeast Res*. 9:161-177.

Moseley, J.B., A. Mayeux, A. Paoletti, and P. Nurse. 2009. A spatial gradient coordinates cell size and mitotic entry in fission yeast. *Nature*. 459:857-860.

Muller, P., G. Weinzierl, A. Brachmann, M. Feldbrugge, and R. Kahmann. 2003. Mating and pathogenic development of the Smut fungus Ustilago maydis are regulated by one mitogen-activated protein kinase cascade. *Eukaryot Cell*. 2:1187-1199.

Ni, M., M. Feretzaki, S. Sun, X. Wang, and J. Heitman. 2011. Sex in fungi. *Annu Rev Genet*. 45:405-430.

Ogura, Y., A. Sakaue-Sawano, M. Nakagawa, N. Satoh, A. Miyawaki, and Y. Sasakura. 2011. Coordination of mitosis and morphogenesis: role of a prolonged G2 phase during chordate neurulation. *Development*. 138:577-587.

Otsubo, Y., and M. Yamamoto. 2012. Signaling pathways for fission yeast sexual differentiation at a glance. *Journal of cell science*. 125:2789-2793.

Pan, K.Z., T.E. Saunders, I. Flor-Parra, M. Howard, and F. Chang. 2014. Cortical regulation of cell size by a sizer cdr2p. *Elife*. 3:e02040.

Perez-Martin, J. 2009. DNA-damage response in the basidiomycete fungus Ustilago maydis relies in a sole Chk1-like kinase. *DNA Repair (Amst)*. 8:720-731.

Pérez-Martín, J. 2009. DNA-damage response in the basidiomycete fungus Ustilago maydis relies in a sole Chk1-like kinase. *DNA Repair (Amst)*. 8:720-731.

Pérez-Martín, J. 2012. Cell cycle and morphogenesis connections during the formation of the infective filament in Ustilago maydis. *In* Morphogenesis and Pathogenicity in Fungi. J. Perez-Martin and A. di Pietro, editors. Springer-Verlag, Berlin Heidelberg. 97-114.

Pérez-Martín, J., and S. Castillo-Lluva. 2008. Connections between polar growth and cell cycle arrest during the induction of the virulence program in the phytopathogenic fungus Ustilago maydis. *Plant Signal Behav*. 3:480-481.

Perez-Martin, J., S. Castillo-Lluva, C. Sgarlata, I. Flor-Parra, N. Mielnichuk, J. Torreblanca, and N. Carbo. 2006. Pathocycles: Ustilago maydis as a model to study the relationships between cell cycle and virulence in pathogenic fungi. *Mol Genet Genomics*. 276:211-229.

Perez-Nadales, E., M.F. Almeida Nogueira, C. Baldin, S. Castanheira, M. El Ghalid, E. Grund, K. Lengeler, E. Marchegiani, P.V. Mehrotra, M. Moretti, V. Naik, M. Oses-Ruiz, T. Oskarsson, K. Schafer, L. Wasserstrom, A.A. Brakhage, N.A. Gow, R. Kahmann, M.H. Lebrun, J. Perez-Martin, A. Di Pietro, N.J. Talbot, V. Toquin, A. Walther, and J. Wendland. 2014. Fungal model systems and the elucidation of pathogenicity determinants. *Fungal Genet Biol*. 70C:42-67.

Pope, P.A., S. Bhaduri, and P.M. Pryciak. 2014. Regulation of cyclin-substrate docking by a G1 arrest signaling pathway and the Cdk inhibitor Far1. *Curr Biol*. 24:1390-1396.

Puhalla, J.E. 1968. Compatibility reactions on solid medium and interstrain inhibition in Ustilago maydis. *Genetics*. 60:461-474.

Rowell, J. 1955. Functional role of compatibility factors and an in vitro test for sexual compatibility with haploid lines of Ustilago zeae. *Phytopathology*. 45:370-374.

Sambrook, J., E. Fritsch, and T. Maniatis. 1989. Molecular cloning: a laboratory manual.

Saunders, D.G., S.J. Aves, and N.J. Talbot. 2010. Cell cycle-mediated regulation of plant infection by the rice blast fungus. *Plant Cell*. 22:497-507.

Schirawski, J., H.U. Bohnert, G. Steinberg, K. Snetselaar, L. Adamikowa, and R. Kahmann. 2005. Endoplasmic reticulum glucosidase II is required for pathogenicity of Ustilago maydis. *Plant Cell*. 17:3532-3543.

Schulz, B., F. Banuett, M. Dahl, R. Schlesinger, W. Schafer, T. Martin, I. Herskowitz, and R. Kahmann. 1990. The b alleles of U. maydis, whose combinations program pathogenic development, code for polypeptides containing a homeodomain-related motif. *Cell*. 60:295-306.

Sgarlata, C., and J. Perez-Martin. 2005a. The cdc25 phosphatase is essential for the G2/M phase transition in the basidiomycete yeast Ustilago maydis. *Molecular microbiology*. 58:1482-1496.

Sgarlata, C., and J. Perez-Martin. 2005b. Inhibitory phosphorylation of a mitotic cyclin-dependent kinase regulates the morphogenesis, cell size and virulence of the smut fungus Ustilago maydis. *Journal of cell science*. 118:3607-3622.

Sia, R.A., E.S. Bardes, and D.J. Lew. 1998. Control of Swe1p degradation by the morphogenesis checkpoint. *The EMBO journal*. 17:6678-6688.

Snetselaar, K., and C.W. Mims. 1993. Infection of maize stigmas by Ustilago maydis: light and electron microscopy. *Phytopathology*. 83:843-850.

Snetselaar, K.M., and C.W. Mims. 1992. Sporidial fusion and infection of maize seedlings by the smut fungus Ustilago maydis. *Mycologia*. 84:193-203.

Spellig, T., M. Bolker, F. Lottspeich, R.W. Frank, and R. Kahmann. 1994. Pheromones trigger filamentous growth in Ustilago maydis. *The EMBO journal*. 13:1620-1627.

Steinberg, G., and J. Perez-Martin. 2008. Ustilago maydis, a new fungal model system for cell biology. *Trends Cell Biol*. 18:61-67.

Stern, B., and P. Nurse. 1997. Fission yeast pheromone blocks S-phase by inhibiting the G1 cyclin B-p34cdc2 kinase. *The EMBO journal*. 16:534-544.

Stern, B., and P. Nurse. 1998. Cyclin B proteolysis and the cyclin-dependent kinase inhibitor rum1p are required for pheromone-induced G1 arrest in fission yeast. *Mol Biol Cell*. 9:1309-1321.

Straube, A., I. Weber, and G. Steinberg. 2005. A novel mechanism of nuclear envelope break-down in a fungus: nuclear migration strips off the envelope. *The EMBO journal*. 24:1674-1685.

Sudbery, P., N. Gow, and J. Berman. 2004. The distinct morphogenic states of Candida albicans. *Trends Microbiol*. 12:317-324.

Wu, L., and P. Russell. 1993. Nim1 kinase promotes mitosis by inactivating Wee1 tyrosine kinase. *Nature*. 363:738-741.

Yamaguchi, S., H. Murakami, and H. Okayama. 1997. A WD repeat protein controls the cell cycle and differentiation by negatively regulating Cdc2/B-type cyclin complexes. *Mol Biol Cell*. 8:2475-2486.

Yamaguchi, S., H. Okayama, and P. Nurse. 2000. Fission yeast Fizzy-related protein srw1p is a G(1)-specific promoter of mitotic cyclin B degradation. *The EMBO journal*. 19:3968-3977.

Zarnack, K., H. Eichhorn, R. Kahmann, and M. Feldbrugge. 2008. Pheromone-regulated target genes respond differentially to MAPK phosphorylation of transcription factor Prf1. *Molecular microbiology*. 69:1041-1053.

Zheng, X., and Y. Wang. 2004. Hgc1, a novel hypha-specific G1 cyclin-related protein regulates Candida albicans hyphal morphogenesis. *The EMBO journal*. 23:1845-1856.